An improved model of $CaCO_3$ crystallization

An improved kinetics-model for the calcium carbonate crystallization
in the fluidized bed softening reactors
at the Weesperkarspel drinking water treatment plant

Eleftheria Chiou

Delft University of Technology

TU Delft Delft University of Technology

An improved model of $CaCO_3$ crystallization

An improved kinetics-model for the calcium carbonate crystallization

in the fluidized bed softening reactors

at the Weesperkarspel drinking water treatment plant

By

Eleftheria Chiou

Student number: 4517547

in partial fulfilment of the requirements for the degree of

Master of Science

in Civil Engineering-Water Management

at the Delft University of Technology

Thesis committee:

Prof. dr. ir. J.P. van der Hoek MBA (Chair)	Delft University of Technology Department of Water management Section of Sanitary engineering
Prof. dr. ir. H.J.M. Kramer	Delft University of Technology Department of Process and Energy
Ing. E.T. Baars	Waternet Waterkwaliteit en Procesondersteuning
Ir. P.J. de Moel	Delft University of Technology Department of Water management Section of Sanitary engineering Waternet Waterkwaliteit en Procesondersteuning
PhD candidate Ir. O.I.J. Kramer	Delft University of Technology Department of Water management Section of Sanitary engineering Waternet Waterkwaliteit en Procesondersteuning

TU Delft Delft University of Technology

Acknowledgements

The successful completion of this thesis was a team effort. I would like to thank a number of persons that have worked on this project for their contribution.

Firstly I would like to thank Prof. Jan Peter van der Hoek for giving me the opportunity to do a Master thesis in this interesting topic. Prof. Jan Peter van der Hoek has not only coordinated the effort between the parties involved in this thesis but also gave me important feedback whenever it was needed. In addition, I would like to thank the Water Quality team at Weesperkarspel water treatment plant and especially Mr Leon Kors for allowing me to participate in this research of TU Delft and Waternet.

Most importantly, I would like to thank Mr Peter de Moel and Eric Baars for helping me daily with my work. I am grateful to Mr Eric Baars for organizing the experimental part of my thesis and always supporting me despite the adversities during my thesis. From the beginning of my research, he was the first person I would go for assistance and support.

I wouldn't have managed to complete my thesis without the help of Mr Peter de Moel. His contribution to this thesis was crucial and I am grateful for him being part of my daily supervisors' team. He always helped me find a solution and continue whenever a serious problem in my research was presented.

I would also like to thank Prof. Herman Kramer for his precious advice on his field of expertise. With his guidance I was able to clarify and understand confusing concepts and complete my experiments in TU Delft laboratory.

Furthermore, I would like to thank Onno Kramer for his emotional support and very interesting philosophical conversations. His way of thinking, was an invaluable lesson for me. He also dedicated a lot of time and helped me during the writing of my report.

Last but not least, I would like to thank my parents and Takis for always being there for me and supporting me in every project I have ever undertaken. I wouldn't have achieved anything without them.

Amsterdam, June 2018,

Eleftheria Chiou

Summary

One of the main targets of Waternet, the water-cycle company of Amsterdam, is to increase the sustainability of water treatment. To achieve this goal, it is necessary to improve the efficiency and to decrease the use of chemicals during pellet softening process. However, the model of Van Schagen et al. (2008 b,c) that is currently used to optimize the pellet softening process is not predicting accurately enough the pH and calcium profile over the height of the pellet softening reactor. The calcium carbonate crystallization is calculated, in this model, using a linear relationship between the rate of crystallization and supersaturation with an additional diffusion parameter to take into account the flow conditions inside the reactor.

To determine more accurately the rate of calcium carbonate during the pellet softening process, two types of experiments were conducted during this research: STR batch and PFR fluidized bed experiments. Firstly, the experimental results were compared with the predictions of two linear models: the model of Wiechers et al. (1975) from literature and the one-rate-constant model developed in this research. Based on the results, it was concluded that it is not possible to improve the prediction of calcium carbonate crystallization kinetics if a linear model with one-rate-constant is used as proposed by Van Schagen. When the rate of crystallization is plotted against supersaturation a bending of the curve is observed at low supersaturation due to a sharp decrease in the rate of crystallization. Other researchers, such as Dreybrodt et al. (1997) has also observed that the rate of calcium carbonate crystallization is not linearly related to supersaturation when water or seeding material with inhibiting compounds is used. To describe this bending of the curve, two models were considered: the exponential model of Lasaga (1998) and the two-rate-constants model that consists of two linear equations. In this research, the two-rate-constants model was chosen instead of the exponential Lasaga model because it is easier to fit to the experimental results and gives a better overview of the dependence of the rate of crystallization from supersaturation. The two-rate-constants model significantly improves the prediction of calcium carbonate crystallization in a pellet softening fluidized bed reactor. The average relative error of this model, for the prediction of the calcium profile in a full-scale reactor, is only 2-5% while the average relative error of the one-rate-constant model is approximately 15-30%. Therefore, the two-rate-constants model predicts better the calcium carbonate crystallization and can be used to describe much more accurately the pellet softening process compared to the models found in literature.

Based on the results of the research, it can be concluded that the performance of a pellet softening fluidized bed reactor cannot be significantly improved by increasing the height of the reactor. On the other hand, it is possible that performance is enhanced by removing inhibitors such as organic carbon from the water. Nevertheless, further research is necessary to determine the effect of inhibitors, such as organic carbon, on water softening. Also, in order to determine more accurately the model parameters, the experimental set up should be adjusted in order to represent better the conditions inside a pellet softening fluidized bed reactor. In particular, increasing the height of the reactor and mixing the caustic soda at the bottom of the column is necessary.

An improved model of calcium carbonate crystallization inside a pellet softening fluidized bed reactor:

$$-\frac{dCa}{dt} = k_i * K_{sp} * S(SR - A_i)$$

dCa/dt is the calcium carbonate crystallization rate (mmol L^{-1} s^{-1}), SR or Ω is the calcite saturation ratio, S is the specific surface area (SSA) (m^2/m^3)

- the high rate constant is k_H =0.1224 (mol/ L *s^{-1}*m^3/m^2) for calcite SR>13.5
- the low rate constant $k_L = 0.004$ (mol/ L *s^{-1}*m^3/m^2) for calcite SR<13.5
- the intercept of the high rate constant line is $A_H = 13$
- the intercept of the low constant line is A_L =1

The saturation ratio of change is the intersection of the two lines.

Contents

List of figures

List of tables

1

Introduction

1.1. Thesis background and motivation

1.1.1. The water-cycle company Waternet

Waternet is the water company of Amsterdam and controls the water-cycle on an integral and socially responsible way, based on the four values: safety, customer orientation, sustainability and innovation (Waternet, 2010). Therefore, Waternet is focusing on providing cheap and clean water to its customers and at the same time on increasing the sustainability of water treatment. In particular, one of the strategic goals of Waternet is having CO_2 neutral water treatment plants by 2020. However, in order to achieve this goal the water treatment plant needs to be operated in an efficient way that would minimize the impact on the environment. As a result, reuse of materials and minimization of the use of chemicals in all water treatment steps is necessary.

1.1.2. The pellet softening process of drinking water

An important process in a drinking water treatment plant is softening. The main goal of the softening process is to reduce the dissolution of copper and lead from the pipes of the distribution system in the water. In addition, advantages of the hardness reduction in the water are: avoiding scaling in heating equipment and appliances, improving the taste of the water, reducing the use of detergents and esthetical consumer aspects [De Moel et al. (2007)]. A common and effective process for calcium concentration reduction is the softening of water in a pellet softening reactor. Waternet played a vital role in the introduction of the pellet softening in a fluidized bed reactor [Van Dijk and Wilms (1991), Kramer et al. (2015)]. During this treatment step, water is pumped through a cylindrical vessel filled with seeding material in an upward direction maintaining the bed in a homogeneous fluidized condition. Alkaline chemicals are injected in the bottom of the reactor, the pH of the water increases and the solubility product of calcium carbonate is exceeded. As a result, calcium carbonate crystallizes at the surface of the seeding material and the calcium concentration in the solution is reduced [Van Dijk, (1993)].

1.1.3. Applied process changes

Traditionally, garnet sand is used as a seeding material in the pellet softening reactors. However, Waternet replaced, in 2016, garnet sand with crushed calcite in Weesperkarspel (WPK) drinking water treatment plant (WTP) in order to increase the sustainability of the softening process. The reuse of crushed calcite decreases the amount of waste produced during this treatment step [Schetters et al. (2015)]. Also, calcite pellets that do not include impurities, such as garnet sand, have numerous industrial and commercial uses. Other important process changes were: in 2010 the CO_2 dosage in the pre-treatment plant in Loenderveen have stopped and in 2017, hydrochloric acid was replaced by CO_2 for the conditioning of the water after softening. Therefore, major parameters of the pellet softening process has recently changed. Due to the changes in the seeding material and the operation of the pellet softening

reactors, the calcium carbonate crystallization rate in Weesperkarspel fluidized bed pellet softening reactors has decreased and a higher dose of caustic soda is used to reach the goal of hardness reduction.

1.2. Problem analysis

1.2.1. Operational changes

To optimize the operation of the pellet softening reactors the model developed by Van Schagen et al. (2008 b,c) was used in the two drinking water treatment plants of Waternet, in Weesperkarspel and Leiduin. The model by Van Schagen et al. (2008 b,c) has been developed and calibrated considering that garnet sand (§1.1.3) is used as a seeding material. Currently, a different type and diameter of seeding material are used and therefore the fluidization conditions in the pellet softening reactor are different.

1.2.2. Prediction model

Additionally, Van Schagen et al. (2008 b,c) has used the calcium carbonate crystallization rate equation of Wiechers et al. (1975), which is explained in §2.6.2, to predict the calcium carbonate kinetics inside the reactor. However, the experiments conducted by Wiechers took place at different flow conditions than the conditions inside a pellet softening fluidized bed reactor in full-scale installations. In order to be able to use the Wiechers equation, under the chemical and flow conditions in a pellet softening fluidized bed reactor, Van Schagen et al. (2008) has introduced a diffusion parameter. However, the role of this diffusion parameter is not clear and further improvement of the calcium carbonate crystallization model is necessary to describe more accurately the calcium and pH profile over the height of a pellet softening reactor. The model should be derived using experiments conducted in similar conditions as in a pellet softening fluidized bed reactor.

1.2.3. Water quality parameters

In theoretical models like Wiechers and applied models like Van Schagen, the effect of inhibitors have not be taken into account. Inhibitors are dissolved compounds in the water like phosphate, natural organic matter and magnesium (§2.3.5). Inhibitors adversely affect the crystallization of calcium carbonate by blocking the transfer of calcium carbonate ions at the surface of the seeding material.

1.2.4. Starting point of research

The Calcium Carbonate Crystallization Potential (CCCP) is the calcium that remains after the maximum amount of calcium carbonate has been crystallized. In the practical application at the Waternet full-scale pellets softening reactors, it has been found that the determined calcium carbonate crystallization potential (CCCP) in the field under current conditions ($\approx$0.3 mmol/L), is higher than the expected value based on experience from pellet softening reactors ($\approx$0.1 mmol/L).

Important factors which affect the performance are specific surface area, caustic soda dosing and mixing, temperature and the presence of inhibitors. To be able to improve the process performance, an accurate prediction model which takes into account these factors is useful. The currently applied Van Schagen model does not take into account all of these factors and does not predict accurately the pH and total calcium profile inside the reactor. According to the linear model by Van Schagen, the rate of crystallization is proportional to the decrease of supersaturation over the height of the reactor. Since supersaturation in the bottom of the reactor is high, a large amount of calcium is removed in this region ($\approx$90%). In the

higher region of the reactor, supersaturation decreases and therefore the rate of crystallization also reduces. Van den Hout (2016) and Van Schagen assumed that the rate of crystallization remains proportional to supersaturation in this region and a lower but significant amount of calcium is removed in this part of the reactor. However, according to observation in the full-scale installation only a relatively small amount of calcium is removed in the upper part of the reactor since the rate of crystallization has significantly decreased. As a result, the operational guidelines derived using the Van Schagen model are not appropriate for the optimization of the pellet softening process in the full-scale installations.

1.3. Research questions

The main challenge issued in this research, is the determination of a model that would be able to predict the rate of calcium carbonate crystallization in a pellet softening fluidized bed reactor. The following research questions will be examined:

- Is it possible to predict the rate of calcium carbonate crystallization using the rate constant and equation derived by Wiechers in a fluidized bed reactor?
- Is it possible by changing the value of the rate constant in the linear equation between the rate of crystallization and supersaturation, as proposed by Van Schagen et al. (2008 b,c), to predict accurately the hardness reduction process?
- Is there a model that can describe more accurately than the existing models, the rate of the calcium carbonate crystallization process in the chemical and hydraulic conditions of a pellet reactor?

1.4. Hypothesis

The hypothesis of this research is that it is possible to improve the pellet softening process by using a more accurate predictive model for the calcium carbonate crystallization. An improved model derived and validated from small-scale experiments and in the pilot plant installation can be calibrated to fit the measurements of a full-scale reactor. In this case, it would be possible to determine accurately the pH and calcium concentration profile over the height of a full-scale pellets softening reactor. The model can be used to test operational scenarios. In these operational scenarios, several set-point changes and process adaptations can be applied until the operation of the pellet softening reactor is optimized. The scenario results can be used as a blueprint for process design rules. In this way, the use of chemicals can be minimized and consequently the cost of the softening process can be reduced and sustainability can be increased.

1.5. Thesis objective

The aim of this research is to improve the model of calcium carbonate seeded crystallization kinetics in order to be able to optimize the pellet softening fluidized bed reactor in full-scale installations. With an improved model it is possible to study different scenarios of operation under different conditions.

1.6. Research approach and challenges

In order to be able to determine the calcium carbonate crystallization kinetics in a pellet softening reactor two types of experiments took place in this research. Stirred Tank Reactor (STR) batch experiments were conducted at TU Delft Process and Energy laboratory and Plug Flow Reactor (PFR) fluidized bed experiments at Weesperkarspel pilot plant. By comparing the results of the two types of experiments the effect of flow conditions on calcium carbonate crystallization was determined. In both types of

experiments, the reactor was filled with seeding material and a caustic soda solution was added to natural hard water increasing the pH of the solution and therefore exceeding the solubility of calcium carbonate. The decrease of the solution's pH due to calcium carbonate crystallization was then measured. Based on the pH reduction curve, a chemical equilibrium model, PHREEQC coupled with Excel, [De Moel et al. (2012)] was used to determine the total calcium (Ca) concentration in the water during the experiments. Consequently, it was possible to calculate the rate of calcium reduction over time. The results of this analysis were used to derive the equation that best describes the rate of calcium carbonate crystallization. The equation was incorporated in a model, that is used to predict the (Ca) and pH profile in a pellet softening fluidized bed reactor. Using this model, it is possible to optimize the pellet softening process and minimize the use of caustic soda during this treatment step.

One of the major challenges of this research was to overcome the limitations of the experimental set-up of both types of experiments. In the STR batch experiments, a high stirring velocity of 1000 rounds per minute (rpm) was necessary to keep the seeding material in suspension. It was not possible to keep in suspension a high concentration of large particles of seeding material. On the other hand, in the PFR fluidized bed experiments, the measurements were limited by the height of the reactor (only 1m) and the amount of conditioned water that was available for each experiment. Also, due to the highly scaling conditions during the experiments the equipment was affected. It was, therefore, important that the measuring devices and the experimental set up were regularly checked.

1.7. Thesis outline

This report is divided into seven chapters. In the first two chapters, the aim of the thesis and the background information necessary for this research are shown. In Chapter 3 and Chapter 4 the materials and methods and the experimental results of the STR batch and PFR fluidized bed experiments are presented. In the last two chapters, the research results are discussed and conclusions are reached. Also, recommendations for future research are made.

- Chapter 1. Introduction - In this chapter, the aim and scope of this research are presented.
- Chapter 2. Theoretical background - In this chapter, the necessary theoretical background for this research is presented. The chemical, as well as the physical part of a pellet softening reactor, is explained and basic concepts related to the softening process are analyzed. Furthermore, an overview of the existing models for calcium carbonate crystallization in addition to the models used in this research is presented.
- Chapter 3. STR batch experiments - In this chapter, the results of the STR batch experiments are presented. The experimental setup and the methodology that was used are described in detail.
- Chapter 4. PFR fluidized bed experiments - In this chapter, the results of the PFR fluidized bed are presented. The experimental setup and the methodology that was used are described in detail.
- Chapter 5. Modeling of a pellet softening fluidized bed reactor - In this chapter, the predictions of several models are compared with the experimental results. The equation that best describes the rate of calcium carbonate crystallization is determined. The model that was derived from the experimental results is validated using data from a full-scale pellet softening reactor.
- Chapter 6. Discussion - In this chapter, the experimental results of both STR batch and fluidized bed reactor experiments are discussed. Furthermore, the effect of factors that may influence the rate of calcium carbonate crystallization such as, temperature, using different types of seeding material and the presence of inhibiting compounds in the influent water of Weesperkarspel water treatment plant is analyzed.
- Chapter 7. Conclusions and Recommendations - In this chapter, the conclusions of this research are summarized. Recommendations for future research are also made.

2

Theoretical background

In this chapter, the theoretical framework of this research is presented. Firstly, an overview of the water treatment processes in Weesperkarspel water treatment plant is shown. Especially, the pellet softening process is presented in detail.

The literature research about a pellet softening fluidized bed reactor is separated in a chemical (§2.3) and physical part (§2.4). In the chemical part, basic concepts of aquatic chemistry and crystallization theory are explained. On the other hand, in the physical part, the type of the seeding material that is used and basic concepts and parameters about the fluidization of the bed are explained. Additionally, the flow conditions inside the most common ideal reactors are described and compared with the flow conditions inside a pellet softening fluidized bed reactor.

Furthermore, the existing literature about the modeling of a fluidized bed pellet reactor is shown. Especially the equations that are used in literature to model the crystallization of calcium carbonate kinetics are presented. Secondly, the hydraulic model that describes the fluidization of the bed in a pellet softening fluidized bed reactor is briefly explained. Finally, the Layers-model that has been used in the past to determine the calcium reduction in a pellet softening reactor is mentioned and its performance is assessed.

2.1. Overview of drinking water treatment at Weesperkarspel WTP

The drinking water treatment plant of Weesperkarspel consists of several processes that aim at purifying and improving the aesthetic characteristics of the water. Firstly, natural raw water is abstracted from Bethune polder and Amsterdam-Rhine canal. Afterward, the water is transferred to the Loenderveen pre-treatment plant where coagulation, sedimentation, reservoir storage and rapid sand filtration takes place (Figure 1). Until 2016, HCl was added before transportation to the main water treatment plant in order to avoid scaling in the pipelines. However, this practice recently changed and the water is no longer conditioned.

The pre-treated water is pumped to Weesperkarspel water treatment plant. At Weesperkarspel four main processes take place for the purification of the water. Initially, ozonation is used for disinfection and oxidation of organic matter and other pollutants. Next, the water is pumped in a pellet softening fluidized bed reactor where the hardness of the water is reduced. Then the water is transferred to an activated carbon bed where pesticides and micropollutants are either absorbed or removed by biological activity. Finally, slow sand filtration takes place to remove any remaining organic or inorganic particles. In Figure 1 the pre-treatment and treatment step is sown at Loenderveen and Weesperkarspel WTP [Van Der Helm et al. (2015)].

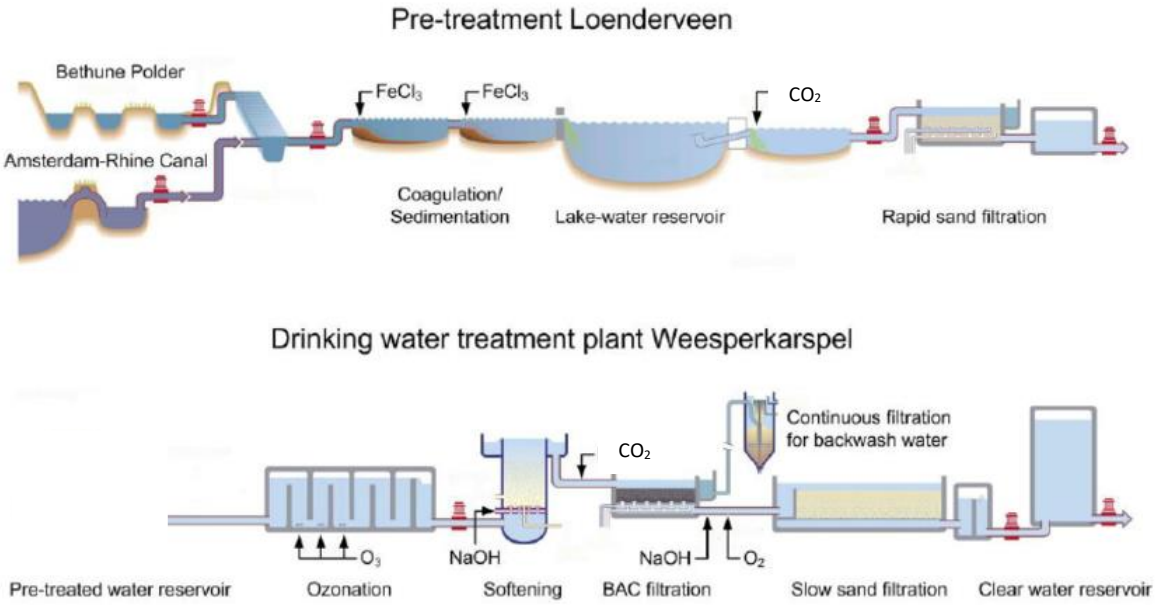

Figure 1 Process scheme of pre-treatment processes at Loenderveen and drinking water treatment at Weesperkarspel WTP of Waternet [Van Der Helm et al. (2015)]

This research is focusing on the improvement of the softening process at Weesperkarspel WTP.

2.2. Pellet softening fluidized bed process

Softening is an important treatment step of the drinking water treatment production. Most of the water companies in the Netherlands reduce the calcium concentration in drinking and industrial water. The reasons that hardness reduction in drinking water is applied are [De Moel et al. (2007)]:

- For the protection of public health: By reducing the calcium concentration the pH of the distributed water is higher and the dissolution of copper and lead from the distribution system is reduced.
- For the protection of the environment: Due to softening, the content of heavy metals in the sludge of wastewater treatment plants is decreased since less lead and copper is dissolved in the water from the distribution system. Also, with softer water, less detergent dosing for washing is required reducing the concentration of phosphate in wastewater and therefore preventing eutrophication in surface water.
- For economy: When softening is applied scaling in heating equipment and appliances is avoided and they use less energy. Also, the amount of detergents that is used for washing is reduced.
- For increasing user's comfort: Softened water has a better taste and it is not damaging or staining the clothes during washing.

Waternet is using fluidized bed pellet softening reactors in the Weesperkarspel water treatment plant to reduce the calcium content of the drinking water that it is produced. Waternet played a vital role in the development and introduction of the pellet softening in a fluidized bed reactor [Graveland et al. (1983), Van Dijk and Wilms (1991), Kramer et al. (2015)]. In Figure 2, a pellet softening fluidized bed reactor is shown.

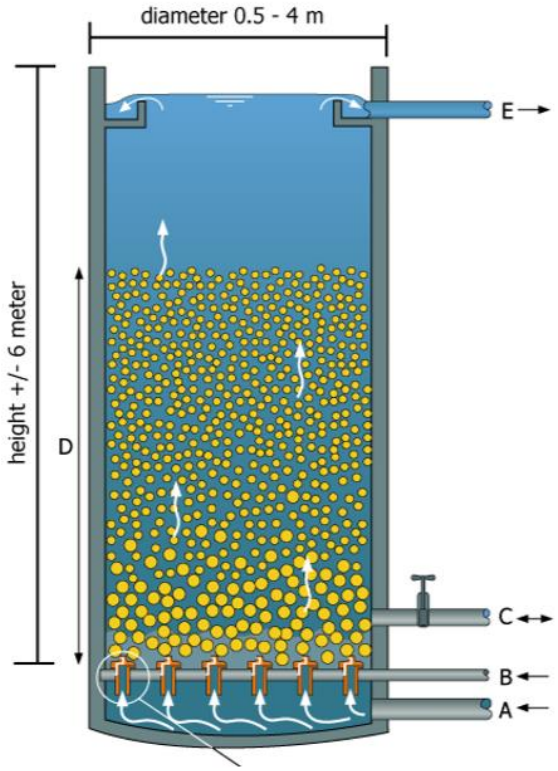

Figure 2 Pellet softening fluidized bed reactor [Rietveld (2015)]

During the pellet softening process the water is pumped in an upward direction in a cylindrical vessel partially filled with seeding material. As a result, the seeding material bed is in a fluidized condition. Alkaline chemicals are added at the bottom of the reactor increasing the pH of the solution. Therefore, the solubility product of calcium carbonate is exceeded and calcium carbonate crystallization takes place on the surface of seeding material [Van Dijk and Wilms (1991)].

The pellet softening process is depending on the chemical dose as well as, the flow and hydraulic conditions inside the reactor. Therefore, the pellet softening process can be divided in a chemical and physical part. In the following sections, the most important concepts and parameters of the chemical, physical and reactor part of the pellet softening process are described.

2.3. Chemical part of a pellet softening fluidized bed reactor

For the determination of the chemical behavior of natural water inside a pellet softening fluidized bed reactor, it is important to determine basic concepts of aquatic chemistry and crystallization theory. In particular, in this section, the reaction of calcium carbonate formation is presented and the most important factors that affect the crystallization of calcium carbonate are underlined. Especially, the effect of inhibitors such as organic carbon is analyzed according to existing literature.

2.3.1. Aquatic chemistry

Aquatic chemistry is the study of chemical interactions in the aqueous phase. Water can be a solvent or a chemical compound. In particular, aquatic chemistry deals with the species distribution in aqueous solutions as well as chemical reactions and interactions with solid and gas phases.

To describe the chemical reactions that take place in a solution, the reactions' chemical constantσ are necessary. The chemical equilibrium constant is the measure of the extent that the reactants are converted to products. For example in the reaction of equation (1)

$$A + B \leftrightarrow AB \quad (1)$$

The chemical equilibrium constant for this reaction is described by equation (2)

$$K_{eq} = \frac{[AB]}{[A][B]} \quad (2)$$

Where [A], [B] are the activities of the reactants and [AB] is the activity of the product. Alternatively, the equilibrium solubility product can be calculated. The equilibrium solubility product is the product of the concentrations of the reactants in equilibrium (equation (3))

$$K_{sp} = [A]_{eq}[B]_{eq} \quad (3)$$

Using the chemical equilibrium constants of all the compounds, the distribution of species in a solution can be determined. It is also possible to calculate saturation index [equation (4)] in order to define if a solution is saturated, supersaturated or undersaturated in respect to a mineral:

$$SI = Log_{10}(\frac{IAP}{K_{sp}}) \quad (4)$$

Where IAP is the ion activity product of the reactants and Ksp is the solubility product. If SI =0 then equilibrium is reached while if SI>0 the solution is supersaturated or if SI<0 the solution is undersaturated in respect to the particular mineral. Alternatively, the saturation ratio SR or Ω can be used to describe supersaturation (equation (5)):

$$SR\ or\ \Omega = \frac{IAP}{K_{sp}} = 10^{SI} \quad (5)$$

Another important concept of thermodynamic theory is Gibbs energy. The standard Gibbs free energy of a compound is the energy needed to form that compound from the elements in the standard state (for example the standard of oxygen is the O_2 molecule, for calcium the Ca-atom, for carbon the carbon-atom etc.) whose standard Gibbs free energies are all zero by definition [Faure (1998)].

The change in Gibbs free energy in a reaction $\Delta GR°$ is equal to the sum of the standard Gibbs free energy of all the products minus the sum of the standard Gibbs free energy of all the reactants as it shown in equation (6).

$$\Delta G^o = \Sigma niGfi^0(products) - \Sigma niGfi^0(reactants) \quad (6)$$

Where Gfi is the standard Gibbs free energy of a substance and ni is the amount of that substance. ΔG = 0 when the reactants and the products are in equilibrium. ΔG < 0 when there are too few products and too many reactants in the system. Therefore, when ΔG < 0 reactants will form a product and when ΔG > 0 products will form a reactant - on condition that a reverse reaction is possible [Faure (1998)].

Kinetics

The equilibrium constants can be used to determine the species distribution in a solution when equilibrium has been reached. In this case, the time needed for equilibrium to prevail has not been taken into account. However, it is often important to determine the time that is needed for a reaction to take place. As a result, obtaining information of the kinetics of the reaction is necessary. The rate of a reaction is the time that it takes for a quantity of reactants to transform to products. By determining the rate, it is therefore possible to determine the concentration of a water component in a solution, in time.

2.3.2. Crystallization theory

There are two main processes related to crystallization: nucleation and crystal growth. The driving force of crystallization is supersaturation. The level of supersaturation and the presence of seeding material is determining the type of crystallization that is going to take place since it is the driving force of crystallization. In order to define the supersaturation of the solution the chemical equilibrium model PHREEQC (pH-redox-equilibrium-calculations) was used. In the following paragraphs, the general theoretical concepts regarding crystallization and the main nucleation and crystal growth theories are summarized.

Classical nucleation theory and Non-classical nucleation theory

There are two main theories describing the nucleation process: the classical and non-classical nucleation theory. Based on the classical crystallization theory, the three possible mechanisms for the formation of crystals are [Lewis et al. (2015)]:

1. Primary homogeneous nucleation
2. Heterogeneous nucleation
3. Secondary nucleation

If the solution already contains crystals of the same compound that is being crystallized, then seeded or secondary crystallization takes place. In a solution without parent crystals, primary nucleation takes place. Primary nucleation can be homogeneous or heterogeneous.

Primary homogeneous nucleation is the formation of nuclei in a solution without small solid particles. In a supersaturated solution, single solute entities are attached or detached into clusters. These clusters can either grow and form a nucleus or fall apart. The formation of a nucleus depends on the Gibbs free energy of the cluster.

There are two competing terms that are defining the Gibbs free energy of the cluster. The addition of a compound entity is decreasing the free energy of the cluster. On the other hand, the additional cluster surface that is created when an entity is added is increasing it. The increase in the Gibbs free energy is depending on the interfacial free energy which is the difference between a surface molecule and its ionic compounds in the solution [De Yoreo and Vekilov (2003)]. When these clusters reach a critical size the Gibbs free energy is reaching a maximum. If the radius of the cluster increases above this critical size, the nucleus will grow as each new entity that is attached to the cluster will only decrease the Gibbs free energy [Lewis et al. (2015)].

In primary heterogeneous nucleation, the nuclei formation takes place in the surface of a foreign substrate. The presence of a surface is decreasing the interfacial free energy of the cluster, therefore, enabling the formation of stable nuclei. In practice, homogeneous nucleation rarely takes place as it is difficult to obtain a solution free of dust particles. Usually, heterogeneous nucleation takes place at the surface of the small particles that are present in the solution. Only in the case that a very high supersaturation is reached heterogeneous nucleation is no longer favored compared to homogeneous nucleation and spontaneous nucleation may take place [Lewis et al. (2015)].

In addition to the classical nucleation theory described above, the non-classical nucleation theory is used to describe phenomena that do not follow the classical nucleation process. According to the non-classical nucleation, an intermediate metastable phase may proceed before the stable crystalline phase. The energy barrier between the intermediate metastable phase and the solution is lower than the energy barrier of the stable phase and the solution. Therefore, the intermediate phase is formed before it is finally crystallized to the stable phase. The intermediate could be a liquid or a solid phase [Lewis et al. (2015)].

Induction time and metastable zone

After a solution becomes supersaturated a certain period of time passes before a detectable amount of nuclei is formed. This time is called "induction time". The induction time varies, based on the supersaturation of the solution and the experimental conditions. For a defined induction time *t,* the metastability limit can be determined. The metastable limit is the maximum supersaturation that a solution can have in order to remain in the metastable zone for the particular induction time. The metastable limit of a solution depends on the temperature as well as the type of nucleation that takes place in the solution as it can be seen in Figure 3 [Lewis et al. (2015)].

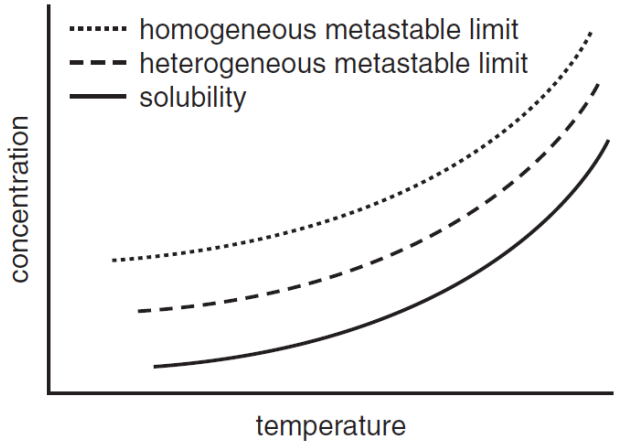

Figure 3 Metastable limit for homogeneous and heterogeneous nucleation [Lewis et al. (2015)]

If the concentration of the solute is above the metastable limit then the solution is oversaturated and nucleation starts to take place. If the concentration of the solute is lower than the solubility limit the solution is undersaturated. In this area no crystallization takes place and the clusters of the solute are not stable and tend to decay. Between the metastable limit and the solubility line lies the metastable zone. If the solution is in this zone a certain induction time should elapse before the start of crystallization. It can be clearly seen from the (Figure 3) that the metastable area for heterogeneous nucleation is smaller than the metastable area for homogeneous nucleation. Therefore, the presence of foreign-surfaces for crystallization can cause the start of nuclei formation in a solution that otherwise would be in the metastable area for homogeneous nucleation. The determination of the induction time is important as it can be used to define the moment that the crystallization of a compound starts. As a result, it is a significant parameter for the determination of the crystallization rate of a certain compound [Lewis et al. (2015)].

Crystal growth

Crystal growth is the crystallization of a compound to a parent crystal of the same material as the one that is being crystallized [Lewis et al. (2015)]. According to Jones (2002), the crystal growth process consists of two steps, the mass transport to the crystal surface and the integration step.

Based on Dhanaraj et al. (2010) the factors that have the most significant effect on the crystal growth is

1. Supersaturation
2. The characteristics of the preparation procedure of the solution and solute-solvent interactions
3. Impurities that absorb to the surface of the crystal and modify the crystallization surface

The crystallization surface plays an important role in the crystal growth process. Based on the model by Kashchiev (2008) the surface of the crystals consists of steps and terraces. The growth of the crystal mainly takes place at the kinks of the steps (Figure 4).

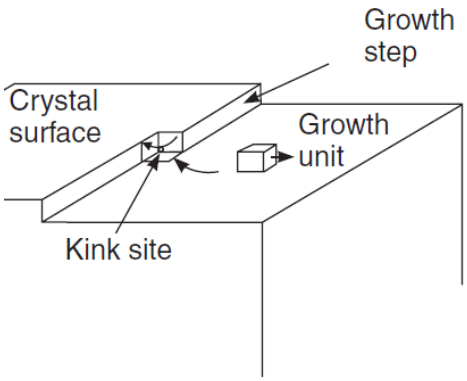

Figure 4 Crystal growth due to attachment and integration of a compound to a kink site [From Lewis et al. (2015)]

The level of the driving force is defining the smoothness of the growth. Based Lewis et al. (2015) when the driving force is moderate to low, smooth surfaces are formed during crystallization while in the case of a high driving force rough surfaces are created. The rate of crystallization is largely affected by the crystallization surface. The presence of impurities can also modify the ability of the crystallized compound to attach to the crystallization surface and integrate to the parent crystal lattice.

2.3.3. Calcium carbonate crystallization reaction

Calcium carbonate is one of the most studied minerals. The crystallization of calcium carbonate has been investigated in studies from different scientific fields, as it is involved in geological, chemical and biological processes. The following chemical equation [equation (7)] shows the calcium carbonate crystallization reaction:

$$Ca^{2+} + CO_3^{2-} \rightleftharpoons CaCO_{3(s)} \quad (7)$$

The solubility product (K_{sp}) of the calcium carbonate formation reaction is [equation (8)]:

$$K_{sp} = [Ca^{2+}][CO_3^{2-}] \quad (8)$$

The rate of calcium carbonate crystallization is depending on the distribution of the carbonate species in the water. As shown above, the higher the concentration of the carbonate species the higher the concentration of the calcium carbonate that crystallizes. The reaction equation of the carbonic species is shown below [equation (9) and equation (10)]

$$H_2CO_{3\,(aq)} \rightleftharpoons H^+ + HCO_3^- \quad (9)$$

$$OH^- + HCO_3^- \rightleftharpoons H_2O + CO_3^{2-} \quad (10)$$

The concentration of the carbonic species in the solution depends on the experimental conditions such as concentration and pH. In the graph of Figure 5, the distribution of the inorganic carbonate species based on pH is shown.

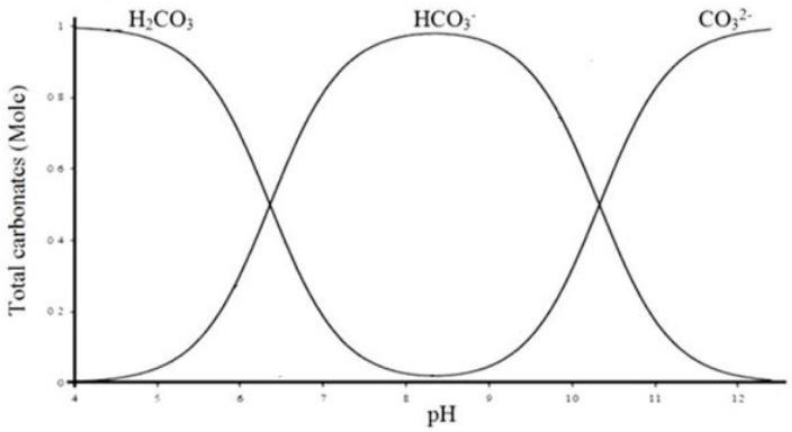

Figure 5 Distribution of carbonate species as a fraction of total dissolved carbonate with pH [Lindsay (1979)]

From Figure 5, it can be clearly seen that the higher the pH, the higher is the percentage of the total inorganic carbonates that is in the carbonate (CO_3^{2-}) form. Therefore, by increasing the pH the calcium carbonate crystallization also increases. In a pellet reactor caustic soda (NaOH) is added in order to increase the pH to 9-10 [equation (11)].

$$NaOH \rightleftharpoons Na^+ + OH^- \tag{11}$$

As a result, the bicarbonate (HCO_3^-) is transformed to carbonate species (CO_3^{2-}) [equation (4)]. Due to the increased concentration of the carbonate species (CO_3^{2-}), the calcium carbonate crystallizes in the surface of the pellets.

It is also important to determine the concentration of the different calcium species that are present in the solution. In Wiechers research the following calcium species have been considered in the speciation calculations: $Ca^{2+}, CaCO_3^0$ and $CaHCO_3^+$. In this research, the presence of $CaOH^+$is also included in the calculations. Based on the calcium species distribution, the calcium carbonate crystallization potential (CCCP) can be calculated. CCCP is the difference between the calcium concentration in the solution and the calcium concentration when the solution has been reached equilibrium and the SI of calcite is 0

There are several polymorphs of calcium carbonate that can be created under different conditions. According to Brečević and Kralj (2007), there are three hydrated forms of calcium carbonate and three anhydrous polymorphs. The hydrate forms of calcium carbonate are calcium carbonate amorphous (ACC), calcium carbonate hexahydrate (HCC), calcium carbonate monohydrate (MCC). The anhydrous polymorphs of calcium carbonate are aragonite, vaterite and calcite. The most thermodynamically stable polymorph of calcium carbonate is calcite. According to Oswald law of Stages [Ostwald (1897)], the least stable form of calcium carbonate is formed first since it has the lowest solubility. After a short period of time, it is transformed to calcite which is the most stable state of calcium carbonate. The saturation indices of the anhydrous polymorphs of calcium carbonate in the water during the pellet softening process are calculated using PHREEQC in order to investigate the formation of these polymorphs under the conditions inside a pellet reactor.

2.3.4. Nucleation and crystal growth of calcium carbonate

There are several theories about the mechanism of calcium carbonate crystallization. The mechanism of crystallization is largely depending on the level of the supersaturation, the presence of the seeding material and the morphology of the surface in which calcium carbonate crystallizes. In this part, the nucleation process for calcium carbonate as well as the growth of calcium carbonate crystals is presented.

In the classical nucleation theory, a cluster of calcium carbonate entities of critical size is considered to be the first step of the crystallization process. If the cluster exceeds its critical size it grows into a stable nucleus otherwise it decays. The nuclei grow into stable calcium carbonate particles.

According to the non-classical nucleation theory, the formation of stable pre-clusters proceeds the creation of a stable nucleus. Gebauer et al. (2008) suggest that the aggregation of these pre-clusters results in the formation of a nucleus that is later transformed into crystal particle. In the following figure, the new nucleation theory proposed by Gebauer et al. (2008) is shown, compared to the classical nucleation theory.

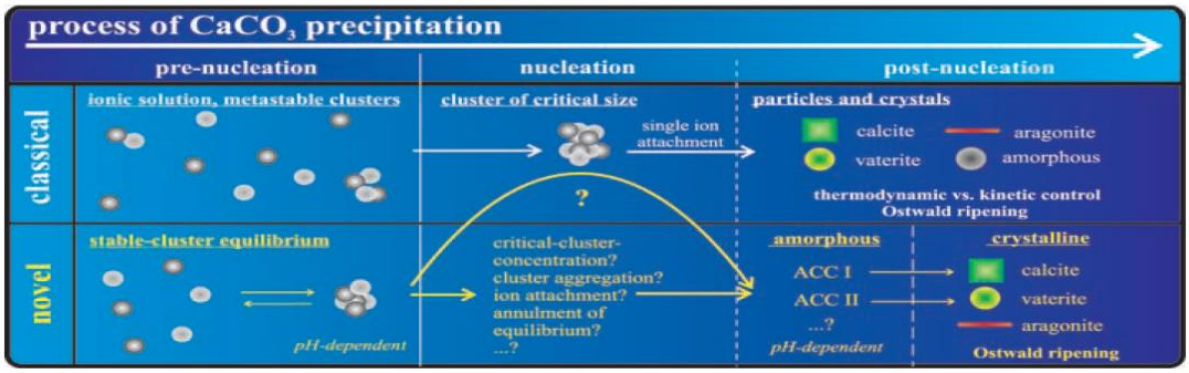

Figure 6 Classical and novel nucleation theory of calcium carbonate [From Gebauer et al. (2008)]

The pre-nucleation clusters in the solution contribute to the growth of the calcium carbonate crystals due to the lower energy barrier that needs to be overcome for the formation of solid $CaCO_{3(s)}$ (figure 5).

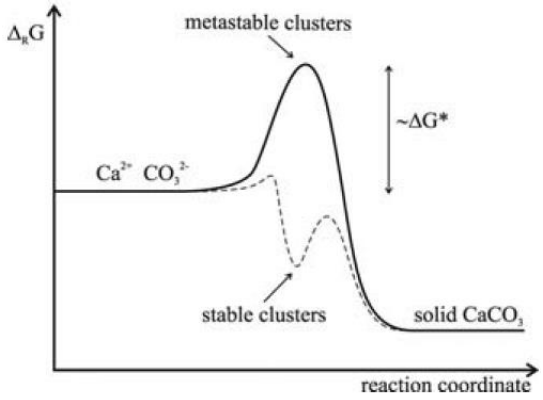

Figure 7 Energy barrier for nucleation if stable pre-nucleation clusters or metastable clusters are formed [From Gebauer et al. (2008)]

According to Lewis et al. 2015 during the earliest stages of calcium carbonate crystallization pre-nucleation clusters of ACC are formed. After a certain period of time, an aggregation of amorphous calcium carbonate clusters in the surface of the template (for example organic template) takes place. In these clusters oriented crystals of calcite and vaterite grow.

In the presence of seeding material, secondary nucleation and crystal growth takes place. The crystal growth of calcium carbonate on a seeding material can be divided into two steps:

- the mass transfer of the crystallizing compounds to the surface of the seeding material and
- the integration of calcium carbonate to the crystal of the seeding material.

The slowest step is the one that is defining the rate of calcium carbonate crystallization. In the following figure, the concentration profile in the surface of the parent crystal is shown.

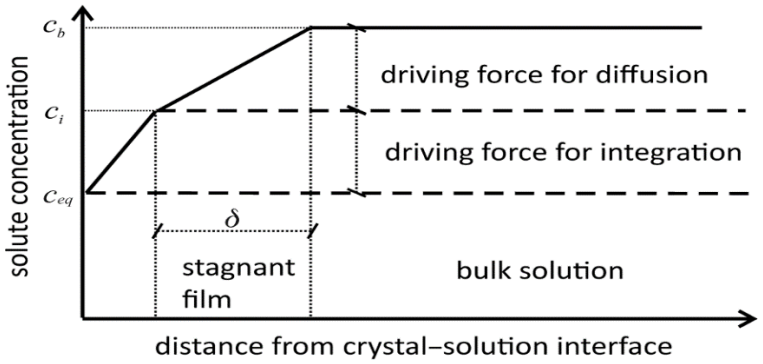

Figure 8 Concentration profile perpendicular to the crystal surface [From Lewis et al. (2015)]

The rate of calcium carbonate crystallization is therefore either limited by the diffusion of the solute to the surface of the seeding material or the reaction of crystallization. In this research, the importance of diffusion on calcium carbonate crystal growth is going to be investigated.

As mentioned in §2.3.2 the crystal growth takes place in the kinks of the steps at the crystal surface. The growth of calcite crystals can be described with the kink-step-terrace theory. According to Nielsen et al. (2013), the calcium carbonate ions incorporation to the growth sites (kinks) in the surface of the calcium carbonate crystal govern the crystallization kinetics. Also, Reddy (2012) claimed that the incorporation of the calcium ion at the growth site of the parent crystal is the rate-limiting step.

The presence of impurities affects the growth of calcium carbonate crystals. The hampering of a crystallization rate is caused mainly due to a higher energy barrier that needs to be overcome in order the crystallization to proceed when inhibitors are absorbed in the surface of the parent crystal (altering the crystallization surface, competing against crystallization compounds or not allowing integration to the crystal lattice [Nielsen et al. (2013)]. The influence of inhibitors in the reaction of calcium carbonate crystallization is analyzed in the following section.

2.3.5. Effect of impurities on crystallization rate of calcium carbonate

The presence of impurities in the solution even at relatively low concentrations can have a significant effect on the crystallization process. Usually, the impurities do not directly affect the supersaturation of the solution but alter the conditions at the crystallization surface. The impurities or additives can either inhibit crystallization or act as a template for nucleation [Lewis et al. (2015)]. In this section the compounds that can act as inhibitors are determined. Their concentration in Weesperkarspel raw water is compared with the minimum concentration that is having an inhibiting effect on calcium carbonate crystallization based on literature.

According to Lewis et al. (2015), there are several substances that can inhibit crystallization. In particular, small organic molecules can adsorb or be incorporated in the crystal lattice and compete with the growth entities. As a result, the rate of crystallization can be remarkably decreased. The extent of the influence of these compounds depends on the type of the inhibitor and the crystal phase. Large organic molecules, on the other hand, can inhibit crystallization due to the adsorption of the compound in the surface of the crystal, therefore creating an inhibiting layer between the crystal lattice and the growth units. Therefore, the growth steps that follow the attachment to the crystal phase no longer take place [Lewis et al. (2015)].

Several researchers have tried to determine the effect of inhibitors on calcium carbonate crystallization rate. Lebron and Suarez (1996) suggest that the crystallization rate of calcium carbonate decreases with an increasing dissolved organic carbon (DOC) content under atmospheric CO_2 partial pressure. According to Lebron and Suarez (1996), the crystallization of calcium carbonate was completely inhibited when the concentration of dissolved organic carbon (DOC) is around 0.1mM and the saturation ratio (SR or Ω) is 1.9. Inskeep and Bloom (1986) have also investigated the effect of DOC in calcium carbonate seeded

crystallization. Based on their results, the crystallization of calcium carbonate is inhibited when a concentration of 0.15mM of DOC is added to the solution and the saturation ratio is Ω= 8-9. Organic carbon is adsorbing to the surface of the crystal and creates a coating on the surface of the seeding material. Consequently, the crystallization of calcium carbonate in the surface of the crystal is significantly reduced. Hamer (2017) has proved that the inhibiting effect of the humic acid depends on the initial supersaturation of the solution. The higher the supersaturation of the solution the lower the effect of the concentration of humic acids on calcium carbonate crystallization.

Reddy (2012) has demonstrated that in particular fulvic and humic acid, as well as magnesium components in the water, inhibit the crystallization of calcium carbonate. Based on the research of Reddy (2012) humic acid is twice as effective inhibitor as fulvic acid. Also, in this research, the combined effect of Mg and fulvic acid was studied. According to the results, the combined effect of the two inhibitors causes a higher reduction in the crystallization of calcium carbonate than each of the inhibitors individually. The magnesium ions inhibit the crystallization of calcium carbonate due to the substitution of calcium in the growth sites of the crystal lattice. On the other hand, in the presence of fulvic acid, it is the binding of the carboxylate groups in the surface of seeding crystals that is responsible for inhibiting the crystallization of calcium carbonate, as the calcium and carbonate ions cannot approach the crystallization surface. It must be noted that in the research of Reddy (2012) the supersaturation of the solution that is used is much lower (approximately Ω=4.5) than in the experiments of this research.

Astilleros et al. (2010) and Zhang and Dawe (2000) have also conducted seeded crystallization experiments of calcium carbonate in a solution with magnesium ions (Mg^{2+}). Zhang and Dawe (2000) support that the mechanism of magnesium inhibition is the blocking of the active kinks that the calcium carbonate crystallization takes place. Another mechanism of inhibition that has been reported, is the substitution of the calcium ions by magnesium in the crystal lattice, forming a more soluble solid and consequently reducing the amount of calcium carbonate that crystallizes. On the other hand, Astilleros et al. (2010) suggest that the presence of the magnesium ions in the solution change the microtopography of the surface of the parent crystal causing an inhibition of the calcite formation. In the research of Astilleros et al. (2010) the concentration of magnesium ions that was used was 0.05-4mM and the calcite saturation ratio of the solution Ω=5 while Zhang and Dawe (2000) used a solution with magnesium ions ranging between 1-27 mM and calcite saturation ratio ranging between Ω=5.3 and Ω=6.6. A total inhibition of calcium carbonate crystallization was not observed. However, when the concentration of magnesium increases above 25 mM only a small amount of calcium carbonate crystallizes. It is, therefore, necessary to decrease the concentration of magnesium below 25mM in the water in order to increase the calcium carbonate crystallization rate.

Flaathen et al. (2011) have investigated the effect of dissolved sulfate species in the calcite kinetics. A concentration of 20mM of sulfate in the solution seems to inhibit the crystallization of calcium carbonate by a factor of 2 when calcite crystals are used as a seeding material and with a constant saturation ratio Ω of 2.6. Lin and Singer (2006) on the other hand, focused on the influence of orthophosphates. In this research, it is suggested that phosphate species adsorb to the surface of the parent crystal and block the crystal growth sites. There seems to be a great reduction of calcium carbonate crystallization when the total phosphorus concentration is ranging between 4-5μM was and the saturation ratio is approximately Ω= 5.3.

Herzog et al. (1989), Taksaki et al. (1994) and Parsiegla and Katz (1999, 2000) has investigated the influence of cations such as Fe(II), Fe(III) and Cu(II) on calcium carbonate crystallization. According to their results, 1μM of ferric ions can completely inhibit the crystallization of calcium carbonate in a solution with calcite saturation ratio of 4. Adding 0.1 -1μM of copper [Cu (II)] can also have a significant effect. However, the influence of copper [Cu (II)] is largely depending on supersaturation [Parsiegla and Katz (1999)].

In Table 1, the concentrations of the compounds in the Weesperkarspel (WPK) influent water that can cause a reduction of calcium carbonate crystallization rate are shown. Also, the concentrations above which these compounds affect the crystallization process are shown.

Table 1 Concentration limits of inhibitors that influence the calcium carbonate crystallization process [modified from Hamer (2016)]

Inhibitor	Reference	Limit	Raw Water WPK	Saturation ratio (Ω)
		mM	mM	(-)
Mg^{2+}	Astilleros et al. (2010), Nielsen et al. (2013), Reddy (2012), Zhang and Dawe (2000)	0.25	0.27	5-6.6
SO_4^{2-}	Flaathen et al. (2011)	20	0.07	2.9
PO_4^{3-}	Lin and Singer (2006)	0.001	<0.001	5.3
Fe^{2+}	Herzog et al. (1989)	0.1	-	25
Fe^{3+}	Takasaki et al. (1994)	0.001-0.005	-	4
Cu^{2+}	Parsiegla and Katz (1999,2000)	0.1-1	-	2.5-10
DOC	Lebron and Suarez (1996), Inskeep and Bloom (1986), Reddy (2012), Hsu and Singer (2009), Grefte (2013), Liu et al. (2005)	0.1*	0.55 Total Organic Carbon (TOC)	1-9

*complete inhibition at 0.3

It can be clearly seen from Table 1, that in WPK influent natural water the compounds that most likely inhibit the crystallization of calcium carbonate are, magnesium ions and organic carbon. According to Reddy (2012), the combined effect of magnesium and organic carbon can have an even more profound effect on calcium carbonate crystallization.

It must be noted though, that the effect of an inhibitor on crystallization largely depends on the supersaturation of the solution. In these studies, the saturation ratio of calcium carbonate of the solution that was used to determine the inhibition of calcium carbonate kinetics is much lower than the saturation ratio inside a pellet softening fluidized bed reactor. Based on literature, it is expected that higher concentrations of inhibitors need to be present in order to have an important effect in crystallization when the saturation of calcium carbonate in the solution is higher.

2.3.6. Effect of natural organic carbon on calcium carbonate crystallization in the softening process

The effect of Natural Organic Matter (NOM) to calcium carbonate crystallization during the softening process has been studied by various researchers [Hsu and Singer (2009), Grefte (2013), Liu et al. (2005)]. In the study of Liu et al. (2005), the hardness removal during the softening process was investigated using different concentrations of fulvic acid ranging from 0 to 5 mg/L. Based on the results of this research, the inhibiting effect of the fulvic acid is depending on the total carbon to calcium ratio (Ct/Ca) and the type of fulvic acid compounds that were present. Three types of fulvic acid with different molecular weight were used in the experiments of this research. The compound with the highest molecular weight (MW) (approximately MW=1360 g/mol) almost fully inhibited calcium carbonate crystallization for a Ct/Ca=1 while the fulvic acid with a lower MW decreased the calcium removal 20%. Therefore, the highest degree of inhibition was observed from the NOM with the highest molecular weight and aromatic carbon content. At the Weesperkarspel water treatment plant, the Ct/Ca ratio is approximately 1.8. As a result, it is possible that the NOC in the influent water can affect significantly the calcium carbonate crystallization in the pellet softening process especially if compounds with high molecular weight such as humic acid are present.

Hsu and Singer (2009) have also studied the effect of NOM in lime precipitation softening process. In particular concentrations of 0, 1.5 and 8.3 mg/L of NOM were tested. In order to increase the NOM

content, fulvic acid was added to the water and the inhibition of the crystallization of calcium carbonate during the precipitation softening process due to the presence of organic carbon was observed. For the same dose of lime, approximately 25% less calcium concentration was removed from the water during the softening process, when the concentration of the NOM in the solution was 8.3 mg/L compared to a content of DOC of 0 or 1.5 mg/L. It can, therefore, be concluded that a high concentration of NOM close to 8mg/L can cause a serious decrease in the performance of the softening treatment step.

Furthermore, Magnetic Anion exchange was used in this research to reduce the carbon content in order to improve the softening process. A MIEX resin is a strong-base anion exchange resin that contains iron oxides integrated in a porous matrix. The resin has magnetic characteristics to facilitate settling. Due to the high surface to volume ratio of the resins a high rate of exchange and low resin fouling is observed. The resins were inserted in a slurry reactor before treatment and recovered in a settling tank. Using the MIEX resins the concentration of carbon in the water decreased from 7.7 mg/L to 2.6 mg/L. It was observed that in the water that was treated with anion exchange, the performance of the softening process was improved since the residual calcium concentration was decreased 1 to 5% using a lower dose of lime <100 mg/L. Therefore, IEX can be an effective process to remove the DOC in the water to improve the softening process.

2.4. Physical part of a pellet softening fluidized bed reactor

The physical part of a pellet softening fluidized bed reactor consists mainly of the fluidized bed. In this section, the main physical parameters of the water such as velocity and viscosity are explained as well as the basic characteristics of a fluidized bed. The characteristics of the fluidized bed play an important role in the pellet softening process.

Characteristics of the fluidized bed

The seeding material used at Weesperkarspel WTP consists of crushed calcite and calcite pellets with a diameter ranging between 0.5 and 1.1 mm. Due to the crystallization of calcium carbonate in the surface of the pellets during the pellet softening process, the diameter of the pellets increases. As a result, the larger pellets become heavier and remain in the bottom of the reactor while the pellets with that smaller diameters stay at the top of the reactor. The pellets remain inside the reactor for a specific residence time. Afterward, a number of pellets from the bottom of the reactor is discharged and new seeding material with a smaller diameter is added. The residence time of the pellets is chosen based on experience with the fluidized bed and hydraulic models like the model presented in §2.7. As a result, a steady diameter profile is reached over the height of the reactor that does not change significantly in time.

Based on the diameter of the pellets, the porosity in each part of the reactor is determined using the [equation (12)]:

$$p = \frac{V_v}{V} = \frac{V - V_p}{V} \tag{12}$$

Where $V_v$the volume of is void, V_p the volume of pellets and V is the volume of the reactor. The volume of pellets can be easily determined by measuring the weight of the pellets before they are added to the reactor. Assuming that the pellets consist of pure calcite, the volume of the pellets can be determined by dividing this weight with the specific weight of calcite 2.71 g/cm^3 [Mineral data publishing, (2001-2005)]. It must be noted though, that the density of calcite may deviate slightly in reality from the value found in literature. However, it is considered accurate enough for this research.

The specific surface area (SSA) of the seeding material is an important parameter for the softening process as it influences significantly the calcium carbonate kinetics. Based on the porosity and assuming perfect round pellets the SSA is determined using the equation (13) of Van Schagen et al. (2008) was used for the :

$$S_r = \frac{6(1-p)}{d_p} \quad (13)$$

Where S_r is the SSA in $m^2/(m^3$ of reactor), p is the porosity and d_p is the diameter of the pellets. In order to be able to compare the SSA in a pellet reactor with the surface area in other types of reactors or under different fluidization conditions the specific surface area per volume of water is calculated [equation (14)]:

$$S = \frac{S_r}{p} = \frac{6(1-p)}{d_p * p} \quad (14)$$

Where S in $m^2/(m^3$ of water), S_r is the SSA in $m^2/(m^3$ of reactor), p is the porosity and d_p is the diameter of the pellets.

Velocity of water in a pellet softening reactor

The porosity and the specific surface area inside a pellet softening reactor depend on the upward velocity inside the reactor. The superficial velocity (v_s) of the water inside the reactor is ranging between 60 m/h and 100 m/h. The higher the superficial velocity the higher the fluidization of the bed. Since the reactor is filled up with seeding material the actual velocity between the pellets is v_s/p.

Viscosity

Another important parameter for the fluidization of the bed is the viscosity of the water. There are two types of viscosity, dynamic and kinematic viscosity. Dynamic viscosity is the resistance of a fluid to gradual deformation by shear or tensile stress. It can be calculated using the equation (15):

$$\eta = \frac{\tau}{\gamma} \quad (15)$$

Where η is the dynamic viscosity in $N*s/m^2$, τ is the shear stress in N/m^2 and γ is the stress rate in s^{-1}. Kinematic viscosity is a measure of the resistive flow of a fluid under the influence of gravity. The kinematic viscosity can be calculated by dividing the dynamic viscosity with the density of the fluid [equation (16)]

$$\nu = \frac{\eta}{\rho} \quad (16)$$

Where ν is the kinematic viscosity in $m^2\ s^{-1}$, η is the dynamic viscosity in $N*s/m^2$ and ρ is the density of the liquid in kg/m^3. The viscosity of the water is a temperature dependent parameter. The lower the temperature of the water the higher the resistance of the water to flow and therefore the higher the fluidization of the pellet bed.

2.5. Reactor theory and flow conditions in a pellet softening fluidized bed reactor

According to Van Schagen et al. (2008 b,c) the flow conditions inside a pellet softening fluidized bed reactor affect the rate of calcium carbonate crystallization. Therefore, it is important to determine the type of reactor that is used during the softening process. In this research two types of reactors were used during the experiments to determine the rate under different flow conditions. In this section, the most common ideal reactors are explained and compared with the reactors that were used during the experiments as well as a pellet softening fluidized bed reactor.

The most common types of ideal reactors are batch, CSTR and PFR reactor:

- A batch rector consists of a tank and a stirrer. The reactor is discontinuous. It is filled with the reactants, the reaction starts and it is emptied after the reaction is completed. A batch reactor has a constant volume of reactant and homogeneous composition.

- A continuous stirred tank reactor (CSTR) consists of a stirrer and a tank that also has an inlet and outlet. As a result, a continuous flow in and out of the reactor is allowed. It is considered that inside the reactor the conditions are homogenous.

- A plug flow reactor (PFR) is a continuous tubular reactor, where the reactants flow steadily through the pipe or column. The composition of the reactants do not vary radially within the reactor but form a concentration profile along the height or length of the reactor [(Mazzotti (2015)]. The main assumption made in the design of the PFR is, that each differential volume inside the reactor behaves like a batch reactor as it moves through a pipe. As a result, the concentration profile along the length of a PFR looks much like the concentration profile in a batch reactor over time.

During this research two types of experiments took place. The flow conditions during these experiments deviate from the ideal conditions. Firstly, the calcium carbonate crystallization was measured in a stirred tank that was operated discontinuously. The reactants were inserted in the reactor and there was no flow in or out of the tank. However, in contrast with a batch reactor, the conditions inside this experimental reactor were not homogeneous since it was difficult to keep the calcite pellets that were used in a seeding material in suspension. Therefore, the reactor used in these experiments is considered to be a stirred tank reactor STR operated in a batch mode (discontinuously). Secondly, a column was used to measure the calcium carbonate crystallization in a fluidized bed of seeding material. The conditions inside the reactor approached a plug flow reactor. However, in the inlet of the water radial flow of water was observed. Also, the presence of a fluidized bed of pellets caused a deviation from plug flow conditions inside the column. As a result, the experimental column cannot be considered an ideal plug flow reactor. Overall, it is considered that while the flow conditions during the experiments were not ideal, the reactors used in the STR batch and PFR fluidized bed experiments approach sufficiently well a batch and plug flow reactor respectively.

A pellet softening fluidized bed reactor is assumed to be similar to a PFR reactor. Therefore, the concentration of calcium does not change radially but over the height of the reactor. The fluidized bed is separated into layers that act as a series of batch reactors. In each layer, homogeneous conditions are assumed (§2.8.). However, in reality, a pellet softening fluidized bed reactor deviates significantly from an ideal PFR. Due to the mixing of the caustic soda at the bottom of the reactor, changes in pH and calcium take place radially within the reactor. As a result, the flow in the bottom of the reactor is more similar to a CSTR than a PFR. In contrast, on the top of the reactor, the flow conditions approach more a plug flow reactor.

According to crystallization theory, there are two possible factors that may be limiting and therefore defining the rate of calcium carbonate crystallization, the rate of mass transfer of the reactants and the reaction kinetics (§2.3.2). The flow conditions inside the reactor play a significant role in the mass transfer of reactants to the crystallization surface. In particular, the mass transfer of reactants is depending on the diffusion of ions, to the crystallization surface. Molecular diffusion is the flow of solute molecules from a region of higher concentration to a region of lower concentration solely due to the kinetic energy of the molecules in the solution. In the case of calcium carbonate crystallization, the concentration gradient between the high concentration of the reactants in the solution and the low concentration in the surface of the pellets (since they have been transformed to calcium carbonate) is causing the diffusion of the ions to the crystallization surface.

Van Schagen et al. (2008 b,c) has used a diffusion coefficient to take into account the difference between the rate of crystallization in a batch reactor and a plug flow reactor (§2.6.2). On the other hand, various

studies such as Wiechers, Nancollas and Reddy (1971) claimed that diffusion is not affecting the calcium carbonate kinetics. In this research, the role of diffusion on calcium carbonate crystallization and the way the mass transfer is affected by different flow conditions inside a softening reactor was investigated.

2.6. Modeling of the chemical part of a pellet softening fluidized bed reactor

For the modeling of the chemical part of a pellet softening fluidized bed reactor two important components are necessary:

- A chemical equilibrium model to determine the concentration of the water components in equilibrium. In this case, the water quality in a specific moment in time is defined.
- A model that describes the kinetics of calcium carbonate crystallization. The model is used to predict the calcium reduction in time.

In this section, the chemical equilibrium model used in this research, as well as the models of calcium carbonate crystallization kinetics available in literature, are described. The kinetic models that are chosen in this research to predict the calcium reduction in a pellet softening fluidized bed reactor are also shown.

2.6.1. Chemical equilibrium model-PHREEQC

The processes related to crystallization such as nucleation and crystal growth take place in supersaturated solutions. Supersaturation is the driving force of crystallization. In order to define the supersaturation of the solution that the chemical equilibrium model PHREEQC (pH redox equilibrium calculations) was used. PHREEQC is a speciation model that can be used to define the distribution of species as well as the saturation indices, density and electrical conductivity in an aquatic solution. Also, the interaction of the solution with solids and gas can be simulated. In this research, PHREEQC coupled with Excel developed by De Moel et al. (2012) is used. As a result, the calculations for the modeling and the presentation of the output is facilitated and improved. PHREEQC is used to define the equilibrium and species distribution of calcium and carbonic species in the solution. For the speciation calculations, the solubility constants of Stimela database (De Moel et al. 2012) were used based on the PHREEQC database (USGS, 2017). Based on the calculations of the calcium species distribution, the calcium carbonate crystallization potential (CCCP) is calculated.

2.6.2. Models of calcium carbonate crystallization rate

The crystallization of calcium carbonate is a widely studied reaction. Many researchers such as Tai et al. (1999), Tai and Hsu (2001), Nancollas and Reddy (1971), Wiechers et al. (1975) has developed a model that macroscopically describes the crystallization process of calcium carbonate in combination with hydraulic parameters. In each of these researches different hydraulic and chemical conditions were applied during the experiments. The model that best describes the calcium carbonate crystallization kinetics in each case, depends on the conditions that the crystallization takes place. In particular, the rate of crystallization depends on the water quality, the presence of inhibitors, the presence of seeding material, the temperature and the calcium and carbonate concentration in the water. In the following table, the most important models of calcium carbonate crystallization for this research are shown. The models presented in this paragraph are separated into two main categories:

- Models derived from experiments using synthetic water (artificial hard water).
- Models derived from experiments using natural water.

Exp. Cond.	Research	Model	Eq.	Parameters
Artificial hard water	Reddy and Nancollas (1971)	$-\frac{\mathrm{dCa}}{\mathrm{dt}} = \mathrm{k_G} * \mathrm{C} * (\mathrm{m_{Ca^{2+}} m_{CO_3^{2-}}} - \frac{\mathrm{K_{sp}}}{\mathrm{f_2^2}})$	(17)	dCa/dt is the rate of total calcium concentration reduction (mol L^{-1} s^{-1}) k_G is a kinetic constant (L mol^{-1} s^{-1} L mg^{-1}), C is the concentration of the seeding material in mg/L $m_{Ca^{+2}}$, $m_{CO_3^{2+}}$ are the concentrations of the calcium and carbonate ions respectively in mol L^{-1}, K_{SP} is the solubility product and f_2 is the calcium activity coefficient.
	Wiechers et al. (1975)	$-\frac{\mathrm{dCa}}{\mathrm{dt}} = \mathrm{k_{w,T}} * \mathrm{C} * [(\mathrm{Ca^{2+}})(\mathrm{CO_3^{2-}}) - \mathrm{K_{sp}}]$ Where $k_{W,T} = 0.0255 * 1{,}053^{(T-20)}$	(18)	dCa/dt is the rate of total calcium concentration reduction (mol L^{-1} s^{-1}) $k_{w,T}$ is a temperature dependent constant (L mol^{-1} s^{-1} L mg^{-1}) C is the concentration of the seeding material in mg/L, T is the temperature in ^{0}C, (Ca^{2+}) and (CO_3^{2+}) are the activities of calcium and carbonate ions in mol L^{-1}, K_{SP} is the solubility product and f_2 is the calcium activity coefficient.
Natural hard water	Van Dijk and Wilms (1991)	$-\frac{\mathrm{dCa}}{\mathrm{dt}} = \mathrm{k_{W,T}} * \mathrm{S} * [(\mathrm{Ca^{2+}})(\mathrm{CO_3^{2-}}) - \mathrm{K_{sp}}]$	(20)	dCa/dt is the rate of total calcium concentration reduction (mol L^{-1} s^{-1}) $k_{W,T}$ is the temperature dependent constant of Wiechers (L mol^{-1} s^{-1} m), S is the specific surface area in (m^2/m^3),(Ca^{2+}) and (CO_3^{2+}) are the activities of calcium and carbonate ions in mol L^{-1}, K_{SP} is the solubility product and f_2 is the calcium activity coefficient.
	Van Schagen et al. (2008 b,c)	$-\frac{dCa}{dt} = \frac{k_{W,T} * k_f}{kw_{,T} + k_f} * S * [(\mathrm{Ca^{2+}})(\mathrm{CO_3^{2-}}) - \mathrm{K_{sp}}]$	(21)	dCa/dt is the rate of total calcium concentration reduction (mol L^{-1} s^{-1}) $k_{W,T}$ is a temperature dependent constant (L mol^{-1} s^{-1}m) k_f is the transportation coefficient that is defined by the equation $k_f = \frac{S_h * D_f}{d_p}$, S is the specific surface area in (m^2/m^3),(Ca^{2+}) and (CO_3^{2+}) are the activities of calcium and carbonate ions in mol L^{-1}, K_{SP} is the solubility product and f_2 is the calcium activity coefficient.
	Tai and Hsu (2001):	$\frac{\mathrm{G}}{\mathrm{K_{d0}} * \mathrm{L^a}} + \left(\frac{\mathrm{G}}{\mathrm{K_{ro}} * \mathrm{L^b}}\right)^{\frac{1}{\mathrm{r}}} = \sigma$	(22)	G is the linear crystal growth rate (m/s), σ the overall supersaturation, L the crystal size (um), r the surface-reaction order, K_{do} and K_{ro} are the mass-transfer and surface-reaction coefficients. exponents a, b are derived from the experimental results
	Hu et al. (2017)	$G = K_g * L_o^m * SV^n * S_s^j$	(23)	G is the linear particle growth rate (m s^{-1}), K_g is the coefficient of linear growth rate, L_0 pellet size of seed (mm). S_s is supersaturation, SV is the superficial velocity (m/h) and m, n, j are exponents.
	Lasaga (1998)	$\mathrm{r_n} = \mp \mathrm{K_n} * \mathrm{S} * \left(1 - \Omega^{\Theta}\right)^{\eta}$	(24)	r_n (mol s^{-1}Kg w^{-1}) is the reaction rate, k_n (mol/L m s^{-1}) is a constant, S is the specific surface area (SSA) (m^2Kg w^{-1}) and Ω_n is the saturation ratio. The saturation ratio is expressed as: $\Omega = \frac{\mathrm{IAP}}{\mathrm{K_n}}$Where IAP is the ion activity product and K_n is the solubility product. The exponent θ and η are empirically determined.
	One-rate-constant model (this research)	$-\frac{dCa}{dt} = k * K_{sp} * S * (SR - 1)$	(29)	dCa/dt is the rate of total calcium concentration reduction (mol L^{-1} s^{-1}) k is a rate constant (L mol^{-1} s^{-1} m) S is the specific surface area in (m^2/m^3), SR is the saturation ratio (-), K_{SP} is the solubility product
	Two-rate–constants model (this research)	$-\frac{dCa}{dt} = k_H * K_{sp} * S * (SR - A_H)$ for SR>SR_{CH} $-\frac{dCa}{dt} = k_L * K_{sp} * S * (SR - 1)$ for SR<SR_{CH}	(32)	dCa/dt is the rate of total calcium concentration reduction (mol L^{-1} s^{-1}), k_H is a high rate constant (L mol^{-1} s^{-1} m), k_L is alow rate constant (L mol^{-1} s^{-1} m), S is the specific surface area in (m^2/m^3), SR is the saturation ratio (-), K_{SP} is the solubility product and SR_{CH} is the saturation ration of change between the high and the low rate constant. It is calculated by $SR_{CH} = -\frac{k_L - A_H * k_H}{k_l - k_H}$ since it is the intersection between the two lines

Several researchers used artificial hard water instead of natural water to conduct calcium carbonate crystallization experiments. Firstly, in the research of Reddy and Nancollas (1971) the following equation (17) was proposed, for the description of calcium carbonate crystallization based on the results of STR batch experiments.

$$-\frac{dCa}{dt} = k_G * C * (m_{Ca^{2+}} m_{CO_3^{2-}} - \frac{K_{sp}}{f_2^2}) \quad (17)$$

Where dCa/dt is the rate of total calcium concentration reduction (mol L^{-1} s^{-1}), k_G is a kinetic constant (L mol^{-1} s^{-1} L mg^{-1}), C is the concentration of the seeding material in mg/L, $m_{Ca^{+2}}$, $m_{CO_3^{2+}}$ are the concentrations of the calcium and carbonate ions respectively in mol L^{-1}, K_{SP} is the solubility product and f_2 is the calcium activity coefficient. In this case, the calcium carbonate crystallization rate is linearly related to the driving force which is the difference between the calcium and carbonate concentration in a supersaturated solution from the concentrations of these ions in equilibrium. A similar linear relationship (equation (18)) between supersaturation the rate of calcium carbonate crystallization was used by Wiechers et al. (1975):

$$-\frac{dCa}{dt} = k_{W,T} * C * \{(Ca^{2+})(CO_3^{2-}) - K_s\} \quad (18)$$

Where dCa/dt is the rate of total calcium concentration reduction (mol L^{-1} s^{-1}), k_T is a temperature dependent constant (L mol^{-1} s^{-1} L mg^{-1}) that can be calculated using equation (19):

$$k_{W,T} = 0.0255 * 1.053^{(T-20)} \quad (19)$$

C is the seeding material concentration (mg/L), (Ca^{2+}) and (CO_3^{2+}) are the activities of calcium and carbonate ions and K_s is the calcium carbonate solubility product. Although it was claimed that the crystallization of calcium carbonate is a surface controlled reaction, the mass of the seeding material is used in equation (18) instead of the specific surface area (SSA) in m^2/m^3. The concentration of the seeding material in the Wiechers et al. (1975) research ranged between the 0.2 -1 mg L^{-1} of calcite powder.

In the research of Wiechers et al. (1975), Noiriel et al. (2012), Nancollas and Reddy (1971) artificial hard water has been used to conduct the experiments for the determination of the calcium carbonate crystallization. Therefore, the effect of inhibitors such as dissolved organic carbon, magnesium ions or orthophosphates was not taken into account. While, Nancollas and Reddy (1974) underlined that the presence of polyphosphates and sulfate in the water can markedly reduce the calcium carbonate crystallization rate, no model that would consider the rate reduction due to the presence of inhibitors was proposed.

Furthermore, Van Dijk and Wilms (1991) used a similar equation (20) as Wiechers to model the crystallization of calcium carbonate inside a pellet softening fluidized bed reactor. The equation that was used was:

$$-\frac{dCa}{dt} = k_T * S * [(Ca^{2+})(CO_3^{2-}) - K_{sp}] \quad (20)$$

Where dCa/dt is the calcium carbonate crystallization rate (mol L^{-1} s^{-1}), k_T is a temperature dependent constant(L mol^{-1}L m s^{-1}), S is the specific surface area m^2/m^3, (Ca^{2+}) and (CO_3^{2+}) are the activities of calcium (mol/L) and carbonate ions and K_{sp} is the solubility product. The main difference between the equation used by Van Dijk and Wilms and Wiechers is that specific surface area (SSA) m^2/m^3 is used instead of the concentration of the seeding material.

Van Schagen et al. (2008b), Van Schagen et al (2008c) has also used an equation similar to the Wiechers to model the pellet softening process in the fluidized bed reactor. The equation that was used is [equation (21)]:

$$-\frac{dCa}{dt} = \frac{k_{W,T} * k_f}{k_{W,T} + k_f} * S * [(Ca^{2+})(CO_3^{2-}) - K_s] \quad (21)$$

Where the dCa/dt the calcium carbonate crystallization (mol L^{-1} s^{-1}), $k_{W,T}$ is a temperature dependent constant(L mol^{-1}L m s^{-1}), k_f is the transportation coefficient that is defined by the equation:

$$k_f = \frac{S_h * D_f}{d_p}$$

Where S_h was the Sherwood number, D_f is the diffusion coefficient and d_p is the diameter of the pellet. Van Schagen used the transportation coefficient k_f to take into account the flow conditions inside the reactor. In this research, the role of diffusion in calcium carbonate crystallization was further investigated.

Alternatively, Tai et al. (1999) and Tai and Hsu (2001) used the two-step model to describe the growth rate of the seeding calcite particles. According to the two-step model, the growth rate of the seeding material particle depends on the mass transfer of the reactants to the surface of the pellet and the reaction of crystallization. The slowest process is limiting the overall calcium carbonate crystallization rate and it is controlling the calcium reduction in the solution. For the modeling of the growth rate of the seeding material particles the following equation (22)has been proposed by Tai and Hsu (2001):

$$\frac{G}{K_{d0} * L^a} + \left(\frac{G}{K_{ro} * L^b}\right)^{\frac{1}{r}} = \sigma \quad (22)$$

Where G is the linear crystal growth rate (m/s), σ the overall supersaturation, L the crystal size (um), r the surface-reaction order, K_{do} and K_{ro} are the mass-transfer and surface-reaction coefficients. The exponents a, b are derived from the experimental results. The coefficients and exponents have been determined using fluidized bed reactor experiments under different water velocities and using different types of seeding material. The main problem regarding this equation is that more than four parameters should be determined experimentally.

Hu et al. (2017) have also used the two-step model to describe the rate of seeded calcium carbonate crystallization. In contrast to the research of Tai and Hsu (2001), in this case, the hydraulic parameters of the experiment were also included in the growth equation (23).

$$G = K_g * L_o^m * SV^n * S_s^j \quad (23)$$

Where G is the linear particle growth rate (m s^{-1}), K_g is the coefficient of linear growth rate, L_0 pellet size of seed (mm), S_s is supersaturation, SV is the superficial velocity (m/h) and m, n, j are exponents. The results from experiments in a pilot plant installation were used to determine the values of the parameters in equation (23). In this research natural groundwater was used instead of artificial hard water during the experiments. Therefore, in this case, the effect of inhibiting compounds was taken into account. In the model of Hu et al. (2017) a number of parameters need to be calibrated in order to be able to predict the kinetics of calcium carbonate crystallization. It is therefore difficult to be used.

Regarding the mechanism of calcium carbonate crystallization, Hu et al. (2017) suggested that the solute molecules diffuse to the template surface and then grow and aggregate. The aggregation of fine crystals and the seeding material is according to this research the mechanism of pellet growth. At the beginning of the crystallization process the surface of the seeding material is rough but as aggregation and adsorption of fine crystals continuous the surface smoothens.

As stated by Marty et al. (2014) there is a high variation between the experimental reaction rates determined by different researchers even when the behavior of the same compound is studied. The difference could be several orders of magnitude. The reason for the discrepancies is differences in the chemical composition of the supersaturated solution and heterogeneities in the media. According to Inskeep and Bloom (1986), Lebron and Suarez (1996) and Lin, Singer and Aiken (2005), at the present

the crystallization of calcium carbonate can only be described with an empirical equation. Therefore, for a large-scale simulation, it is necessary to use an empirical model. The general equation that is proposed by Lasaga (1998) is:

$$r_n = \mp K_n * S * \left(1 - \Omega^{\Theta}\right)^{\eta} \quad (24)$$

Where r_n (mol s^{-1}kg w^{-1})is the reaction rate, k_n (mol/L m s^{-1}) is a constant, S is the specific surface area (SSA) ((m^2kg w^{-1}) and Ω_n is the saturation ratio. The saturation ratio is expressed as:

$$\Omega = \frac{IAP}{K_n} \quad (25)$$

Where IAP is the ion activity product and K_n is the solubility product. The exponent θ and η are empirically determined. Although the Lasaga equation has not a direct physical meaning it can be used to easily determine the rate of crystallization by calibrating only three parameters. As a result, it is suitable for easily modeling the rate of calcium carbonate crystallization by conducting experiments in the same conditions as inside a fluidized bed pellet softening reactor.

Dreybrodt et al. (1997) have also conducted calcium carbonate seeded crystallization experiments using synthetic water with inhibitors. According to their results, two regions can be noticed while measuring the rate of calcium carbonate crystallization. In region A the precipitation rate is following a linear reduction with calcium concentration, and it is not sensitive to inhibition. In region B, a further reduction of the rates is observed, resulting in a bending in the curve in the graph of the rate against calcium concentration as it can be seen from Figure 9:

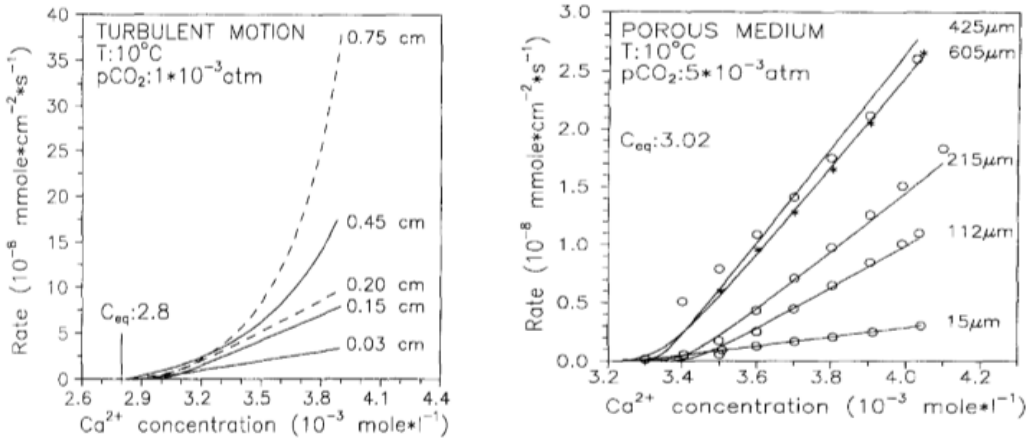

Figure 9 Precipitation rate of calcium carbonate as a function of Ca concentration in a batch reactor with turbulent motion and a porous medium (Dreybrodt et al. 1997)

According to the results of this research, the growth rate for region A can be determined using a linear equation:

$$R = k_4 * [C * K_{sp} - (Ca^{2+})(CO_3^{2-})] \quad (26)$$

Where R is the rate of crystallization, $k_4$is a rate constant, C is a constant, (Ca^{2+}) and (CO_3^{2+}) are the activities of calcium and carbonate ions and K_{sp} is the calcium carbonate solubility product. The value of C is calculated by $C = 1/f$ where f is an inhibition factor that is determined by the equation (27):

$$f = \left(\frac{[Ca^{2+}]_{eq}}{[Ca^{2+}]_{app}}\right) \quad (27)$$

Where $[Ca^{2+}]_{eq}$ is the theoretical calcium equilibrium and $[Ca^{2+}]_{app}$ is the apparent calcium equilibrium. The apparent equilibrium is reached when precipitation no longer takes place due to the presence of

inhibitors. Apparent equilibrium is reached at a higher calcium concentration value than theoretical equilibrium. Therefore, since C>1, this constant reflects an enhancement of the forward reaction.

On the other hand, in region B, a bending of the line is observed due to the presence of inhibitors in the solution or impurities in the surface of the seeding material. No equation, for this region is proposed.

According to Dove and Hocella (1993), Regions A and B exhibit different mechanisms of growth. In region B, surface nuclei are formed, coalesce and continue to grow. The presence of inhibitors is, therefore, blocking the surface available for nucleation and is reducing the aggregation of nuclei. As a result, the rate of calcium carbonate crystallization is significantly decreased. In contrast, in region A, the growth rate is not sensitive to saturation and surface nucleation is not the primary mechanism of crystallization. Consequently, inhibitors do not have a significant impact on calcium carbonate crystallization and the rate of crystallization is decreasing linearly with supersaturation.

According to Dreybrodt et al. (1997), in solutions with saturation ratio 1.5 <SR< 100 the rate law of equation (26) can be applied while at lower supersaturation an inhibition of the carbonic anhydrase is observed. However, it must be noted that the saturation ratio that inhibitors start to have an important impact on calcium carbonate crystallization, is depending on the type and concentration of the inhibitor. In the presence of a higher concentration of inhibitors or a compound with a higher inhibiting effect, it is likely that the saturation ratio that a bending of the curve is observed is higher.

2.6.3. Kinetic models of calcium carbonate used in this research

In order to determine which crystallization model predict better the calcium carbonate crystallization rate three models were compared in this research:

- The Wiechers model
- The one-rate-constant model
- The two-rate-constants model

The Wiechers model

Firstly, it is tested whether the model of Wiechers can predict accurately the rate of calcium carbonate crystallization. Equation (18) is used to define the pH reduction for each STR experiment in this research and the results are compared with the experimental values. The rate constant value that is used in this case is the temperature dependent constant described by equation (19).

The Wiechers model has been derived using STR batch experiments with artificial hard water. However, in this research natural water is used instead and a seeding material with different mass to surface ratio than the calcite powder that was used by Wiechers. Therefore, the validity of the model under different conditions is evaluated.

The one-rate-constant model

The one-rate-constant model has been derived in this research based on the equations found in literature. In particular, a linear relationship between the rate of calcium carbonate crystallization and supersaturation, as Wiechers suggested, is assumed. However, three important changes were applied:

- The concentration of the seeding material in the Wiechers equation was substituted with specific surface area.
- The rate constant was changed
- The equation of Lasaga (equation (24))with $\theta=\eta=1$ is used instead of the equation of Wiechers.

The reasons for implementing those changes to the Wiechers equation are described below

- For using specific surface area instead of concentration of seeding material:

Although Wiechers states that the crystallization of calcium carbonate is surface controlled, in the model of this research it is considered that the rate of crystallization is proportional to the concentration of the seeding material rather than specific surface area. As a result, when a different type of seeding material is used, the surface to mass ratio changes and subsequently the rate of hardness reduction changes. In case a seeding material with a high mass to surface ratio is used the rate of crystallization is overestimated by the model.

To avoid discrepancies due to the use of a different type of seeding material, the specific surface area was used in this research instead of the concentration. Van Dijk and Wilms (1991), Van den Hout (2016) has also replaced the concentration to the specific surface area in the equation of Wiechers and used this rate equation to model the pellet softening fluidized bed reactor. However, in contrast with this research, the rate constant that was used by these researchers is the temperature dependent constant derived by Wiechers equation (19).

- For changing the rate constant value:

Previous researchers such as Van Schagen et al (2008 b,c) has tried to predict more accurately the rate of calcium carbonate crystallization by changing only the rate constant of the Wiechers equation In particular, Van Schagen has introduced a diffusion parameter, to change the rate constant of the linear model in order to fit the measured data. However, the Van Schagen model is not describing accurately enough the rate of calcium carbonate crystallization in a pellet softening reactor.

In this research, it is investigated if the one-rate-constant model can predict the calcium carbonate crystallization when a different rate constant value than the temperature dependent rate constant of Wiechers is used. The rate constant value of this model is determined by calibrating the model to fit the experimental data and is not calculated in advance.

- For using Lasaga (1998) equation with θ=η=1

For clarity, the Lasaga (1998) equation was used instead of the Wiechers equation. By using the modified Lasaga (1998) equation the correlation between the supersaturation and the rate of calcium carbonate crystallization can be more easily seen. Also, since it is a more common equation in literature, it can be compared with the findings of other researchers.

The Wiechers equation is transformed to the equivalent Lasaga (1998) equation if it is assumed that the exponents θ=η=1 and minor modifications are made:

If the Wiechers equation

$$-\frac{dCa}{dt} = k_{W,T} * S * ((Ca^{2+})(CO_3^{2-}) - K_{sp})$$

is multiplied with $\frac{K_{sp}}{K_{sp}}$ then the equation

$$-\frac{dCa}{dt} = k_{W,T} * K_{sp} * C * \left(\frac{(Ca^{2+})(CO_3^{2-})}{K_{sp}} - 1\right) = k_{W,T} * K_{sp} * C * (SR - 1) \\ = K_n * S * (SR - 1) \quad (28)$$

If it is assumed that $K_n = k_{W,T} * K_{sp}$ and C=S is the specific surface area in m^2/m^3 instead of the concentration the equation of Wiechers is equivalent to the Lasaga equation.

Overall, the equation proposed for this research for the one-rate-constant model is:

$$-\frac{dCa}{dt} = k * K_{sp} * S * (SR - 1) \quad (29)$$

Where dCa/dt is the calcium carbonate crystallization rate (mol L^{-1} s^{-1}), k is a rate constant(L mol^{-1}L m s^{-1}), S is the specific surface area m^2/m^3 and SR is the saturation ratio.

The two-rate-constants model

Both in the Wiechers and the one-rate-constant model, the rate of calcium carbonate crystallization is proportional to a rate constant and the product of SSA and supersaturation. As a result, if the rate of crystallization is plotted against supersaturation in a graph the calculated points form a straight line. However, Dreybrodt et al. (1997) have proved that in the presence of inhibitors the line of calcium carbonate crystallization against supersaturation is bending into a curve. This is caused by a large reduction of the rate of crystallization at low supersaturation. There are two possible options to describe this behavior:

- A fluent model using the Lasaga (1998) equation and fitting the curve to the experimental data by changing the exponents θ, η
- A linear model that consists of two equations. The curve of Dreybrodt et al. (1997) can be divided into two or more regions. In each region, a different linear equation is used.

According to the first option, the values of exponents θ, η can be changed in the Lasaga (1998) equation (24) in order to fit the prediction of the model to the curved line observed by Dreybrodt et al. (1997). However, in this case, the dependence of the rate of crystallization from supersaturation is not clear. Hence, it is difficult to determine the sensitivity of the rate of crystallization to supersaturation and distinguish the physical meaning of the equation.

On the other hand, the rate of calcium carbonate crystallization can be divided into two regions as proposed by Dreybrodt et al. (1997). In region A, equation (26) is used. However, modification of this equation is necessary in order to take into account the dependence of the rate of crystallization from the specific surface area of the seeding material. Furthermore, for clarity an equivalent equation similar to Lasaga (1998) equation was used. As a result, the equation that is proposed is:

$$-\frac{dCa}{dt} = k_H * K_{sp} * S * \left[\frac{C - (Ca^{2+})(CO_3^{2-})}{K_{sp}}\right] = k_H * K_{sp} * S * (SR - C) \quad (30)$$

Where dCa/dt is the calcium carbonate crystallization rate (mol L^{-1} s^{-1}), k_H is a high rate constant(L mol^{-1}L m s^{-1}), S is the specific surface area m^2/m^3, SR is the saturation ratio, C is a constant and K_{sp} is the solubility product. Equation (30) is very similar to the one-rate-constant model except from the factor C that is used to describe the slight enhancement of the reaction at high saturation ratio that was observed by Dreybrodt et al. (1997). No researcher has given an equation for region B. It is therefore assumed that a linear equation can be used to determine the rate of crystallization in this area as well. Linearity is not a realistic approach for processes that take place in nature. However, for reasons of simplicity and clarity a linear equation is considered. Therefore, a model that would be able to approximate sufficiently well calcium carbonate kinetics at low saturation ratio and that would clearly demonstrate the dependence of the rate of crystallization on supersaturation was chosen. Overall, the equation that is proposed for region B is:

$$-\frac{dCa}{dt} = k_L * K_{sp} * S * (SR - 1) \quad (31)$$

Where dCa/dt is the calcium carbonate crystallization rate (mol L^{-1} s^{-1}), k_L is a low rate constant(L mol^{-1}L m s^{-1}), S is the specific surface area m^2/m^3 and SR is the saturation ratio In equation

(31) the value of the low rate constants was determined based on the experimental results as well. The value of the low rate constant that was used is much lower than the value of the rate constant in equation (30) in order to approximate the rate of calcium carbonate crystallization near equilibrium. Nevertheless, validation of this equation from experimental data is necessary

Overall, based on this approach the equation of the two-rate-constants model is:

$$-\frac{dCa}{dt} = k_i * K_{sp} * S * (SR - A_i) \quad (32)$$

dCa/dt is the calcium carbonate crystallization rate (mmol L^{-1} s^{-1}), SR or Ω is the calcite saturation ratio, S is the specific surface area (SSA) (m^2/m^3).

- k_H is the high rate constant (mol/ L *s^{-1}*m^3/m^2) for calcite SR>SR_{CH}
- k_L is the low rate constant (mol/ L *s^{-1}*m^3/m^2) for calcite SR< SR_{CH}
- $A_H = C$ is the intercept of the high rate constant line
- A_L is the intercept of the low constant line that is forced to SR=1

The saturation ratio of change is the intersection of the two line and is calculated using the equation:

$$SR_{CH} = -\frac{k_L - A_H * k_H}{k_L - k_H} \quad (33)$$

2.7. Modeling of the physical part

A pellet softening fluidized bed reactor is modeled as an ideal plug flow reactor [Van den Hout (2016)]. It is therefore considered that it consists of a series of batch reactors with homogeneous conditions. As a result, in order to describe the hydraulic conditions inside a pellet softening rector, it is separated into 20 or more layers containing a constant number of particles.

In a fluidized bed classification of the pellets takes place. The pellets with the larger diameter settle in the bottom of the reactor while the pellets with the smallest diameter are in the top of the fluidized bed. As a result, in the higher region of the reactor, a larger number of smaller particles is present while in the bottom of the reactor there is a lower amount of pellets with a large diameter. To model this behavior a number of particles are assumed in the highest layer and it is considered that the number of particles in the lowest layer is approximately 1% of the number of particles in the highest layer. The number of particles in the intermediate layers is reduced gradually. This percentage was chosen based on empirical observations and in order to be to achieve low residence time in each layer. The residence time of the water in each layer is the time step of the simulation. By choosing a small time step, iteration and convergence errors are avoided.

Initially, a diameter and a number of particles is assumed for each layer. After several iterations and trials of different diameters, the height of each layer is determined so that the total height of the fluidized bed to be equal to the height determined by the user. The height of each layer is defined assuming a particular diameter and number of pellets and using an empirical algorithm Fluid Bed Inside (FBI) to determine the fluidization of the seeding material. FBI has been derived from the experimental data acquired in the Weesperkarspel pilot plant by Kramer et al. (2015). [Van den Hout (2016)].

Therefore, the profile of pellets inside the reactor, the height of the fluidized bed and therefore the specific surface area in each layer is calculated. Since the height of each layer is known the contact time can also be determined. Firstly, the velocity of water inside the reactor is calculated using the equation (34).

$$v = \frac{Q}{A} = \frac{Q}{A_r * p} \tag{34}$$

Where Q is the flow of water inside the reactor in m^3/s, A_r is the total area of a cross-section of a reactor, A is the area inside the reactor that water can flow, v is the velocity of water between the pellets in m/s and p is the porosity of each layer [equation(12)] . The contact time is calculated by dividing the height of each layer with the velocity

$$t = \frac{h_i}{v} \tag{35}$$

Where t is the contact time in seconds, $h_i$is the height of each layer in m and v is the velocity in m/s. It is therefore assumed that the time of the calcium carbonate crystallization reaction in a layer is the time that it takes for the water to pass through that layer. As a result, the fluidization of the bed and the contact time of the water with the seeding material can be accurately predicted. This hydraulic part of the model is developed by Van den Hout (2016) and incorporated in the Layers-model.

2.8. Layers-model

The Layers-model was developed by Van den Hout (2016) based on the research of Kramer et al. (2015), to simulate the pellet softening fluidized bed reactor. In the Layers-model, the modeling of the chemical part of the pellet softening reactor is combined with the hydraulic model for the fluidization of the bed.

According to the Layers-model, the pellet softening fluidized bed reactor is an ideal plug flow reactor. As a result, the reactor was divided into consecutive layers containing a constant number of particles. Once, the hydraulic state of each layer has been determined as explained in §2.7 a chemical equilibrium model PHREEQC is used to determine the chemical conditions inside the reactor. For every layer, both the hydraulic state (porosity) and the CCCP is estimated. However, since PHREEQC is a chemical equilibrium model and cannot predict the reaction kinetics, an equation that would describe the calcium removal in time is needed. In the Layers-model, the Wiechers equation is used to determine the rate of crystallization inside the reactor. However, while the Layers-model predicts accurately enough the hydraulic state inside a pellet softening reactor, it fails to predict the pH and calcium profile. Therefore, It is assumed that a different equation for the rate of calcium carbonate crystallization should be used to improve the predictions of the model (§2.8).

3

STR batch experiments

3.1. Aim of STR batch Experiments

The aim of the STR experiments is to determine the rate of calcium carbonate crystallization in a batch reactor, using natural water instead of artificial hard water and a high concentration of seeding material. The results of these experiments are compared to the experimental results of Wiechers to determine the effect of the presence of inhibitors in natural water. Also, it is tested whether the rate of crystallization remains proportional to specific surface area, as Wiechers suggested, when 30 times higher specific surface area is offered during the experiment.

3.1.1. Introduction

Many researchers such as Wiechers et al. (1975), Nancollas and Reddy (1971) (I and II) has used STR batch experiments to determine the kinetics of calcium carbonate crystallization. However, the experimental conditions in these studies, are different than the conditions during the fluidized bed pellet softening process. The most important differences are:

- The specific surface area (SSA) of the seeding material in the experiments of Wiechers et al. (1975) and Nancollas and Reddy (1971), is significantly lower than the one offered in a pellet softening reactor. Consequently, the rate, in this case, is much lower than the rate of calcium carbonate crystallization during the pellet softening process.
- In contrast to the experiments of Wiechers where artificial hard water was used the untreated water from the WPK water contains compounds that might inhibit the softening process.

Therefore, the validity of the experimental results from these researchers should be tested under different conditions.

3.1.2. Goals of STR batch experiments

Several STR batch experiments took place in the TU Delft Process and Energy laboratory in order to determine the effect of using different seeding material and different type of water in the hardness reduction process. The main goals of the STR batch experiments that were conducted in the TU Delft laboratory were:

- To repeat the Wiechers experiments with natural water instead of artificial hard water. By comparing the experimental results with the results of the research by Wiechers et al. (1975) the influence of the presence of inhibitors in the water can be detected.
- To repeat the Wiechers experiments using natural water and a higher concentration of seeding material. It can, therefore, be detected if the rate of crystallization remains proportional to the

specific surface area when higher concentrations of seeding material ranging from 10-30 g/L is used. The specific surface area of the seeding material when 30 times higher concentration of calcite powder is used is similar to the specific surface area offered inside a pellet softening fluidized bed reactor.

- To repeat Wiechers experiments using the same type seeding material that is used in a pellet softening reactor instead of calcite powder. Crushed calcite and calcite pellets were used as seeding material instead of calcite powder.
- To define the effect of diffusion in the calcium carbonate crystallization. The results of the STR batch experiments were compared to the results of the fluidized bed experiments to determine the effect of different hydraulic conditions in the crystallization process.
- To define the effect of temperature ranging from 5-20 ˚C on calcium carbonate crystallization rate.

3.2. Materials and methods

In this section, the materials that were used during the STR batch experiments are shown and the experimental procedure that was followed is described.

Chemical part

The water that was used for the STR batch experiments was abstracted from the influent stream of WPK water treatment plant on 4th and 12th of July 2017. Although the water quality of the WPK raw water does not change significantly on a monthly basis the differences especially in pH and total calcium concentration between the two samples were taken into account. The water quality of the two samples can be seen in Table A. 1 and Table A. 2 (Appendix A).

The caustic soda solution that was dosed, was prepared by diluting NaOH powder with demineralized water. Due to the low volume of the dose, it is considered that no serious change in the water quality took place after dosing. A solution of 0.5% w/w caustic soda was prepared.

For each experiment, 7.25 ml of a solution 0.5% w/w NaOH were added to 492.75 ml of raw water. The concentration of caustic soda added to the solution was 1.81 mmol/L and the $SI_{Calcite}$ in the water after this concentration of NaOH was added was increased approximately to 2 and therefore the SR=100.

Physical part

During the STR batch experiments two types of calcite were used as seeding material:

- Merck calcite powder with d_{50}= 14-24 um.
- Crushed calcite with d= 0.5-0.6 mm

The crushed calcite was sieved in the Pilot plant of WPK treatment plant using Retsch AS 200 test sieves and Sieve shaker. It is important to note that the crushed calcite was sieved but not washed. As a result, an amount of crushed calcite powder was observed to be attached to the surface of the seeding material particles. For the determination of the Specific Surface Area (SSA) of the Merck calcite powder, a particle size distribution analysis took place in TU Delft laboratory with a Microtac S3500 laser diffraction analyzer. For the determination of the particle size distribution inside the reactor, the Focused Beam Reflectance Measurement (FBRM) technology was applied. In particular, the FBRM Particle Track G400 probe-based instrument was used to able to continuously measure the particle size distribution and detect particle changes inside the reactor.

The SSA for each experiment was determined according to the following procedure:

1. Firstly, the weight W (g) of the seeding material that was used as seeding material was determined.

2. In order to determine the total volume of the pellets that was added to the solution, the weight of the pellets was divided with the calcite density. Since pure calcite powder and calcite pellets are used as a seeding material, the density of calcite found in literature is used 2.71 g/cm^3 or 2711 kg/m^3 [Mineral data publishing, (2001-2005)]. It must be noted though, that the actual calcite pellets density is slightly different than the density found in literature.

3. In order to determine the surface area of the seeding material, it is assumed that the calcite pellets are perfect spherical particles with a specific diameter. The assumption of round particles is an oversimplification, especially for crushed calcite pellets. But it is considered accurate enough for the purpose of this research. Based on this assumption the surface area of the seeding material was determined using the equation $A_p = V_p * \frac{A_{single\ pellet}}{V_{singlepellet}} = V_p * \frac{\pi * d^2}{\frac{2}{9} * \pi * d^3}$

   Where A_p is the surface area of the seeding material in m^2, V_p is the volume of the pellets in m^3, $V_{singlepellet}$ is the volume of a single pellet is m^3, $A_{singlepellet}$ is the surface area of a single pellet in m^2 and d is the diameter of the pellet.

Since the volume of solution that was used in each experiment is known the concentration of the seeding material in mg/L of solution and the specific surface area in m^2/m^3 of solution was calculated. The calculations are shown in more detail in Appendix A.2.2.1 and Appendix A.2.6.

Experimental setup

The experimental set up consisted of a glass jar with a volume of 1L that was used as a batch reactor for the experiments. A Heidolph RZR 2021 overhead stirrer was fixed inside the reactor and the stirring velocity was adjusted to 700-1000 rpm in order to keep the seeding material in suspension. The temperature of the reactor was measured and stabilized with a Huber CC231 waterbed. The pH was measured using a Mettler Toledo 914 pH/Conductometer. It must be noted that the accuracy of the pH meter is largely affected by the scaling of the sensor. Hence, the pH meter was calibrated daily. As a result, the error of the pH measurement was below approximately ±0.02.

In Figure 10 the batch reactor set up is shown.

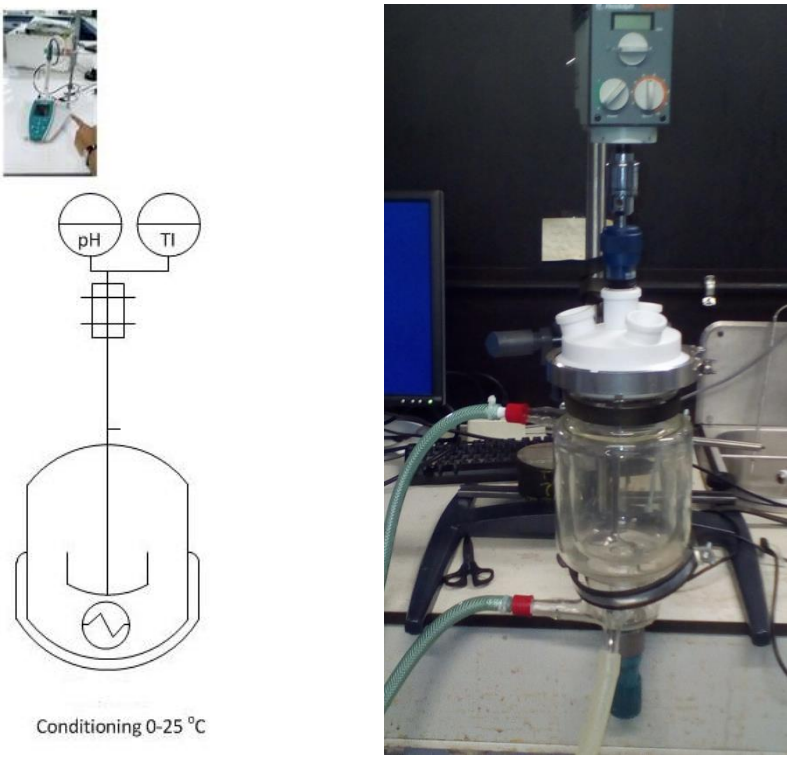

Figure 10 STR batch reactor experiments set up

Experimental procedure

For the STR batch experiments, the following experimental procedure was followed.

- At the beginning of the experiment, the raw water of the WPK influent stream was added to the Jar. The pH meter and the FBRM probe were fixed inside the jar and the openings on the top of the reactor were sealed in order to minimize the exchange of CO_2 between the solution and the atmosphere as much as possible.
- Using a funnel the seeding material was also added to the vessel and the stirring velocity of the impeller was adjusted to around 1000 rpm to keep the particles in suspension.
- The logging of the pH meter was started before the dosing of the caustic soda. A measurement of the pH was taken every second for approximately 900 seconds.
- A few seconds after the beginning of the stirring the caustic soda dose was added.

At the end of the experiment, the reactor was emptied and rinsed with demineralized water. The FBRM probe and the pH meter were also rinsed and stored in an appropriate solution before the beginning of the next experiment.

Initial pH determination

Due to the limitations of the pH measurement instrument, it was not possible to measure the initial pH after dosing. Since the response time of the pH meter is a few seconds, after adding the caustic soda some time elapses before a reliable measurement is available. However, these first few seconds of the reaction are important for the determination of the calcium carbonate rate. For this reason, PHREEQC was used to calculate the initial pH of the solution based on the caustic soda dose. The procedure that was followed to determine the initial pH is:

- For the determination of the initial water quality the online measurements of WPK water treatment plant was used. For the components that are not continuously measured, laboratory results were available. Since the quality of the water from the influent of the WPK treatment plant does not change significantly over time, it is considered that the water composition is adequately described.
- The temperature of the natural water solution in the model was adjusted to the temperature that the experiment was conducted. Then the NaOH dose was added to the solution in PHREEQC input sheet. It must be noted that for the preparation of the NaOH dose, demineralized water was used instead of natural water. Therefore, by assuming that only moles of NaOH are added and not a solution of NaOH is mixed with the water an error is introduced to the calculations. However, since the volume of the dose that was added is lower than 1% of the total volume of the solution, the error in the concentrations of the water components is very small and is considered acceptable for the accuracy of these experiments.

Based on the calculations of the chemical equilibrium model the initial pH at the beginning of the experiment was measured. However, the first 5-10 seconds the pH measurement was not stabilized and a plateau in the pH measurement was observed. These pH values were not considered reliable. Also, during the experiment, a stepwise reduction of pH was observed. This is due to the fact that the pH meter has an accuracy of only two digits. Therefore, the pH meter measurement cannot adequately represent the slow part of the crystallization process. Therefore, a smoothening of the pH measurement line is necessary.

In order to determine the pH the first 5-10 seconds and eliminate the presence of steps in the measured data, a 6^{th} order polynom was used. The polynom was forced to fit the point of the initial pH and the measured points for the first 90 seconds that are considered reliable. This polynom was used to predict the pH during the first 5-10 seconds. This way the first few seconds of the reactions can also be defined, although they cannot be measured.

Overview of STR batch reactor experiments

In the first experiment, 1 g/L Merck calcite powder with d= 14-24 um was added as a seeding material. The temperature was adjusted at 20 ˚C. In this experiment, the same concentration of calcite powder as in the experiments from Wiechers was used.

In Experiments 2a and 2b, Merck calcite powder with d= 14-24 um at a concentration of 30 g/L was added as a seeding material. The temperature was adjusted at 10 ˚C. In this group of experiments, the concentration of the seeding material that was used was more than 30 times higher than the one used in the Wiechers experiments. The specific surface area (SSA) offered in STR batch experiments was calculated assuming perfectly round pellets. Based on the results, the SSA in Experiment 2 is ranging between S =2000-3000 m^2/m^3 while the SSA offered in a fluidized bed softening reactor is ranging between S =4000 and 6000 m^2/m^3 of water. Therefore, the SSA offered in the experiments of this research is comparable to the specific surface area that is usually available in a pellet reactor. Experiment 2 was repeated twice to ensure the reproducibility of the experimental method. In the third group of experiments crushed calcite with a diameter d=0.5-0.6 mm at a concentration of 74 g/L was used as a seeding material. The temperature of the batch experiments was fixed at three different temperatures:

- At 5 ˚C
- At 10 ˚C
- At 20 ˚C

It must be noted that while the crushed calcite was sieved and only the fraction of pellets with a diameter between 0.5-0.6 mm was used, the crushed calcite was not washed. It was observed that calcite powder was attached to the crushed calcite pellets significantly increasing the SSA of the seeding material from 320 m^2/m^3 (which is the SSA of the large pellets). It assumed that the SSA of the seeding material rose to approximately 1000-3000 m^2/m^3 due to the presence of 10% calcite powder particles with diameter approximately d=10um.

In contrast to the fluidized bed experiments, the STR batch reactor experiments have certain limitations concerning the concentration of seeding material that can be used. If the concentration of the seeding material is too high a large part of the seeding material is no longer in suspension and therefore in no contact with the water. As a result, due to lack of specific surface area, spontaneous homogenous nucleation takes place inside the reactor instead of crystallization in the surface of the seeding material. In Figure 11, the case when not sufficient surface area is offered and calcite nuclei are formed is shown:

Figure 11 Spontaneous nucleation due to mixing problems in an STR batch reactor experiment

Several experiments with calcite pellets with diameter d= 0.63-0.71 mm were conducted in the TU Delft Process and Energy laboratory. However, the results of these experiments were not reliable. This was mainly due to the fact that it was not possible to keep the pellets in suspension despite vigorous stirring.

Even if a low concentration of calcite pellets (approximately 90 g/L) was used, the experimental results were not reproducible. Hence, the results are not considered reliable and were not further processed. In Table 2 an overview of the STR batch reactor experiments can be seen:

Table 2 Overview of STR batch reactor experiments

	Date	Temperature	Seeding material	Diameter	Concentration	Specific Surface Area (SSA)
Experiment 1	28/06/2017	20 °C	Calcite Powder	d=14-24 um	1g/L	88 m^2/m^3
Experiment 2 (Duplicate)	13/7/2017	10 °C	Calcite Powder	d=14-24 um	30g/L	2660 m^2/m^3
Experiment 3	6/7/2017	5 °C	Crushed Calcite	d=0.5-0.6 mm	74 g/L	330 m^2/m^3
Experiment 4	6/7/2017	10 °C	Crushed Calcite	d=0.5-0.6 mm	74 g/L	330 m^2/m^3
Experiment 5	6/7/2017	20 °C	Crushed Calcite	D=0.5-0.6 mm	74 g/L	300 m^2/m^3

In the following section, the experimental results of the STR batch experiments are shown.

3.3. Experimental Results

In this section, the results of the STR batch reactor experiments are presented. Firstly, if the water quality as described by the in line and laboratory measurements at WPK treatment plant and the measured values in TU Delft laboratory match, is checked. The charge balance error is calculated to verify that no major components were omitted during the chemical composition analysis. In all of the experiments, the charge balance error is less than 3%, therefore the water analysis is acceptable. In Figure 12 the experimental pH results and the polynom that is used to smoothen the measured pH data and determine the pH the first few seconds of the reaction are shown. Also, the equation of the polynom that is used for each experiment is presented below.

Experiment 1

The polynom that is used to smoothen the measured pH line is:

$$Polynom = 8.35E^{-19}x^6 - 5.37E^{-16}x^5 + 7.37E^{-14}x^4 - 3.14E^{-9}x^3 + 4.77E^{-6}x^2 - 2.57E^{-3}x + 9.853$$

The pH in t=0 sec is not measured but calculated using PHREEQC.

Experiment 2

The polynom that is used to smoothen the measured pH line is:

$$Polynom = 3.29E^{-10}x^6 - 6.88E^{-8}x^5 + 5.71E^{-6}x^4 - 2.41E^{-4}x^3 + 5.63E^{-3}x^2 - 7.96E^{-2}x + 9.99$$

Experiment 3

For Experiment 3, the polynom that is used to smoothen the measured pH line is:

$$Polynom = 4.48E^{-11}x^6 - 1.43E^{-8}x^5 + 1.81E^{-6}x^4 - 1.16E^{-4}x^3 + 3.87E^{-3}x^2 - 6.8E^{-2}x + 10.1$$

Experiment 4

For Experiment 4, the polynom that is used to smoothen the measured pH line and take into account the first few seconds of the experiment is:

$$Polynom = 3.81E^{-11}x^6 - 1.43E^{-8}x^5 + 1.81E^{-6}x^4 - 1.16E^{-4}x^3 + 3.87E^{-3}x^2 - 6.8E^{-2}x + 10.01$$

Experiment 5

For Experiment 5, the polynom that is used to smoothen the pH measured line and take into account the first few seconds of the experiment is:

$$Polynom = 1.9E^{-11}x^6 - 5.98E^{-8}x^5 + 7.48E^{-7}x^4 - 4.8E^{-5}x^3 + 1.74E^{-3}x^2 - 4.19E^{-2}x + 9.87$$

It must be noted that in the last three experiments 5% lower caustic soda was dosed than Experiment 1 and 2. Therefore, the initial supersaturation is lower in this case, than in the previous experiments.

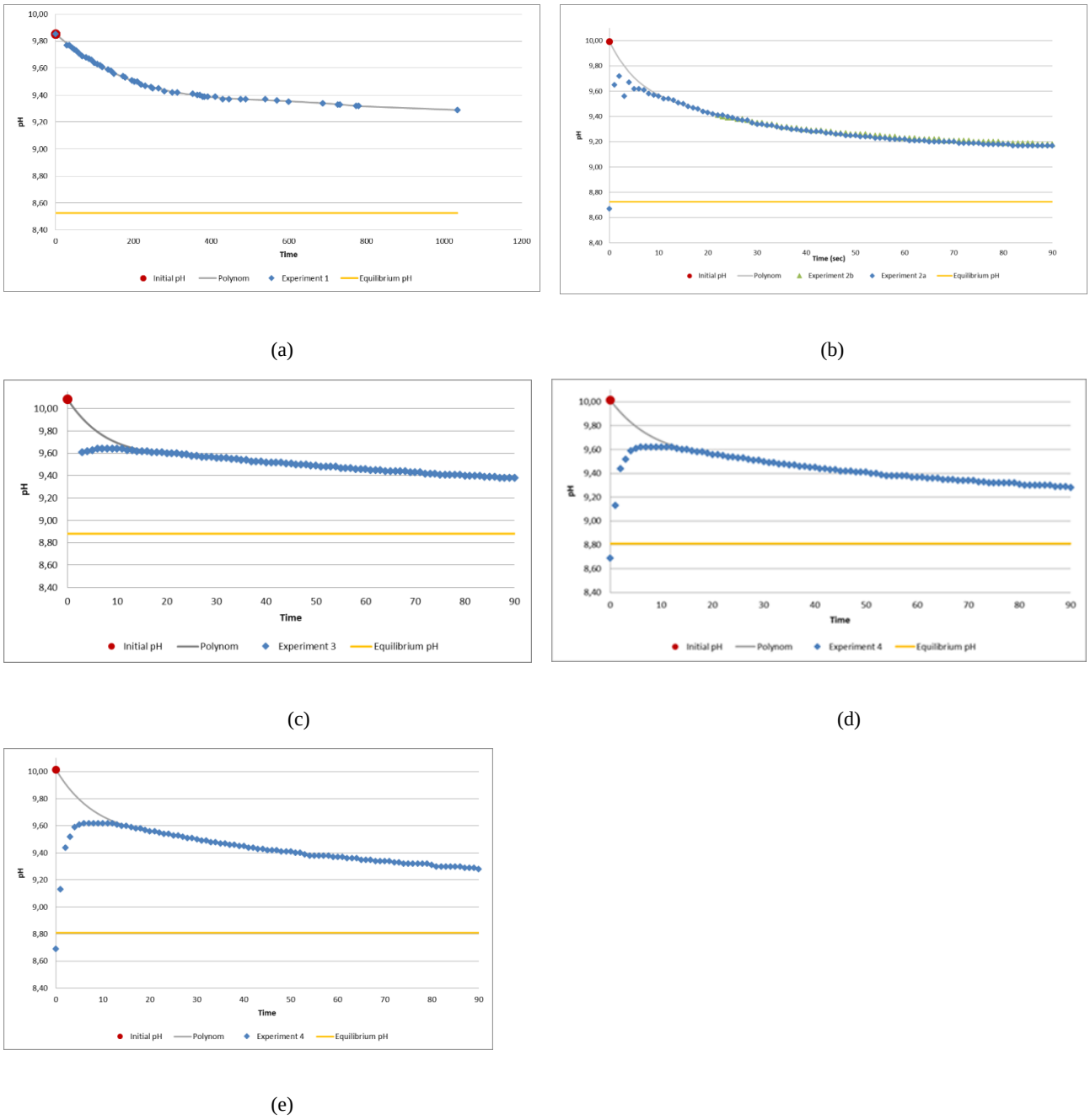

Figure 12 Measured pH and polynomial correction for: (a) Experiment 1 (with calcite powder 1g/L),(b) Experiment 2a (with calcite powder 30g/L) and 2b (c) Experiment 3 (with crushed calcite at 5°C) (d) Experiment 4 (with crushed calcite at 10°C (e) Experiment 5 (with crushed calcite at 20 °C)

At the beginning of the experiment, the supersaturation of the solution is particularly high, as the calcite saturation ratio is approximately 100. In these conditions, spontaneous homogeneous nucleation may

occur when there is not sufficient seeding material for crystallization. To exclude that spontaneous homogeneous nucleation takes place instead of crystal growth during Experiment 2, the particles size distribution inside the reactor was measured continuously using the FBRM technology. In the graph of Figure 13, the counts of particles with a diameter lower than 10 um based on the FBRM measurement is shown.

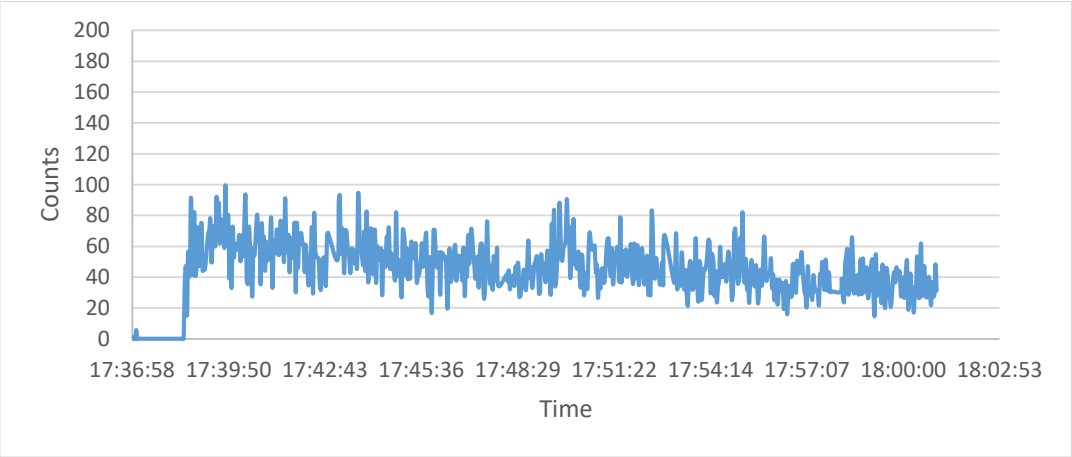

Figure 13 Experiment 2: Number of particles with size <10 um

Around 17:36 the seeding material is added in the reactor and the small calcite particles are counted. It is obvious from the graph the counts of particles with small diameters does not change during the experiment and even decrease after a few minutes as the particles grow. Therefore, the specific surface area offered for crystallization is sufficient and no detectable primary nucleation takes place. Hence, the measured pH can be used to predict the rate of calcium carbonate seeded crystallization.

4

PFR fluidized bed experiments

4.1. Aim of PFR fluidized bed experiments

The aim of the PFR fluidized bed experiments is to determine the effect of the hydraulic and flow conditions on the rate of calcium carbonate crystallization. In this type of experiments, no intensive stirring is applied since the mixing of the caustic soda takes place in a static mixer prior to the reactor. Therefore, the calcium carbonate crystallization kinetics are determined in a reactor without stirring that is operated in a plug flow mode. The results of these experiments are compared with the results of the STR batch experiments to determine the impact of different flow conditions on calcium carbonate crystallization.

4.1.1. Introduction

Many researchers such as Tai et al. (1999), Tai and Hsu (2001), Hsu et al. (2017) have used fluidized bed reactor experiments to determine the kinetics of calcium carbonate crystallization. The chemical and hydraulic conditions during the PFR fluidized bed experiments are almost similar to the conditions inside a pellet softening reactor. In contrast to previous researchers, the fluidized bed reactor experiments in this research are focusing only on the chemical reaction of calcium carbonate crystallization and natural water from the influent of WPK treatment plant. The hydraulic part of the pellet softening process is determined using the Layers-model developed by Van den Hout (2016).

4.1.2. Goals of PFR fluidized bed experiments

The main goals of the fluidized bed reactor experiments is:

- To define the influence of using natural water from the influent of WPK treatment plant instead of artificial hard water. In this way, the effect of inhibitors in the untreated water can be determined.
- To determine the calcium carbonate crystallization rate in a column with the same concentration of seeding material and the same hydraulic conditions as a pellet softening fluidized bed reactor
- To define the effect of temperature ranging from 10-20 ℃ on calcium carbonate crystallization rate
- To define the effect of diffusion in the calcium carbonate crystallization.

4.2. Materials and methods

In this section, the materials that were used during the PFR fluidized bed experiments are shown and the experimental procedure that was followed is described.

Chemical part

The water that was used for the PFR fluidized bed experiments was abstracted from the influent stream of WPK water treatment plant on 14th and 15th of August and 12th of September 2017. Although the water quality of the WPK raw water does not change significantly in a monthly basis the differences, especially in pH and total calcium concentration, between the three days were taken into account. The water quality of the influent stream of WPK water treatment can be seen in Table B. 1 (Appendix B).

Before being used in the experiments the water was stored in a 1 m^3 vessel where its temperature was adjusted using an AEG heat exchanger. Due to limitations of the equipment, it was not possible to reduce the temperature of the water below 10 ˚C. However, the temperature in the WPK water treatment plant is ranging between 3 and 23 ˚C. It was therefore not possible to conduct experiments in the full range of temperatures that can be measured in the pellet softening fluidized bed reactors of WPK.

For the dosing of caustic soda, a solution of 0.7-1.4 % w/w NaOH was used. The solution was prepared by diluting a 10 % w/w NaOH Brenntag solution with demineralized water. The caustic soda solution was dosed using an Iwaki pump with a maximum flow of 2.29 L/h. The caustic soda was mixed with the solution before the column with a static mixer.

During the experiment, the pH, Electrical Conductivity (uS/cm), turbidity (NTU) and temperature (˚C) was simultaneously measured using the appropriate probes. The probes were connected with a Hanna IH 9829 logging device. Before the start of each experiment, each probe was calibrated using Hanna standards.

At the end of each experiment, the pH and EC of the standards was measured again in order to determine the effect of scaling in the pH and EC meter. If the deviation between the standard and the measured value, was relatively high the experiment was repeated. When the column was not used, a Brenntag solution of 10% HCl was used to remove any scaling and blocking of the water inlet of the column.

Physical part

Two types of seeding material were used during the experiments:

- Calcite pellets with d= 1-1.12 mm
- Crushed calcite with d=0.5-0.6 mm

The calcite pellets were sieved in the pilot plant of WPK treatment plant using Retsch AS 200 test sieves and Sieve shaker. In each case, only the fraction with a particular diameter range was used in the PFR fluidized bed experiments.

The seeding material was added gradually in the PFR in layers with a weight ranging between 1-1.5 kg. After each layer was added, the height and volume V_t of the fluidized bed was measured. From the total volume of the column, the volume of the inlet nozzle was subtracted. The volume of pellets V_p was determined by dividing the weight with the specific weight of calcite 2.71 g/cm^3 [Mineral data publishing, (2001-2005)]. It must be noted that the density of calcite may deviate slightly in reality from the value found in literature. As a result, the porosity in each part of the reactor can be determined using the equation (12). Based on the porosity and assuming perfect round pellets the SSA of each layer in the reactor was determined using the equation of Van Schagen et al. (2008) [equation (13)] was used. In order to be able to compare, the SSA in a pellet reactor with the surface area in other types of reactors or under different fluidization conditions the specific surface area per volume of water was calculated using equation (14) (see Appendix B.2).

Experimental setup

The experimental set up consisted of a column with a diameter of 8 cm and a height of 100 cm. The water was pumped from the bottom of the column to the top in order to keep the bed fluidized. A flow meter was used to regulate the flow of water through the column. An overflow was located approximately 85 cm from the bottom of the reactor. The overflow was connected with a vessel with water level indications. Each indication was corresponding to a certain volume. Using a timer, it was, therefore, possible to measure the flow through the reactor and verify the flow meter measurement. In Figure 14 the experimental set up is shown.

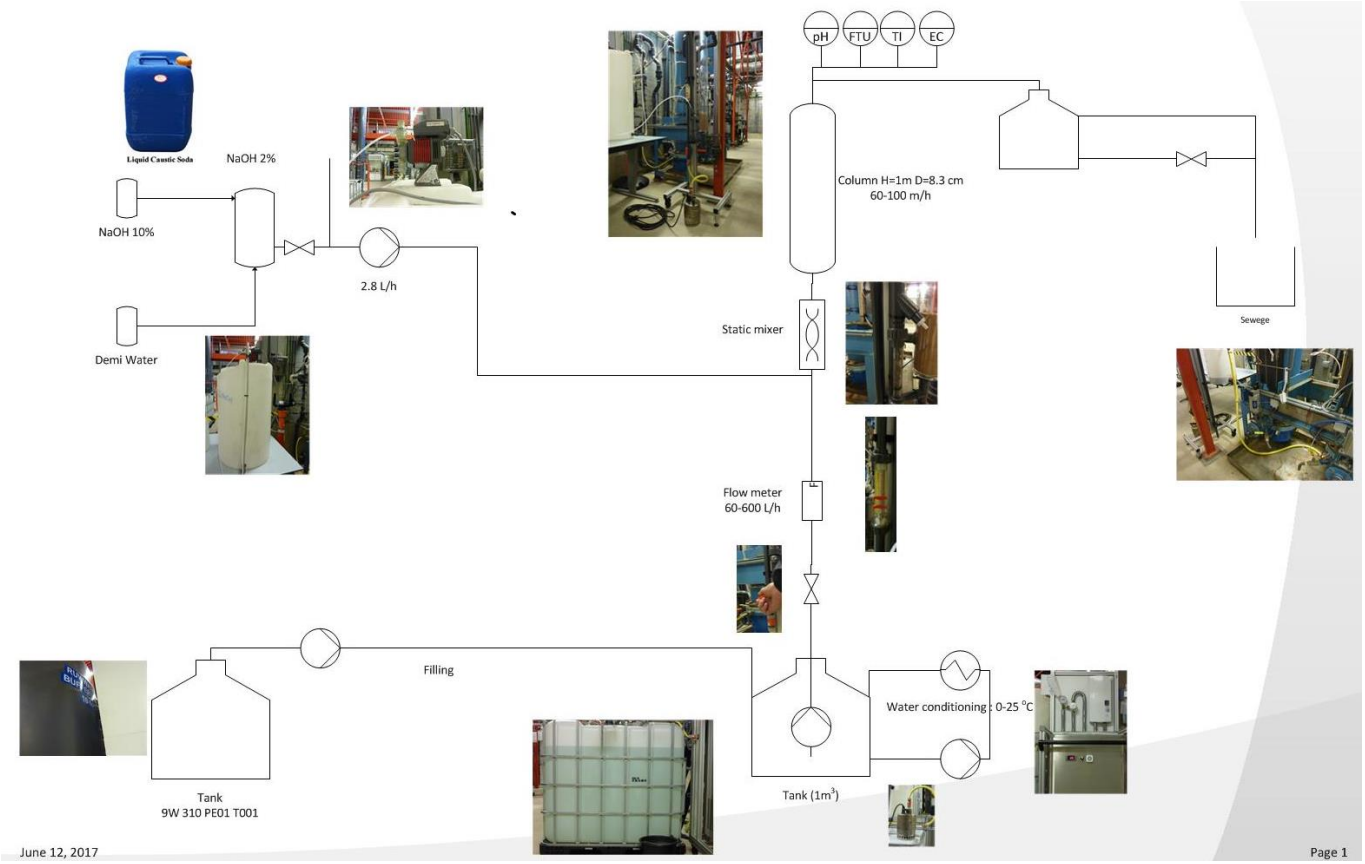

Figure 14 PFR fluidized bed experiments set up

Experimental procedure

The experimental procedure that was followed during the PFR fluidized bed experiments is described below:

- The temperature of the natural water was adjusted using the AEG boiler and heat exchanger before the beginning of each experiment. The conditioned water was stored in the 1m^3 vessel.
- At the beginning of the experiment the conditioned water was pumped through the column and the flow was stabilized to 420-460 L/h in order to achieve a superficial velocity of approximately 80 m/h inside the reactor. The flow of water was checked twice using the flow meter and the marked vessel.
- The pH, EC, turbidity and temperature probes were first calibrated and then inserted into the column and the logging of the measured values was started. The initial values that were obtained were used to verify the in-line and laboratory measurements of the influent stream in WPK water treatment plant.

- In the next step, the volume and the frequency of the caustic soda pump were adjusted in order to achieve the desired pH in the bottom of the reactor. In all experiments, the pH in the bottom of the reactor was, approximately, pH= 9.5 while the flow of the dosing pump was ranging between 1.2-1.3 L/h. The volume of the caustic soda that was added to the solution was verified using the level indicators in the storage vessel.
- In each experiment 4 to 5 layers of seeding material were added with a fixed bed height ranging between 5, 10 and 15 cm. Each layer was weighted before it is added to the column. After a layer was added, the probe remained in the column for approximately 20 minutes until steady-state conditions were reached. Then, the probe was removed for a short period of time, the next layer was added and the probe was placed again inside the column, a few centimeters above the fluidized layer. The measurements of pH, EC, turbidity and temperature on top of every layer were recorded using both logged and handwritten data. The flow of the dosing pump and water pump was checked several times during the experiment and flow adjustments were applied if necessary.
- At the end of the experiment, the dosing of caustic soda was stopped and the column was washed using raw water. Afterward, the column was drained and the seeding material was removed. The seeding material that was used, was put in the oven at 105 ˚C to dry. The same seeding material was reused to later experiments. It is considered that no significant change in the diameter of the seeding pellets takes place since the duration of the experiments is relatively short.
- Due to the scaling of the water input at the bottom of the column, the water flow was reduced during the experiments. To avoid the scaling of the water input after each experiment a 10% w/w HCl was added in the column. The hydrochloric acid was removed before the start of the next experiment.

Overview of PFR fluidized bed experiments

Four PFR fluidized bed experiments took place in WPK pilot plant. In Experiments 6 and 7, 1330 g/L of calcite pellets with diameter d=1-1.12 mm were used and the temperature was adjusted at 11 ˚C and 20 ˚C respectively. The specific surface area (SSA) offered in Experiments 6 and 7, based on the mass and the volume of the fluidized bed is ranging between S=5200-6200 m^2/m^3. On the other hand, in Experiments 8 and 9, 860 to 920 g/L of crushed calcite pellets with diameter d=0.5-0.6 mm were used as a seeding material. The calcium carbonate crystallization rate was investigated again at two temperatures at 11 ˚C and 20 ˚C. The specific surface area (SSA) of the seeding material in Experiments 8 and 9 was ranging between S =4700-6100 m^2/m^3. In Table 5 the overview of the PFR fluidized bed experiments are shown:

Table 3 Overview of fluidized bed experiments

	Date	Temperature	Seeding material	Diameter	Concentration (g/L)	Specific Surface Area
Experiment 6	16/8/2017	11 ˚C	Calcite pellets	d=1-1.12 um	1330 g/L	Ranging from 5200-5900 m^2/m^3
Experiment 7	15/8/2017	20 ˚C	Calcite pellets	d=1-1.12 mm	1360 g/L	Ranging from 5500-6200 m^2/m^3
Experiment 8	15/8/2017	11 ˚C	Crushed calcite	d=0.5-0.6 mm	862 g/L	Ranging from 4700-5600 m^2/m^3
Experiment 9	13/9/2017	20 ˚C	Crushed calcite	d=0.5-0.6 mm	917 g/L	Ranging from 5000-6100 m^2/m^3

4.3. Experimental results

Firstly, the water quality as described by the in line and laboratory measurements at WPK treatment plant and the measured values in the WPK pilot plant is checked. The charge balance error is calculated to verify that no major components were omitted during the chemical composition analysis. In all of the experiments, the charge balance error is less than 3%. Furthermore, the Electrical Conductivity is measured in the WPK laboratory at a temperature of 20 ˚C. PHREEQC is able to calculate the electrical conductivity at the temperature of the solution based on the concentration of the water components and pH. The deviation between the measured and calculated EC is approximately 2%. Overall, the water analysis seems to describe adequately the quality of the natural influent water that was used.

In Figure 15 the experimental results of the PFR fluidized bed experiments are shown.

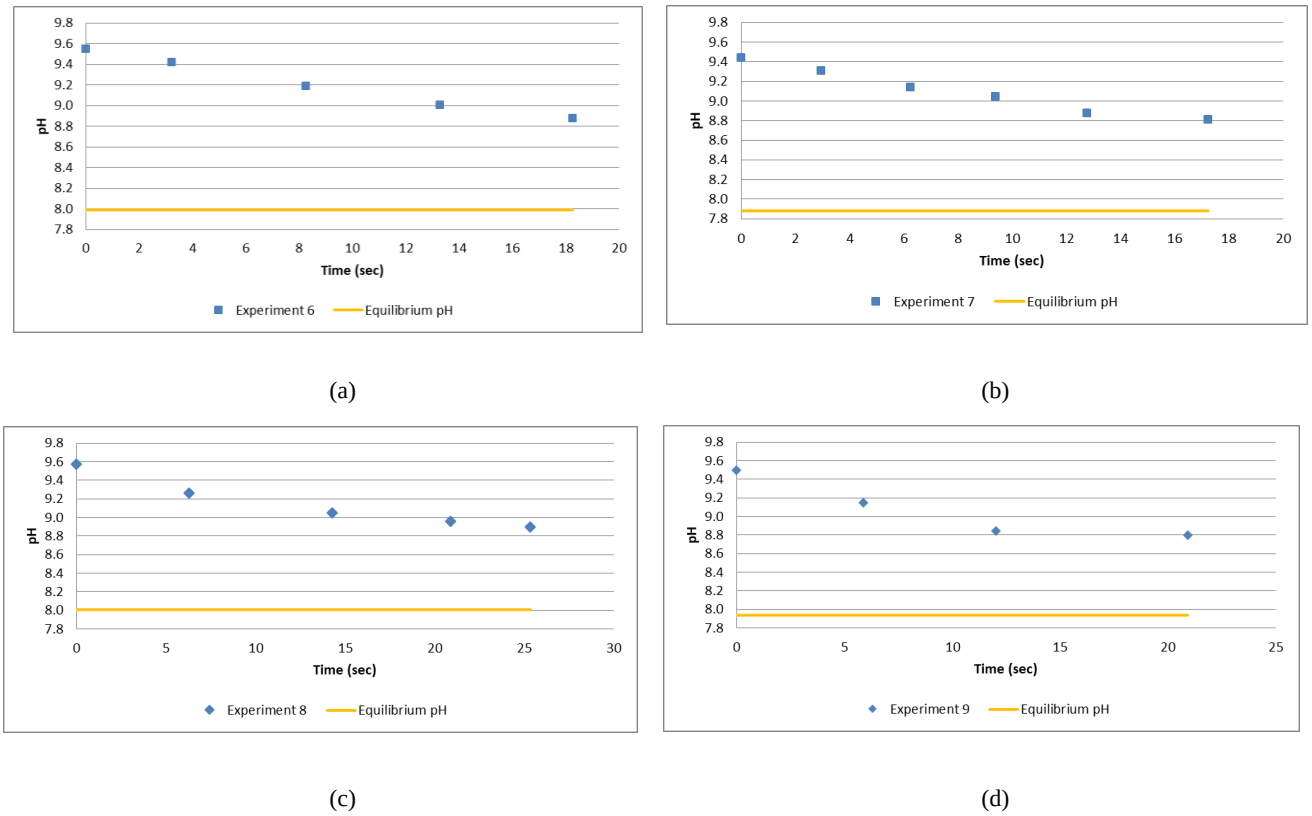

Figure 15 Measured pH values for: (a) Experiment 6 (with calcite pellets at 11°C), (b) Experiment 7(with calcite pellets at 20°C) (c) Experiment 8 (with crushed calcite at 11°C) (d) Experiment 9(with crushed calcite at 20 °C)

5

Modeling of a pellet softening fluidized bed reactor

5.1. Introduction

For the modeling of a pellet softening fluidized bed reactor the model of Van Schagen has been used in WPK water treatment plant. The model of Van Schagen (2008 b,c) is basically an empirical model. It has been derived by fitting to the pH and Ca measurements from full-scale pellet softening fluidized bed reactors to a linear equation between the rate of calcium carbonate crystallization and supersaturation. In order to check the applicability and possibility of improvement of the Van Schagen model several steps were followed.

Firstly, the validity of the equation proposed by Wiechers et al. (1975), that the Van Schagen model, was based, was investigated. Therefore, the results of the experiments of this research were compared with Wiechers research. The main difference in the experimental conditions of this research compared to the experiments by Wiechers is that natural water is used instead of artificial hard water. It can, therefore, be tested if the same rate of crystallization as in Wiechers research can be measured if natural water is used instead of artificial hard water.

Secondly, the general concept of a linear relationship between crystallization and supersaturation was tested. Other researchers such as Van Schagen (2008 b,c), Van Dijk and Wilms (1991) have also proposed a linear relationship between the rate of crystallization and supersaturation (§2.6.2). However, in these cases, the rate constant has been determined to fit the measured data of each research. However, the applicability of the equation was not proven.

The Wiechers equation has several disadvantages such as the fact that the rate constant should be corrected every time a different seeding material is used. It is, therefore, not suitable to prove the linear relationship between the hardness reduction rate and supersaturation. As a result, a new linear equation was proposed, the one-rate-constant model (§2.6.3). The experimental results were compared with the linear model to determine if a linear equation can be used to describe the rate of calcium carbonate crystallization.

Based on the results of this research, the linear relationship cannot be used to predict the calcium carbonate crystallization rate when natural water is used. In order to explain these deviations from linearity, it is assumed that the presence of inhibitors is affecting the rate of crystallization. This assumption is supported by literature. The concentration of organic carbon and magnesium is higher than the minimum concentration that is inhibiting calcium carbonate crystallization found in literature (§2.3.5). The combined effect of the inhibitors can cause a reduction of calcium carbonate crystallization rate at low supersaturation. Dreybrodt has also observed a bending of the curve in the rate of crystallization against supersaturation graph. In this research as well as in the research of Dreybrodt, the bending of the curve was attributed to inhibition in combination with a change in the mechanism of crystallization. Nevertheless, no microscopic research was conducted to confirm this assumption.

However, it is an explanation for the deviation between the experiments of Wiechers and this research of the research of Dreybrodt.

An empirical model needs to be developed that would describe sufficiently well the non-linear relationship between supersaturation and crystallization rate. This model could be used to practical applications in order to predict accurately the calcium removal during softening and maintain an overview of the crystallization process. The linear equation of Dreybrodt was taken into account during the development of the model. There are two possible options to model the curved lines:

- The two-rate-constants model [equation (32)]
- The exponential Lasaga model [equation (24)]

The model of Lasaga (1987) (see §2.6.2) can be calibrated by determining the exponents in order to fit the curve in the graph of the rate of calcium carbonate crystallization against saturation ratio. In this case, a fluent equation is used that is not separated into two pieces. However, if the Lasaga model is used, it is very difficult to maintain an overview of the dependence of the rate of crystallization from the saturation ratio. The physical meaning of the equation, in this case, is no longer visible and the equation is simply curve fitting. On the other hand, when two simple linear equations are used, the linear dependence of the rate of crystallization on the saturation ratio is clear. In our working field simplicity through linearization is important since it is possible to maintain an overview of the dependence of the rate of calcium carbonate crystallization from the model parameters. It must be noted though, that a linear model is not a realistic description of natural processes. Nevertheless, it is considered an accurate approximation for the purpose of this research

In this research, the two-rate-constants model was used instead of the Lasaga model. Therefore, two linear equations that describe the relationship between the rate of calcium carbonate crystallization and the saturation ratio were chosen.

5.2. Methodology of data processing from STR batch experiments

In this section, the method that was used for the processing of the experimental data of the STR batch reactor experiments is shown. The procedure that was followed can be divided into 3 steps. Firstly, the influent water quality was inserted in PHREEQC and the temperature was adjusted in the model. Then the initial pH of the solution was calculated and a polynom was used to smoothen the pH measurements. The method of deriving this polynom is explained in detail in §3.3. Secondly, the rate of calcium carbonate crystallization during the experiment was determined.

Determining the rate of calcium carbonate crystallization based on the pH reduction during the experiment

The pH reduction data that were obtained during the experiments were processed in order to define the calcium carbonate crystallization rate. The data processing methodology is described below. The pH measurement in time (based on the polynom) were inserted to PHREEQC. For each time step, the equilibrium in the solution was calculated. Hence, the concentrations of total calcium, calcium ions and carbonic species were determined. It was also possible to determine the saturation index and the saturation ratio of calcite. The rate of calcium carbonate crystallization was determined using the equation:

$$-\frac{Ca_i - Ca_{i-1}}{t_i - t_{i-1}} \qquad (36)$$

Where Ca_i and t_i is the calcium concentration and the time during time step I and Ca_{i-1}, t_{i-1} are the calcium concentration and time of the previous time step. The rate of calcium concentration was plotted against the saturation ratio SR_{i-1} of the previous time step. In this step, it was investigated whether the

experimental data plot in a straight line or there is a bending in the curve as Dreybrodt et al. (1997) noticed. In order to further investigate which model predicts better the experimental data, three models were used to predict the pH and calcium reduction during the experiments. The modeling results were compared with the measured pH and the equation that best describes the reaction was defined. The models that were tested are:

- The Wiechers model [equation(18)]
- The one-rate-constant model[equation (29)]
- The two-rate-constants model[equation(23)]

The models are described in detail in §2.6.2.

A preliminary rate constant value for the one-rate-constant model can be obtained from the slope of the linear trend line in the graph of calcium carbonate crystallization rate against saturation ratio for the one–rate-constant model. By trial and error, the final values of the model input parameters that result in the best fit between the measured and modeled data were derived.

5.2.1. Comparison of the STR batch experimental results with the model of Wiechers

In this section, it is tested whether the equation (18) and rate constant $k_{W,T}$ that was proposed by Wiechers can sufficiently well describe the experimental results of this research. Wiechers has conducted experiments using calcite powder as seeding material. The $k_{W,T}$ value is calculated using equation (19) for the experiments of this research. The results are shown in Table 4. The pH reduction in time, based on the model of Wiechers, is plotted in the same graph as the experimental results. It can, therefore, be evaluated whether the model is predicting accurately the experimental results of this research.

Table 4 Overview of batch reactor experiments k_T and $k_T * S$ values based on Wiechers

	Temperature	**Seeding material**	**Concentration**	**$K_{W,T}$ (mol L^{-1}* s^{-1} $(mg/L)^{-1}$)**	**$K_{W,T}$ *S (mol L^{-1}* s^{-1})**
Experiment 1	20 °C	Calcite Powder d=14-24 um	Conc=1 g/L	0.0255	25.5
Experiment 2 (Duplicate)	10 °C	Calcite Powder d=14-24 um	Conc=30 g/L	0.0152	456
Experiment 3	5.5 °C	Crushed Calcite d=0.5-0.6 mm	Conc=74 g/L	0.0121	892
Experiment 4	10 °C	Crushed Calcite d=0.5-0.6 mm	Conc=74 g/L	0.0152	1126
Experiment 5	20 °C	Crushed Calcite d=0.5-0.6 mm	Conc= 74 g/L	0.0255	1887

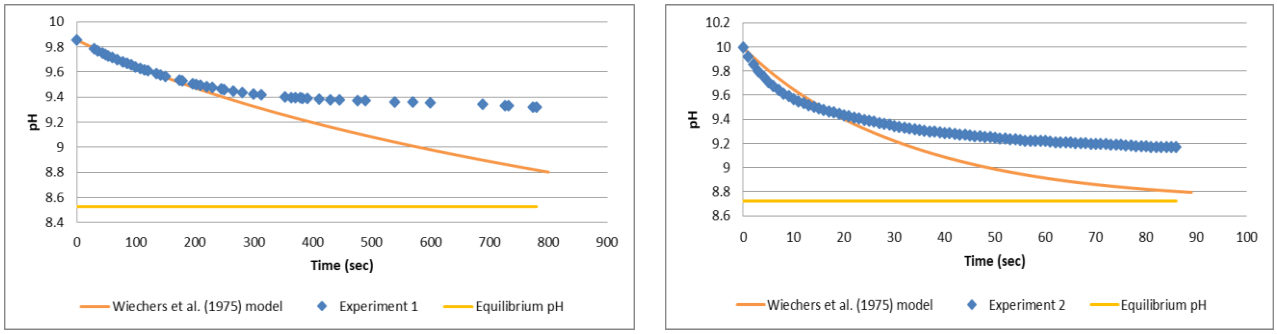

(a) (b)

Figure 16 Comparison between the pH measurement of (a) Experiment 1 and (b) Experiments 2a and 2b with the Wiechers model

It can be clearly seen in Figure 16 (a) that the Wiechers equation (18) follows accurately the experimental results for the first 200 seconds. However, after approximately 200 seconds the rate of crystallization reduces and the predicted values deviate significantly from the measured pH. The same observation can be seen in Figure 16 (b). At the beginning of Experiment 2, the pH measurement is slightly underestimating the Wiechers model prediction. However, after the first 10 seconds, there seems to be a significant reduction in the calcium carbonate crystallization rate and the experimental data deviate from the modeled values.

The reasons that the equation derived by Wiechers cannot approximate the experimental data of this research sufficiently well are:

- The powder that was used in the Wiechers experiments is different than the powder used in the experiments of this research. In particular, the diameter of the calcite powder particles used in the Wiechers research was d_{50}=4.6-10 um while in this research calcite powder particles with a larger diameter d_{50}=24um were used. Therefore, there could be a deviation between the specific surface area offered in this and the experiments of Wiechers.
- In the research of Wiechers et al. (1975) artificial hard water was used while in this research the experiments were conducted with untreated water with various inhibiting compounds. Thus, the reason for the reduced rate could be the inhibiting effect of these compounds on the calcium carbonate crystallization process. Nevertheless, further investigation is necessary to determine the role of the inhibitors in calcium carbonate crystallization kinetics.

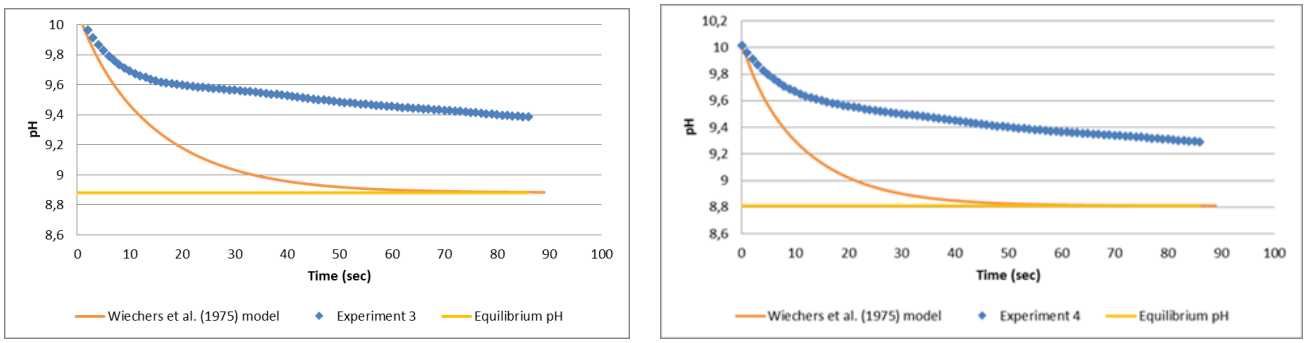

(a) (b)

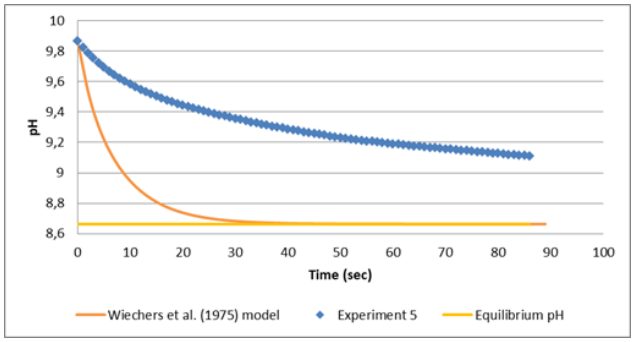

(c)

Figure 17 Comparison between the prediction of the pH by Wiechers model and (a) Experiment 3 (b) Experiment 4 (c) Experiment 5

It can be seen from Figure 17 that in Experiments 3 to 5, Wiechers equation is largely overestimating the calcium carbonate growth rate. The reason for this deviation is that the diameter of the crushed calcite pellets is 3 times larger than the diameter of the calcite powder particles. So, the specific surface area that was offered in Experiments 3, 4, 5 was approximately 3 times lower compared to the specific surface area of the same concentration of powder. Since in Wiechers model the concentration of the seeding is used instead of the SSA, in the case of crushed calcite pellets the equation largely overestimates the surface area of the seeding material and thus the rate of calcium carbonate crystallization. It is not possible to correct the rate constant for using a different kind of seeding material since the diameter of the calcite powder used by Wiechers is not precisely known. Furthermore, a different correction each time a seeding material with a different diameter is used should be applied.

5.2.2. Comparison of the STR batch experiments with one-rate-constant and two-rate-constants model

Firstly, the rate of crystallization is plotted against saturation ratio (Figure 18) to determine whether the linear relationship proposed by Wiechers or the curved line observed by Dreybrodt et al. (1997) is found during the experiments of this research. In particular, it is checked whether the experimental data plot in a straight line that intercepts with the x-axis at (0,1) as it is assumed in the one-rate-constant model. It can be clearly seen that the purple line, that represents the one-rate-constant model, is not giving an accurate description of the experimental results.

Alternatively, if two linear equations are used, a higher correlation between the lines and the experimental data is observed. Therefore, the two-rate-constants model that consists of two linear equations proposed in §2.6.2 is predicting more accurately the experimental data. A preliminary value for the high rate constant can be derived from the slope of the red line while the green line is used to derive a preliminary value for the low rate constant.

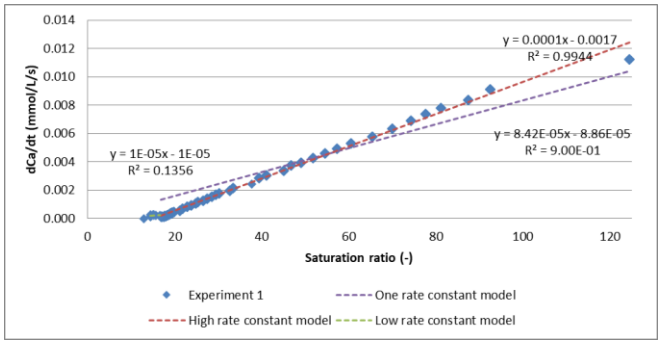

(a)

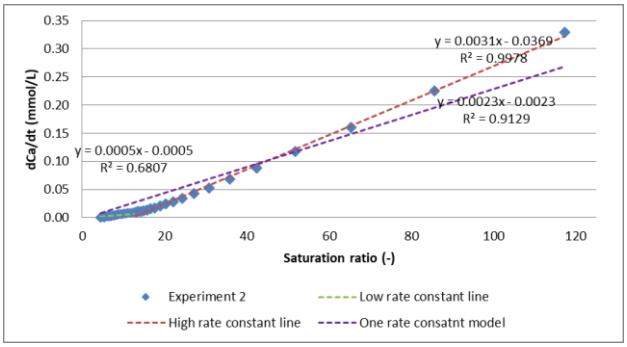

(b)

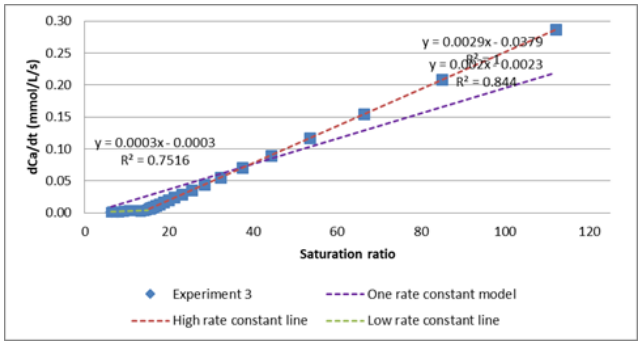

(c)

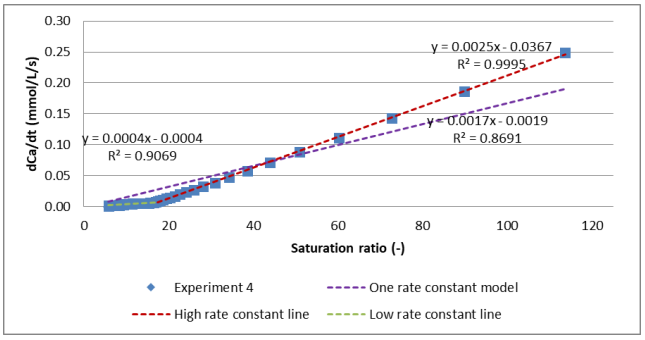

(d)

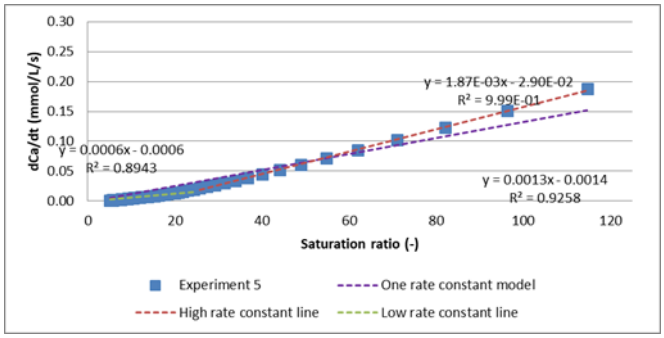

(e)

Figure 18 Crystallization rate against calcite saturation ratio of : (a) Experiment 1 (b)Experiment 2 (c)Experiment 3 (d)Experiment 4 (e) Experiment 5

To confirm the findings above the experimental measurements are also compared with the predictions of the one-rate-constant and two-rate constants model. Using the slope of the purple line in Figure 18 a preliminary value for the rate constant $k * K_{SP} * S$ is determined. The final $k * K_{SP} * S$ value is determined with trial and error based on how well the results of the model approximate the measured values. The pH and Ca reduction graph during the experiments are derived using the one-rate-constant model and are compared with the measured pH during the experiment Figure 19.

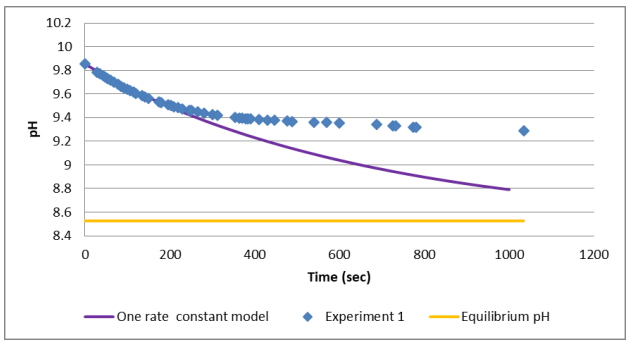

(a)

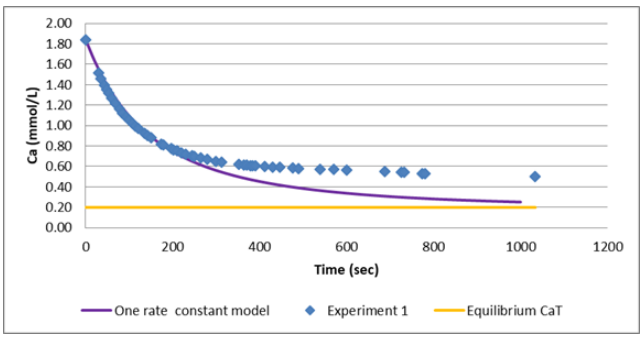

(b)

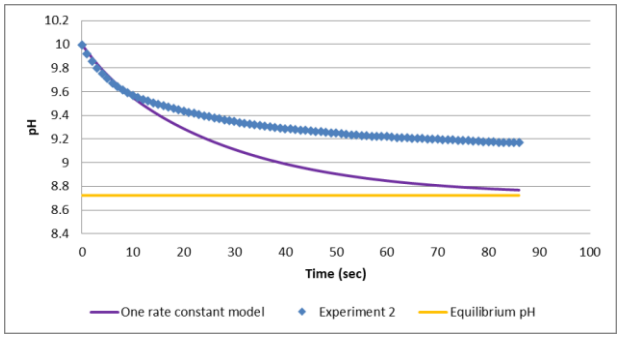

(c)

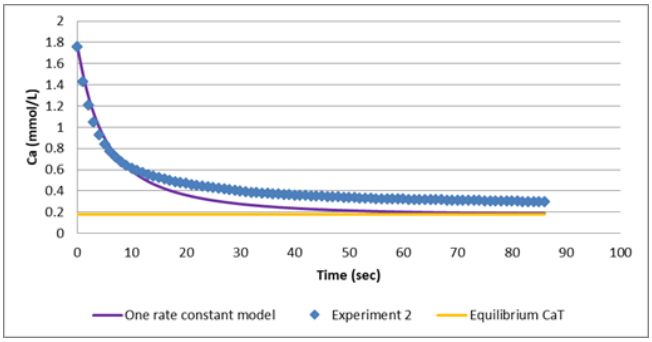

(d)

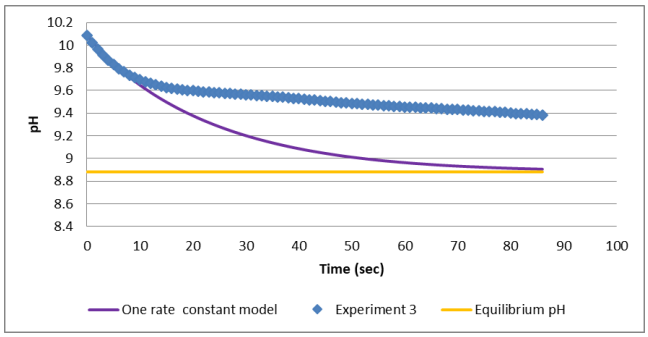

(e)

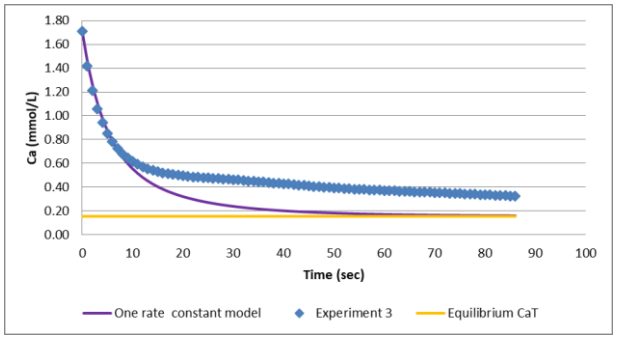

(f)

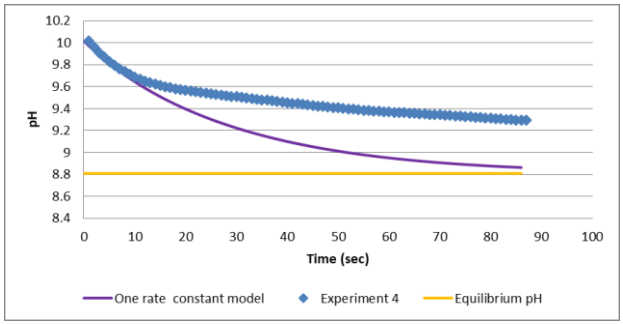

(g)

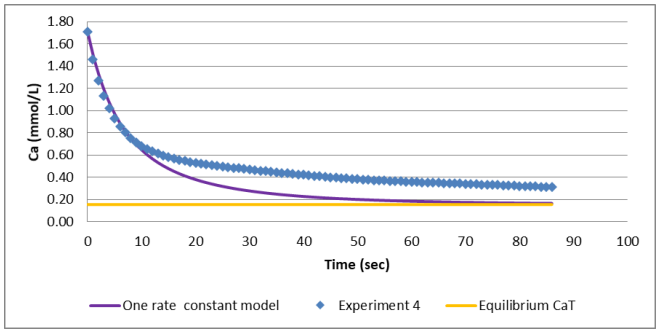

(h)

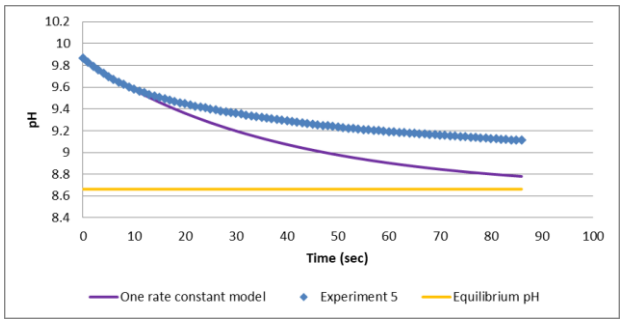

(i)

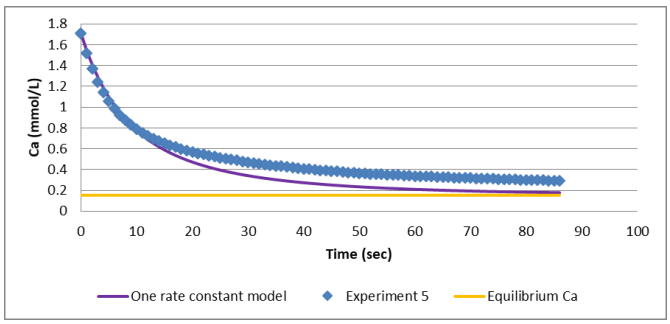

(j)

Figure 19 Measured pH and modeled pH reduction and Ca concentration using the one-rate-constant model of: (a) and (b) Experiment 1, (c) and (d) Experiment 2, (e) and (f) Experiment 3, (g)and (h) Experiment 4, (i) and (j) Experiment 5

As it can be seen from Figure 19 the pH and calcium concentration reduction is predicted accurately for the first seconds of the experiments. After this period, the one-rate-constant model overestimates the calcium and pH reduction. It is, therefore, not possible to predict accurately the beginning as well as the later phase of the experiment using the one-rate-constant model.

Alternatively, a two-rate-constants model can be used. In Figure 20 the measured and modeled pH and calcium reduction using the two-rate constants model is presented.

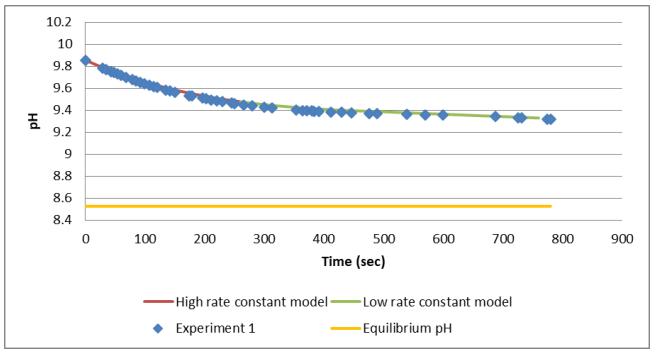

(a)

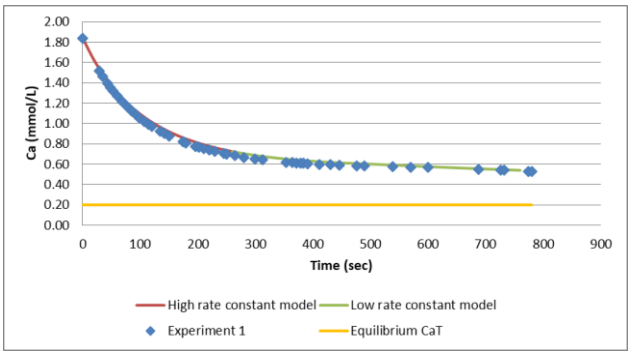

(b)

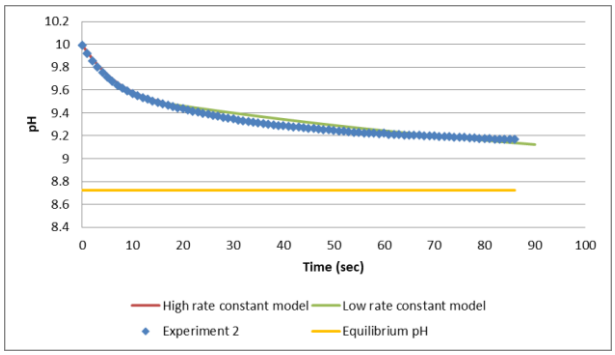

(c)

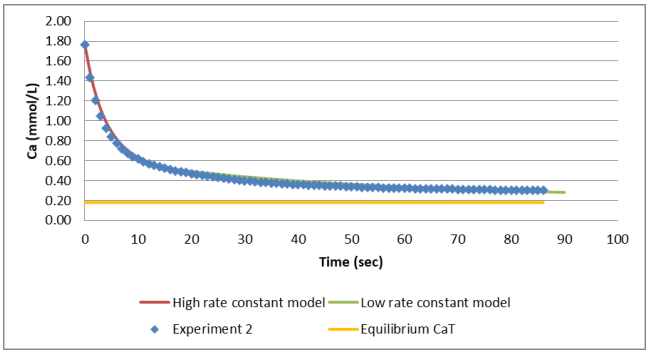

(d)

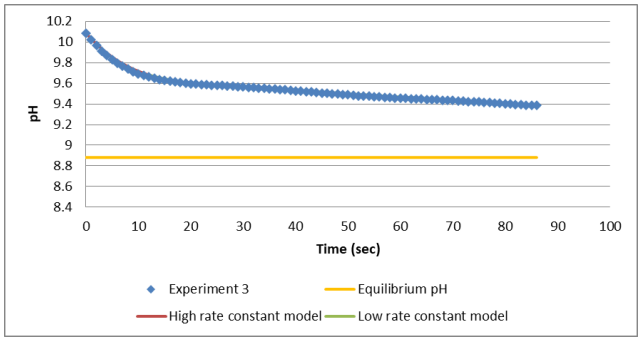

(e)

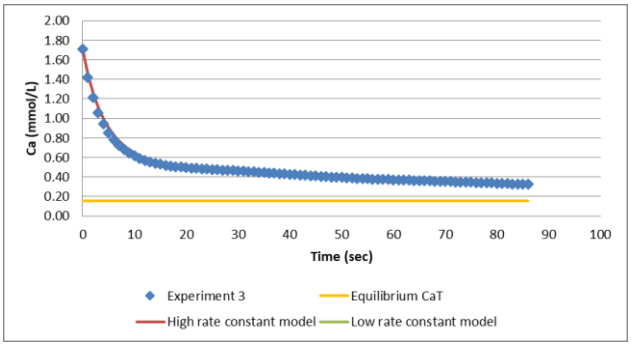

(f)

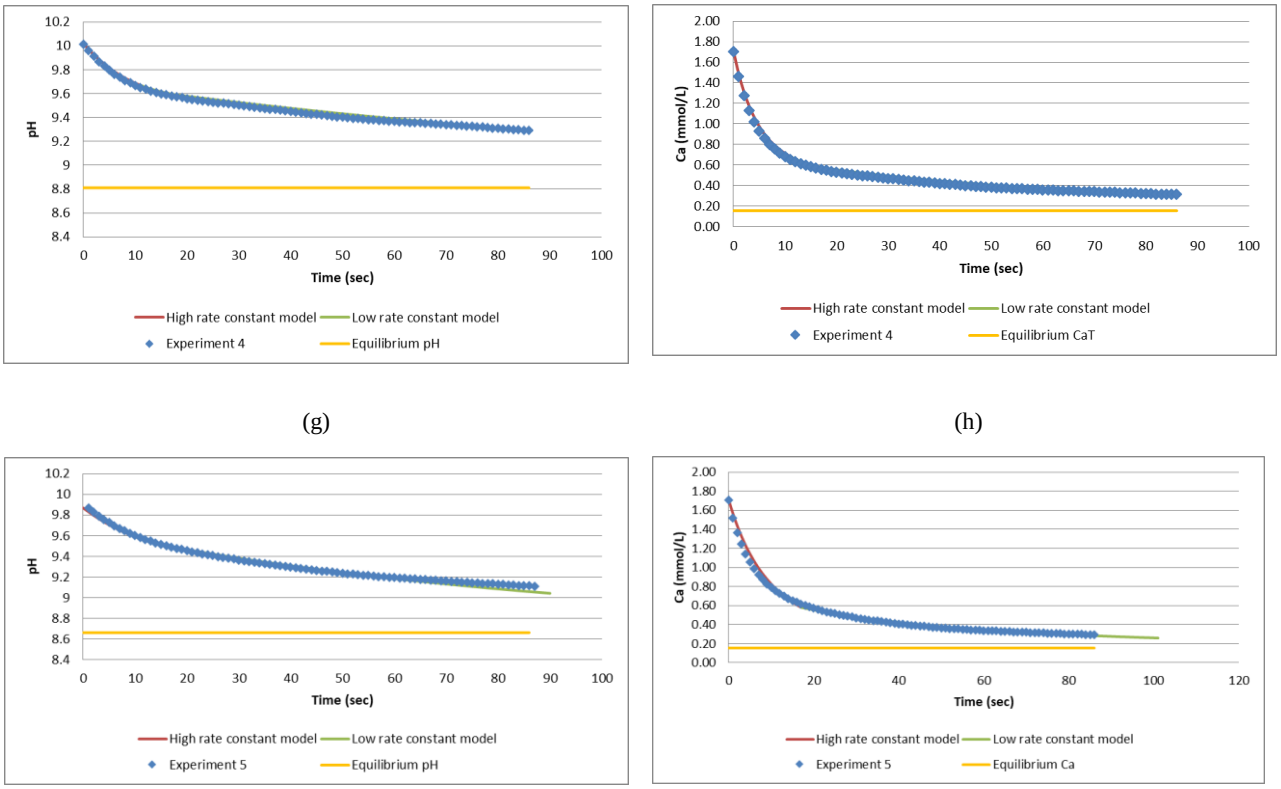

Figure 20 Measured pH and modeled pH reduction and Ca concentration using the two-rate-constants model of: (a) and (b) Experiment 1, (c) and (d) Experiment 2, (e) and (f) Experiment 3, (g) and (h) Experiment 4, (i) and (j) Experiment 5

Based on Figure 20 the two-rate-constants model is predicting much better the experimental results than the one-rate-constant model and the Wiechers model. In the following table, an overview of the results of the two-rate-constants model from the experimental data processing of the STR batch reactor experiments is shown. The $k_H * K_{sp} * S$ and $k_L * K_{sp} * S$ values of the two-rate-constants model are shown as well as the saturation ratio that the change from the "high" rate constant to the "low" rate constant takes place.

Table 5 Overview of the two-rate-constants model $k*K_{sp}*S$ values for the STR batch experiments

	Temperature	Seeding material	Concentration	$k_H*K_{sp}*S$ (mmol/L* s^{-1})	$k_L*K_{sp}*S$ (mmol/L* s^{-1})	SR_{CH}	A_H
Experiment 1	20 °C	Calcite Powder d=14-24 um	Conc=1g/L	0.000114	0.000015	17	15
Experiment 2 (Duplicate)	10 °C	Calcite Powder d=14-24 um	Conc=30g/L	0.0031	0.0005	14	12
Experiment 3	5.5 °C	Crushed Calcite d=0.5-0.6 mm	Conc=74g/L	0.0029	0.00025	14.5	13
Experiment 4	10 °C	Crushed Calcite d=0.5-0.6 mm	Conc=74g/L	0.0025	0.0004	17	15
Experiment 5	20 °C	Crushed Calcite d=0.5-0.6 mm	Conc=74g/L	0.0019	0.0006	21.8	15

In Experiment 1 a concentration of calcite powder similar to the concentration of seeding material in Wiechers experiments was used. In Experiment 2, however, 30 times higher concentration (and therefore SSA) of seeding material was added than in Experiment 1. If the $k_T * K_{sp} * S$ values derived from Experiment 1 and Experiment 2 are compared, it can be seen that in Experiment 2 an approximately 30 times higher value is used. This observation is based on the assumption that the temperature does not have a significant effect on the calcium carbonate crystallization when it is ranging between 10-20 ˚C (as it was shown from the experiments of this research). It can, therefore, be concluded that the rate of crystallization remains proportional to the specific surface area, even if a much higher concentration of seeding material is used than in Wiechers experiments.

5.3. Methodology of data processing from PFR fluidized bed experiments

In this section, the method that was used for the processing of the experimental data from the PFR fluidized bed reactor experiments is shown. The procedure that was followed can be divided into 3 steps.

Determining the natural water quality

For the determination of the initial water quality the online measurements of WPK water treatment plant were used. For the components that are not continuously measured, laboratory results were available. Since the quality of the water from the influent of the WPK treatment plant does not change significantly with time it is considered that the water composition is adequately described.

Determining the water quality of the initial solution after NaOH dose is added

Firstly, the temperature of the natural water solution was adjusted in the model to the temperature that the experiment was conducted. Then the NaOH dose was also added to the solution in the PHREEQC input sheet in order to achieve an initial pH of approximately 9.5. It must be noted that during the experiments demineralized water instead of natural water was used for the preparation of the NaOH solution dose. Therefore, by assuming in the PHREEQC model that only moles of NaOH are added and not a solution of NaOH is mixed with the natural influent water an error is introduced to the calculations. However, since the volume of the dose is lower than 1% of the total volume of the water that was used, the error in the concentrations of the components of the influent water, was very small and is considered acceptable for the accuracy of these experiments.

Determining the rate of calcium carbonate crystallization based on the pH reduction during the experiment

The pH reduction data that were obtained during the experiments were processed in order to define the calcium carbonate crystallization rate. The data processing methodology is described below.

- For each experiment only 4-5 pH measurements, for an empty reactor and on top of every layer, are available. The pH measurements were inserted to the PHREEQC and for each time step, the equilibrium in the solution was calculated. Hence, the concentrations of total calcium, calcium ions and carbonic species were determined. It was also possible to calculate the saturation index and the saturation ratio of calcite.
- The contact time for each layer was determined. For the calculation of the contact time, the following parameters were calculated

  - The porosity was determined using equation (12).

  -The flow Q ($\frac{m^3}{s}$) of the water inside the reactor was known.

  -The area of the reactor A_r was calculated based on the diameter of the column.

However, the reactor was also filled with seeding material

-The area of the reactor $A = \frac{A_r}{p}$ in m² that is not filled with seeding material was calculated.

-The real velocity in the reactor was therefore $v = \frac{Q}{A} = \frac{Q}{A_r * p}$ in (m/s).

The contact time was calculated by dividing the total height of the fluidized bed with the velocity

$$t_i = \frac{H_{tot}}{v} = \left(\frac{\Sigma h_i}{v}\right) \quad (37)$$

Where t is the contact time in s, H_{tot} is the total height of the fluidized bed and v is the velocity in m/s. It was, therefore, assumed that the time of the calcium carbonate crystallization reaction in a layer is the time that it takes for the water to pass through that layer. By determining the rate of crystallization in time the results of the PFR fluidized bed experiments can be compared with the results of the STR batch experiments.

- The rate of calcium carbonate crystallization was calculated and plotted against the supersaturation ratio SR. The calcium concentration and SR in each layer were determined using PHREEQC. Then, equation (36) was used to determine the rate of calcium reduction in time. The time step, in this case, is the time it takes for the water to pass through each layer. The rate of crystallization was plotted against the saturation ratio SR_{i-1} of the previous time step. In this step, it was investigated whether the experimental data plot in a straight line or there is a bending in the curve as Dreybrodt et al. (1997) noticed.
- The one-rate-constant equation and the two-rate-constants model that has been derived from the STR batch experiments were used to predict the hardness reduction during the PFR fluidized bed experiments and produce the pH and calcium graphs. The derived graphs were compared with the experimental results and the model that best fits the measured data was determined. A preliminary rate constant value for the one- rate-constant and two rate constants model can be obtained from the slope of the linear trend line in the graph of calcium carbonate crystallization rate against saturation ratio for the one–rate-constant model.

5.3.1. Comparison of PFR fluidized bed experiments with one-rate-constant and two-rate-constants model

Firstly the rate of crystallization the plot of the rate of calcium carbonate crystallization against supersaturation is shown in Figure 21.

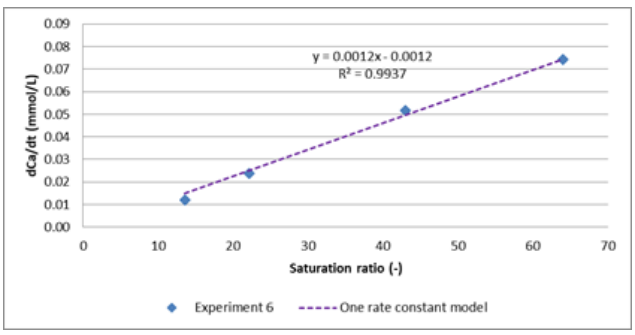

(a)

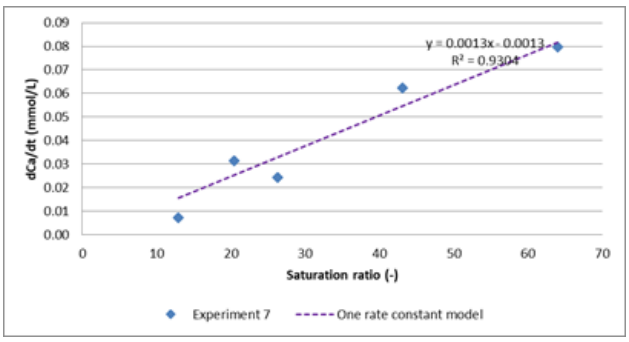

(b)

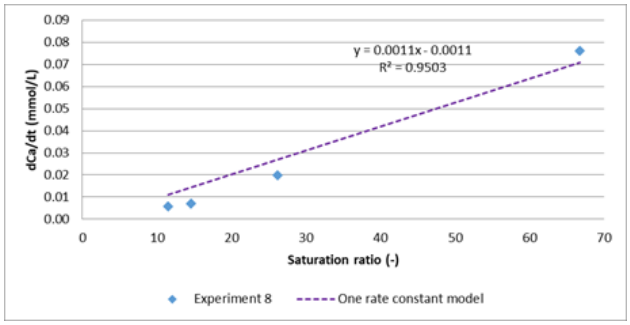

(c)

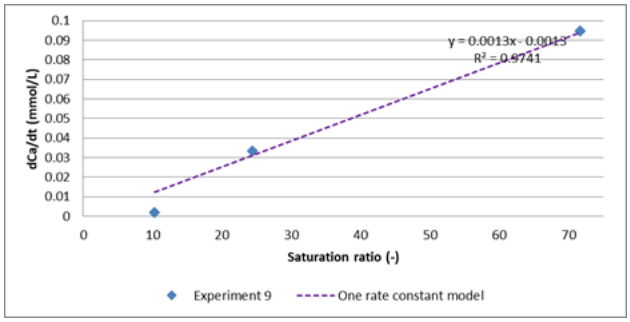

(d)

Figure 21 Crystallization rate against calcite saturation ratio of: (a) Experiment 6, (b) Experiment 7, (c) Experiment 8 (d) Experiment 9

The experimental data in this experiment seem to plot sufficiently well in a straight line that is passing from the point (1,0) in all PFR fluidized bed experiments. Therefore, a linear model can be used to describe the rate of calcium carbonate crystallization in a PFR fluidized bed experiment.

In Figure 22 the measured and modeled pH and Ca reduction using one-rate-constant model is shown:

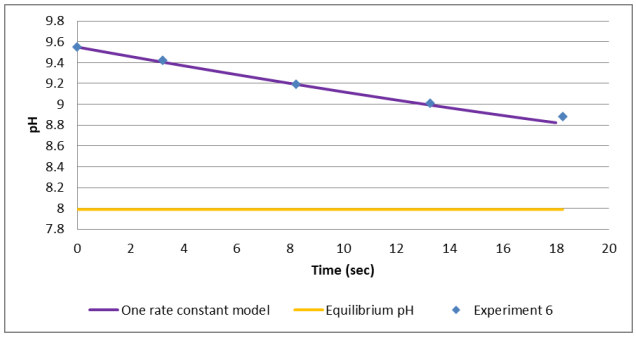

(a)

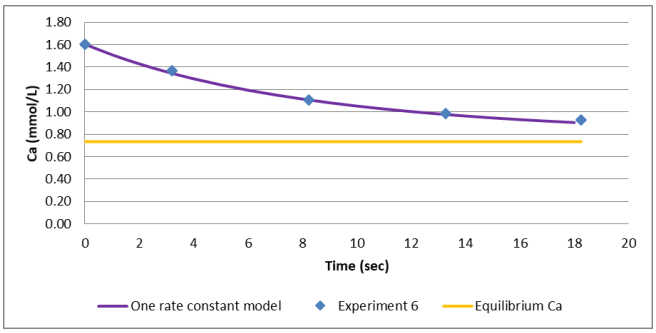

(b)

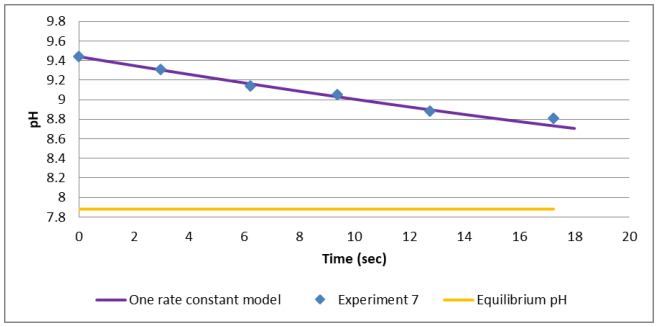

(c)

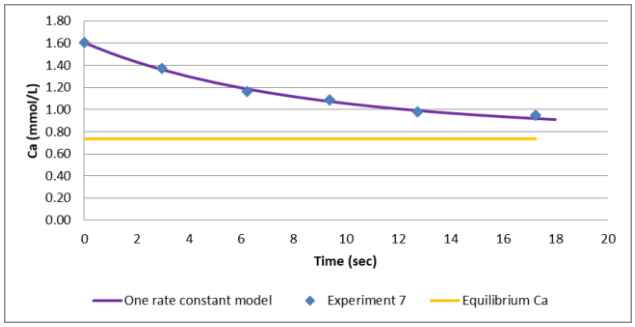

(d)

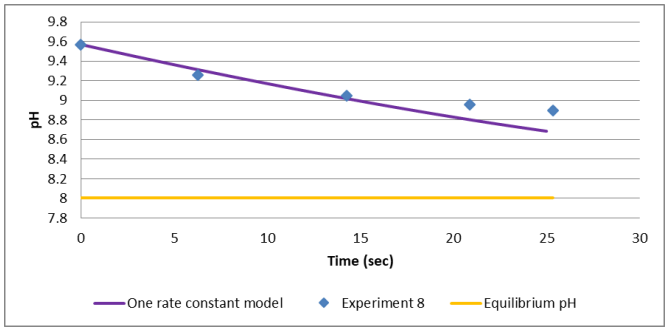

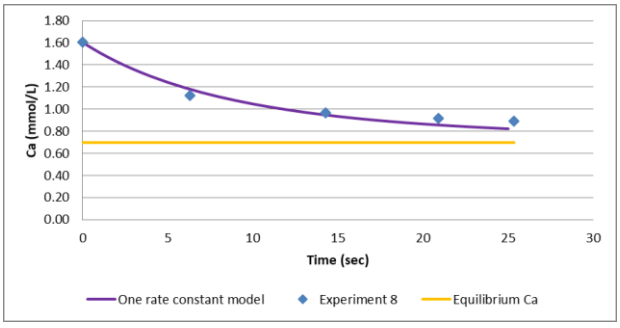

(e) (f)

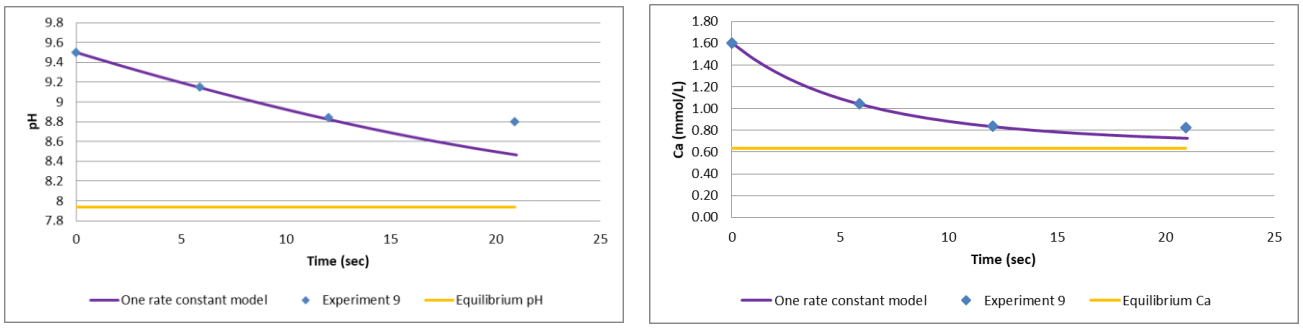

(g) (h)

Figure 22 Measured pH and modeled pH reduction and Ca concentration using the one-rate-constant model of: (a) and (b) Experiment 6, (c) and (d) Experiment 7, (e) and (f) Experiment 8, (g)and (h) Experiment 9

From Figure 22, it can be seen that the one-rate-constant model is describing the experimental results sufficiently well. However, the final measured pH points are deviating from the modeled pH line in all experiments. Therefore, the pH at the top of the reactor is slightly different from the pH value based on the model. The difference is ranging from 0.06 for Experiments 6 and 7 to 0.2-0.3 for Experiments 8 and 9. Therefore, it is possible that these last points are deviating from the low rate constant line because at the upper region of the column, that supersaturation is low, the rate of calcium carbonate crystallization has significantly decreased. It is assumed that the reasons that this reduction of the calcium carbonate rate cannot be clearly observed, as in the STR batch experiments are:

- The contact time during the column experiments is not long enough. A higher column is necessary in order to observe the change from the high rate constant line to the low rate constant line.
- There are not sufficient measured pH points in the upper part of the reactor that the supersaturation has significantly reduced and the effect of the inhibitors may be important.

Alternatively, the two-rate-constants model that is derived from the STR batch experiments can be used. In this case, a preliminary value only for the high rate constant can be derived from Figure 18. In Figure 23 the measured and modeled pH and Ca reduction using the two-rate-constants model are shown:

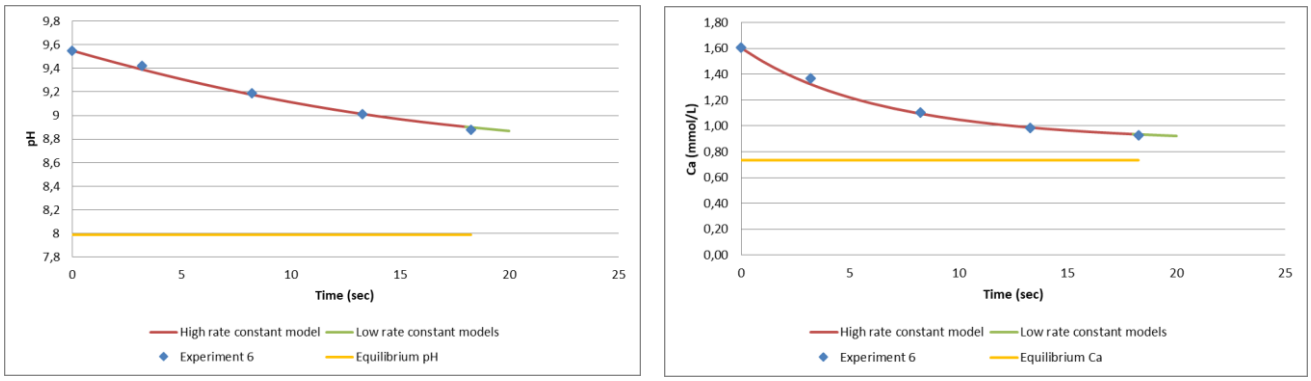

(a) (b)

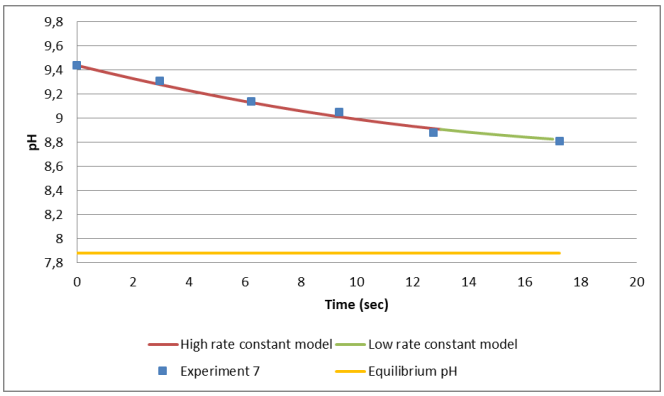

(c)

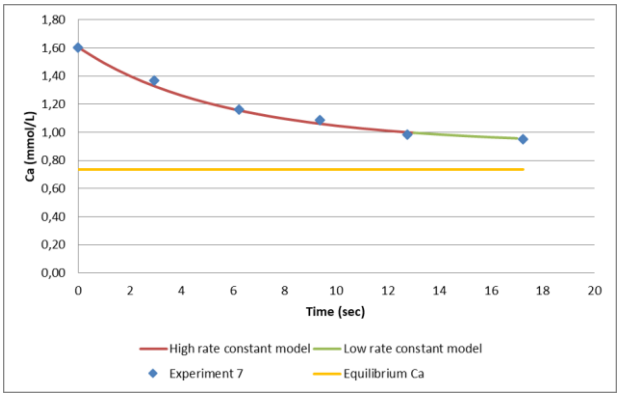

(d)

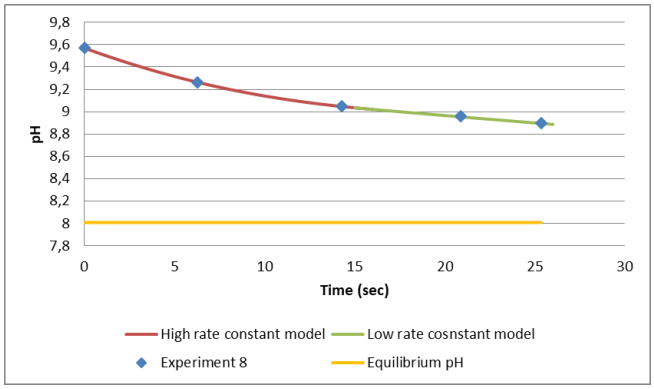

(e)

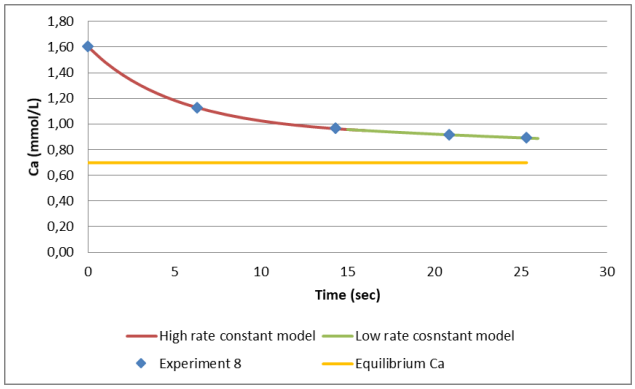

(f)

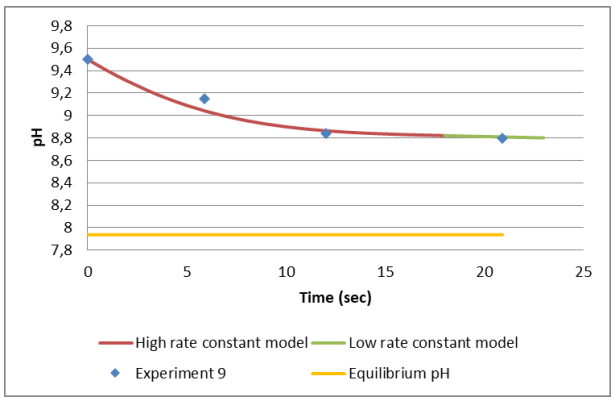

(g)

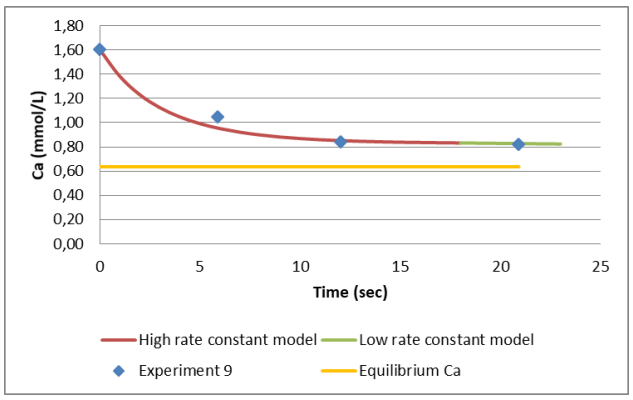

(h)

Figure 23 Measured pH and modeled pH reduction and Ca concentration using the two-rate-constants model of: (a) and (b) Experiment 6, (c) and (d) Experiment 7, (e) and (f) Experiment 8, (g)and (h) Experiment 9

From Figure 23, it can be seen that the two-rate-constants model predicts better the experimental results than the one-rate-constant model but the difference between the two models is not significant.

In the following table, an overview of the results from the experimental data processing of the PFR fluidized bed experiments is shown. The $k_H * K_{sp} * S$ and $k_L * K_{sp} * S$ values of the two-rate-constants model are shown as well as the saturation ratio that the change from the high-rate-constant to the low-rate-constant takes place.

Table 6 Overview of the two-rate-constants model $k*K_{sp}*S$ values for the Fluidized Bed Reactor experiments

	Temperature	Seeding material	Specific Surface Area	$k_H*K_{sp}*S$ (mmol/L* s^{-1})	$k_L*K_{sp}*S$ (mmol/L* s^{-1})	Saturation ratio	A_H
Experiment 6	10 ˚C	Calcite Pellets d=1-1.12 mm	Ranging from 5200-5900 m^2/m^3	0.002	0.0008	10	6.4
Experiment 7	20 ˚C	Calcite Pellets d=1-1.12 mm	Ranging from 5500-6200 m^2/m^3	0.0022	0.0005	10.1	8
Experiment 8	10 ˚C	Crushed Calcite d=0.5-0.6 mm	Ranging from 4700-5600 m^2/m^3	0.0024	0.0006	13.6	10.4
Experiment 9	20 ˚C	Crushed Calcite d=0.5-0.6 mm	Ranging from 5000-6100 m^2/m^3	0.0043	0.0002	9.9	9.5

Based on the results of the fluidized bed experiments it seems that there is no significant change in the crystallization rate if the temperature is ranging between 10 ˚C and 20 ˚C. The SR that the change from the high rate constant to the low rate-constant model takes place, is ranging between 10 and 13. Through comparing the $k_H * K_{sp} * S$ values of the first 3 experiments, it can be seen that the type of the seeding material that is used does not significantly affect the high rate constant of calcium crystallization rate. The low rate constant is also not significantly changing based on the type of seeding material that is used or the temperature. In the last experiment, the high and low rate constants are slightly higher than in the rest of the experiments. However, it is within an acceptable margin of error for a pilot plant installation.

5.4. Overview of the PFR fluidized bed and STR batch experiments modeling results

In Table 7 the rate constant values for the two-rate-constants model based on the measured or assumed specific surface area (SSA) are shown. It is can be seen from Table 7 that the rate constant values for the STR batch experiment are in all experiments more than 3 times higher than in the PFR fluidized bed. It is, therefore, possible that the results of the STR batch experiments are not sufficient to determine the rate of calcium reduction in a plug flow fluidized bed column. The hydraulic conditions seem to play a significant role in the determination of calcium carbonate kinetics. The specific surface area of Experiments 3, 4 and 5 the specific surface area of the seeding material that was used cannot be accurately determined. Therefore, the rate constant values calculated in this case are not reliable.

Table 7 Overview of the two-rate-constants for the PFR fluidized bed Reactor experiments and STR batch experiments

STR Batch Reactor Experiments							
	Temperature	**Seeding material**	**Specific Surface Area (SSA)**	**k_H ((mol/L)$^{-1}$* s^{-1}*m^3/m^2)**	**k_L ((mol/L)$^{-1}$* s^{-1}*m^3/m^2)**	**Saturation ratio of change**	**A_H**
Experiment 1	10 °C	Calcite Powder d=24 um	Ranging 88 m^2/m^3	0.36	0.048	17	19.7
Experiment 2 (Duplicate)	10 °C	Calcite Powder d=24 um	Ranging from 2662 m^2/m^3	0.30	0.048	14.4	11.9
Experiment 3	5 °C	Crushed Calcite d=0.5-0.6 mm	Ranging from 300 m^2/m^3	2.49	0.25	14.5	13
Experiment 4	10 °C	Crushed Calcite d=0.5-0.6 mm	Ranging from 300 m^2/m^3	2.14	0.34	17.3	14.7
Experiment 5	20 °C	Crushed Calcite d=0.5-0.6 mm	Ranging from 300 m^2/m^3	1.80	0.57	15.3	21.8
PFR Fluidized Bed Reactor Experiments							
	Temperature	**Seeding material**	**Specific Surface Area (SSA)**	**k_H ((mol/L)$^{-1}$* s^{-1}*m^3/m^2)**	**k_L ((mol/L)$^{-1}$* s^{-1}*m^3/m^2)**	**Saturation ratio of change**	**A_H**
Experiment 6	10 °C	Calcite pellets d=1-1.12 um	Ranging from 5200-5900 m^2/m^3	0.076	0.038	13	6.4
Experiment 7	20 °C	Calcite pellets d=1-1.12 mm	Ranging from 5500-6200 m^2/m^3	0.088	0.025	13	8
Experiment 8	10 °C	Crushed Calcite d=0.5-0.6 mm	Ranging from 5600-4700 m^2/m^3	0.112	0.030	15	10.4
Experiment 9	20 °C	Crushed Calcite d=0.5-0.6 mm	Ranging from 6100-5000 m^2/m^3	0.132	0.020	10	9.5

5.5. Validation of the two-rate-constants model

The two-rate-constants model that is derived from the PFR fluidized bed experiments can be used to model the rate of calcium carbonate crystallization in a pellet softening fluidized bed reactor. For the simulation of the hydraulic and chemical part of the reactor, the Layers-model that was developed by Van den Hout (2016) is used.

However, in this research, equation (20) that was used to describe the calcium carbonate crystallization kinetics in the Layers-model, is substituted with the two-rate-constants model. In order to validate the new model and investigate the applicability of the two-rate-constants equation under different conditions, the model's results are compared with the pH and total calcium concentration profile of the full-scale reactors and the measurements of previous researchers.

Initially, the PFR fluidized bed experiments that took place in the pilot plant of Weesperkarspel WTP are simulated (Figure 24).

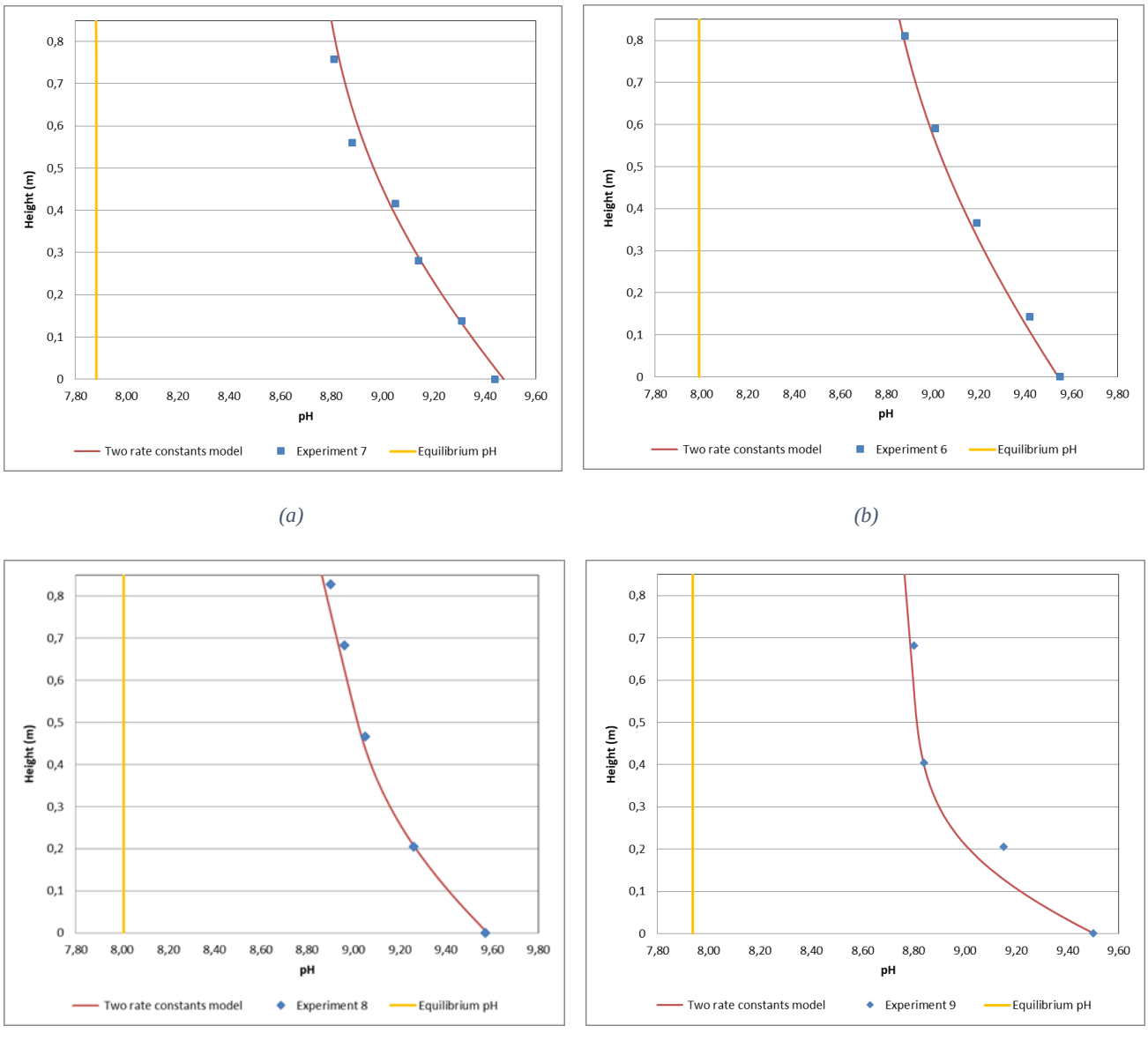

Figure 24 Measured and modeled pH profile over the head of the column of: (a) Experiment 6 (b) Experiment 7 (c) Experiment 8 (d) Experiment 9

Based on the results shown in Figure 24, it can be seen that the Layers-model can be used to approximate sufficiently well the crystallization of calcium carbonate inside the experimental column.

Furthermore, using the Layers-model the pH profile of the reactor is derived and compared with the pH profile that was measured in the pellet softening fluidized bed columns of Weesperkarspel pilot plant by Schetters (2013) (Figure 25). According to this research, the pH at the bottom of the reactor is approximately 11.75. In order to reach this pH a very high dose above 4 mmol/L needs to be added to the solution. Considering the range of the flow of the dosing pump and the strength of the caustic soda solution, it is not possible that such a high dose was used. The high pH measurement is probably caused by a deviation in the measurement of the pH meter caused by scaling of the probe or mixing problems in the bottom of the reactor.

Despite the fact that there is an error in the pH measurement in the bottom, the shape of the pH profile is similar with the pH profile of the PFR fluidized bed experiments and the measurements of previous researchers [Graveland et al. (1983)]. In particular, the largest reduction of the pH takes place in the first one meter of the reactor while the reduction of the pH above this height is very small. This shape is consistent with the results of the two-rate-constants model as it can be seen from Figure 24. While the two-rate-constants model cannot approximate the pH in the bottom, the pH measurements in the rest of the reactor could be predicted using the two-rate-constants model.

In Figure 25 (a) the pH profile that was measured by Schetters (2013) and the modeled pH profile using the two-rate-constants model is shown. Three different doses of caustic soda are considered since the dose has not been accurately determined. In Figure 25 (b) the predicted pH profile based on the measured effluent hardness is shown.

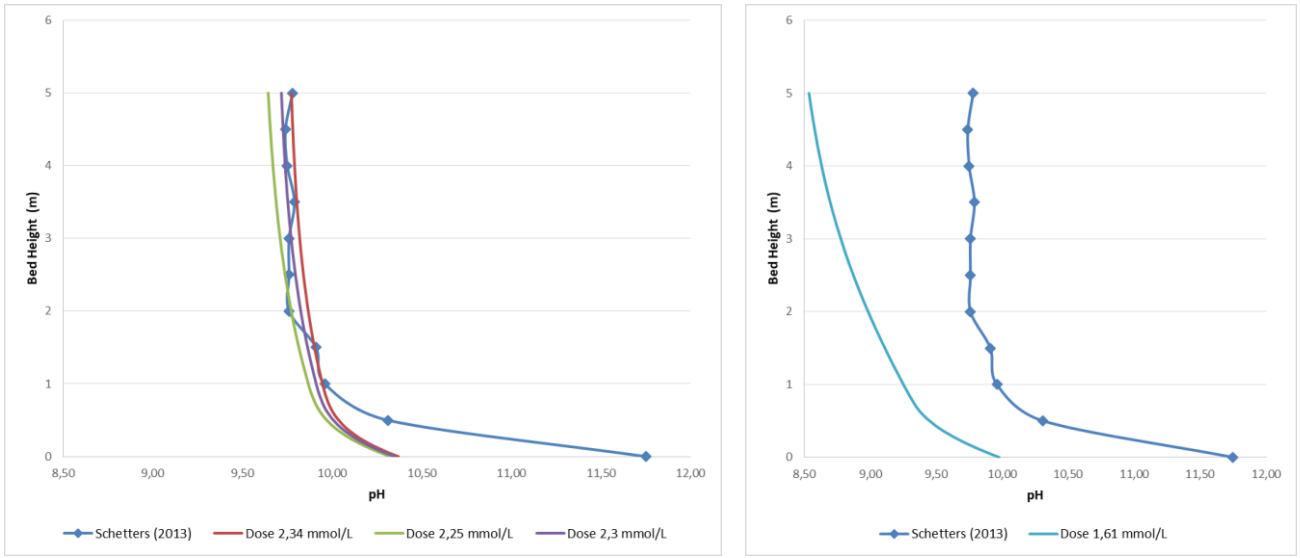

(a) *(b)*

Figure 25 (a) Approximation of the pH profile measurement of Schetters (2013) using the two-rate-constants model (b) the pH profile that should have been measured by Schetters in order to reach a TH=0.8 mmol/L in the effluent of the reactor

In Figure 26 the pH profile from the two-rate-constants model is compared with the pH profile from the Layers-model developed by Van den Hout (2016) using the one-rate-constant equation.

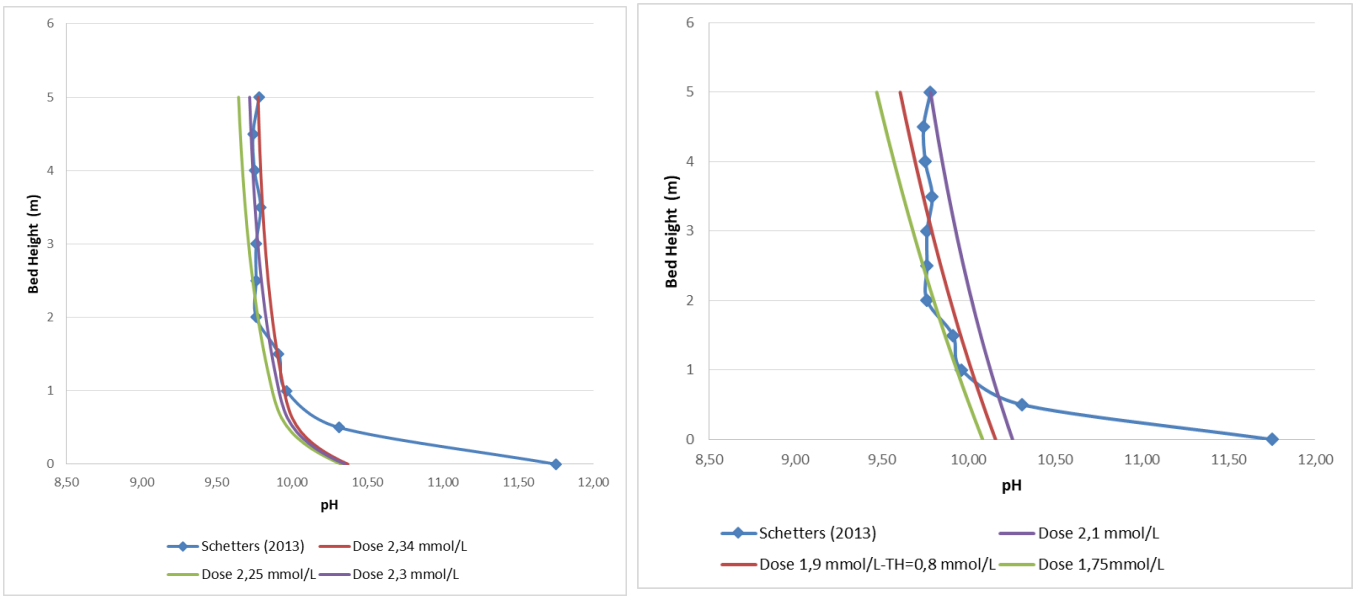

(a) *(b)*

Figure 26 (a) Approximation of the pH profile measurement of Schetters (2013) using the two-rate-constants model (b) Approximation of the pH profile of Schetters using the Layers-model by Van den Hout (2016)

According to the Layers-model, there is a constant rate of calcium reduction over the height of the reactor. However, it is obvious from Figure 26 that neither the bottom nor the top of the reactor is sufficiently well approximated using the Layers-model.

A pH measurement in the pellet softening reactors of the Weesperkarspel water treatment plant is also used to validate the two-rate-constants model. However, it is important to note that a number of parameters can affect the softening process inside a pellet softening reactor. A deviation due to problems in the flow and the mixing conditions inside the reactor is possible. In Figure 27, the approximation of the pH measurement in a full-scale reactor using the two-rate-constants model and the Layers-model is shown. It can be clearly seen the pH profile on the top of the reactor is approximated much better using the two-rate-constants model than the Layers-model. The main difference between the two models is that the two-rate-constants model is assuming that the largest percentage of calcium has been removed in the first meter of the reactor while the decrease of the pH in the rest of the reactor is not significant. On the other hand, the Layers-model in which equation (20) has been incorporated assumes a steady continuous decrease of the pH over the head of the reactor. Nevertheless, neither one of the two models can approximate the pH values in the bottom of the reactor. Mixing or flow problems can cause these unrealistic pH measurements in the caustic soda mixing zone at the bottom.

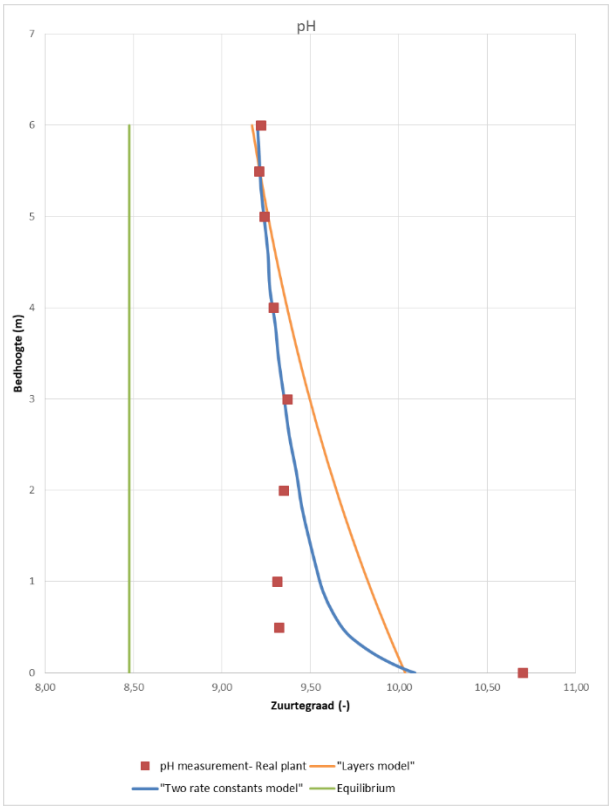

Figure 27 Comparison between the measured pH profile in a full-scale pellet softening reactor and the pH profile derived using the two-rate-constants model and the Layers-model

Additionally, the research of Linssen (1983) is used to validate the two-rate-constants model. In the research of Linssen (1983) the calcium profile inside a pellet softening reactor was measured in various hydraulic and dosing conditions. In Table 8 an overview of the operational conditions and the water quality of the influent during Linssen (1983) experiments is shown. A detailed description of the experimental measurements can be found Appendix C. As it can be seen from the table below the experiments in the research of Linssen (1983) were conducted in different conditions than the experiments of this research. In contrast to the experiments of this research, sand was used as a seeding material and the diameter of the seeding material particles ranged from 0.37 to 0.43 mm. It is also important to note that for the experiments of Linssen (1983) a full-scale reactor was used with a diameter of 2.6 m and a mixing zone at the bottom of the reactor.

By studying the experimental results of Linssen (1983), it becomes clear that the CO_2 influent concentration cannot be used to determine the initial pH of the solution since it is not consistent with the calculated dose and the measured pH effluent. The pH measurement of the influent water in WPK treatment plant in April and May 1983 were used instead. Based on this measurement, the initial pH of the water before dosing was approximately pH= 7.9 and the CO_2 concentration of the hard water was 0.12 mmol/L.

Table 8 Water quality and operational conditions during the experiments of Linssen (1983) in a pellet softening reactor

	Experiment 1	Experiment 2	Experiment 3
Date	21/03/1983	04/05/1983	04/05/1983
Water flow (m^3/h)	420	535	535
Temperature (℃)	9.3	10.8	10.8
NaOH dose (mmol/L)	1.04	1.02	1.38
Fluidized Bed Height (m)	3.85	4.35	4.3
Ca influent (mmol/L)	2.02	1.98	1.98
Ct influent (mmol/L)	3.6	3.63	3.6
CO_2 influent (mmol/L)	0.3	0.3	0.3
Type of seeding material	sand	sand	sand
Diameter of seeding material at the top (mm)	0.37	0.43	0.43
Diameter of seeding material at the top (mm)	0.79	0.68	0.68
pH effluent	8.75	8.75	8.75

Furthermore, it is observed that a slightly different concentration of caustic soda needs to be dosed in all experiments in order to achieve the measured calcium concentration and pH in the effluent. The deviation between the dose calculated by Linssen (1983) and the dose calculated using PHREEQC is ranging between 2-10%. The accuracy of the dosing system is lower than 10% since the flow of the dosing pump, as well as the strength of the caustic soda solution, fluctuate significantly. Therefore a 10% deviation in the dose of caustic soda is possible.

Firstly, the calcium concentration measurements of the experiments of Linssen (1983) are plotted against the saturation ratio (Figure 28). It can be clearly seen that in all three experiments there is a high and low rate constant line and the curve have the characteristic hockey stick shape.

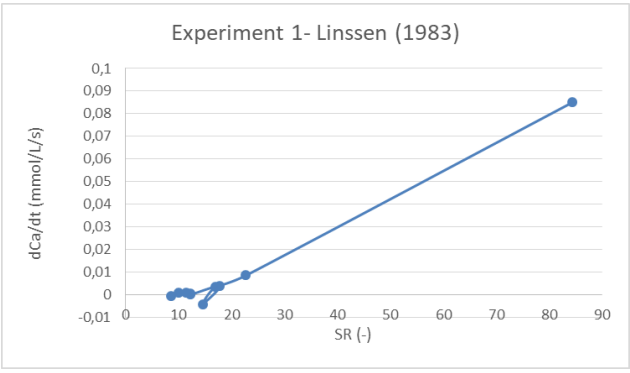

(a)

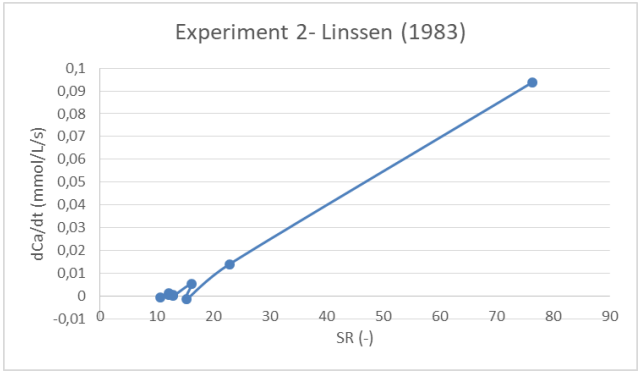

(b)

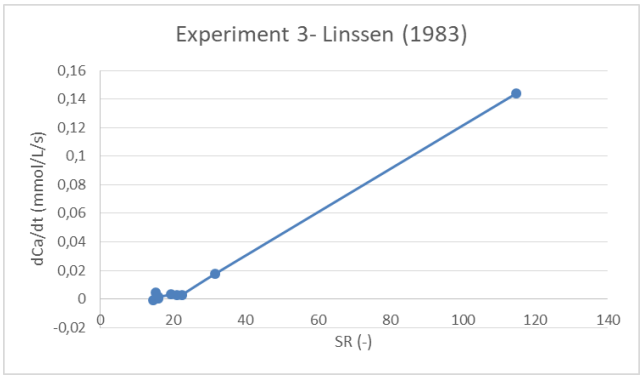

(c)

Figure 28 Rate of crystallization against the saturation ratio of: (a) Experiment 1 (b) Experiment 2 (c) Experiment 3 of Linssen (1983)

Initially, for the validation of the model, the input parameter values from the modeling of the experiments of this research are used. In Table 7 the input values of the two-rate-constants model of the PFR fluidized bed experiments are shown. In Experiment 8 the diameter of the seeding material and the temperature of the experiment is closer to the experimental conditions of Linssen (1983). Thus, the parameter values of Experiment 8 that was conducted in comparable conditions as the experiments from Linssen (1983), are chosen.

The equation that is used in this case is:

$$-\frac{dCa}{dt} = k_i * K_{sp} * S(SR - A_i) \quad (38)$$

- The high rate constant is k_H =0.1224 (mol/ L *s^{-1}*m^3/m^2) for calcite SR>13,53
- the low rate constant k_L = 0.0306 (mol/ L *s^{-1}*m^3/m^2) for calcite SR< 13,53
- the intercept of the high rate constant line is A_H = 10.4
- the intercept of the low constant line is A_L =1

The saturation ratio of change is the intersection of the two line and is calculated using the equation (33). So SR_{CH} = 13.53.

In Figure 26, the measured by Linssen (1983) and calculated calcium reduction is shown. It seems that the two-rate-constants model based on the parameter values of Experiment 8 is approximating sufficiently well the rate of crystallization in the bottom of the reactor that the high rate constant from the PFR fluidized bed is used. However, the low rate constant that was derived from the experiments of this research is largely overestimating the rate of crystallization above a height of approximately 1m. The reason for the overestimation, is probably caused by the limitations of the experimental setup. In most PFR fluidized bed experiments, only one measured point was used to calculate the low rate constant value. Therefore, the value of this parameter is sensitive to small deviations due to inaccurate measurement of this point. Also, it is not possible to determine, if the point that was used to determine the value of the low rate constant k_L is in the gradual period of change between the high rate constant and the low rate constant line. In this case, an overestimation of the value of this parameter is possible. Therefore, a higher column and a larger number of measurements at the top of the reactor is necessary to determine accurately the low rate constant value.

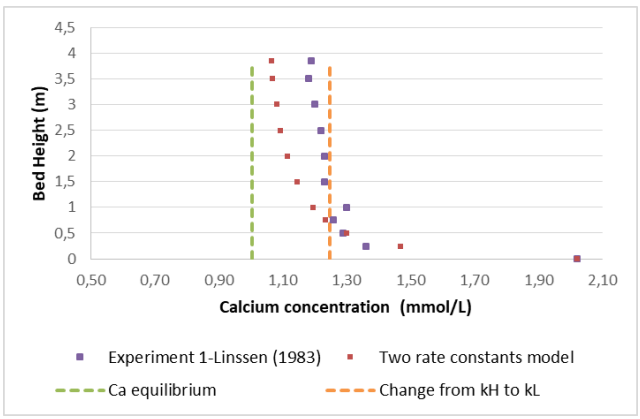

(a)

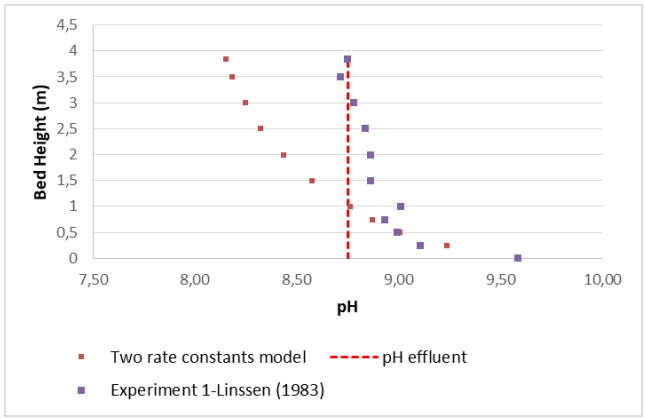

(b)

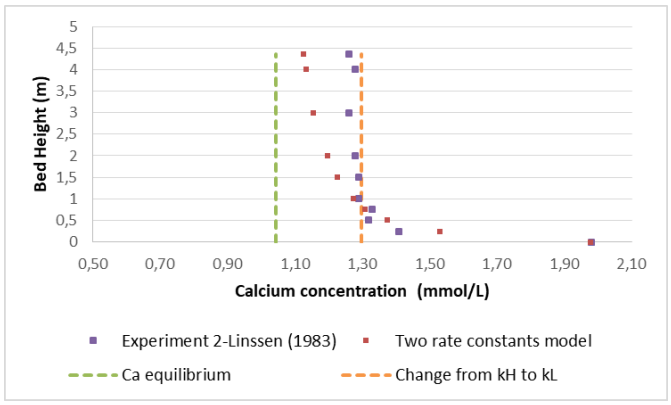

(c)

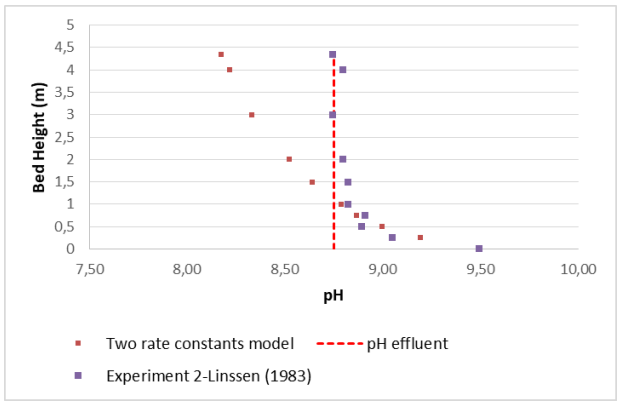

(d)

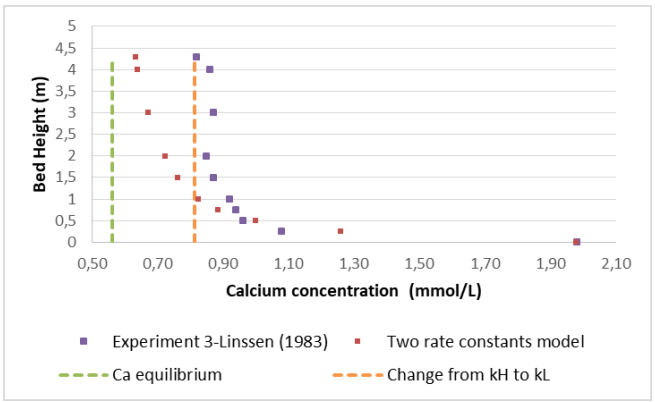

(e)

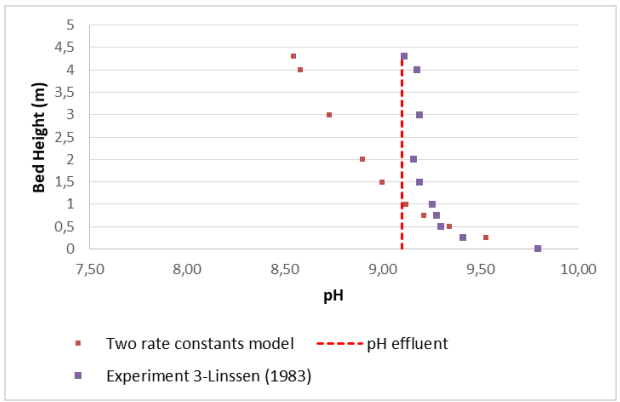

(f)

Figure 29: Measured and modeled pH and calcium reduction using the rate constant values of Experiment 8 (a) and (b) for Experiment 1 from Linssen (1983), (c) and (d) for Experiment 2 from Linssen (1983) (e) and (f) for Experiment 3 from Linssen (1983)

Finally, it is investigated whether the one-rate-constant model proposed by Wiechers et al (1975), Van Schagen et al. (2008 b,c) can also approximate sufficiently well the experimental results of Linssen (1983). The modeled and measured calcium concentration using the one-rate-constant model is shown in Figure 30.

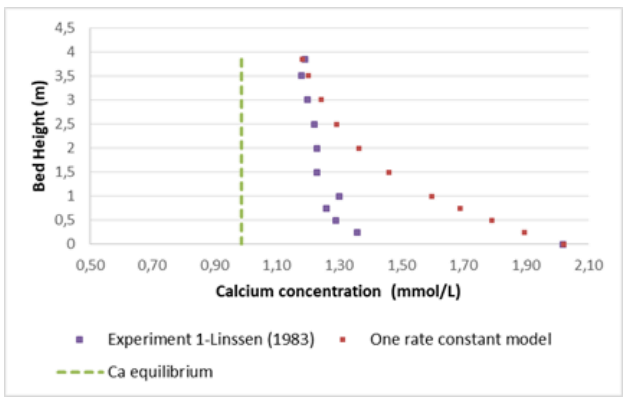

(a)

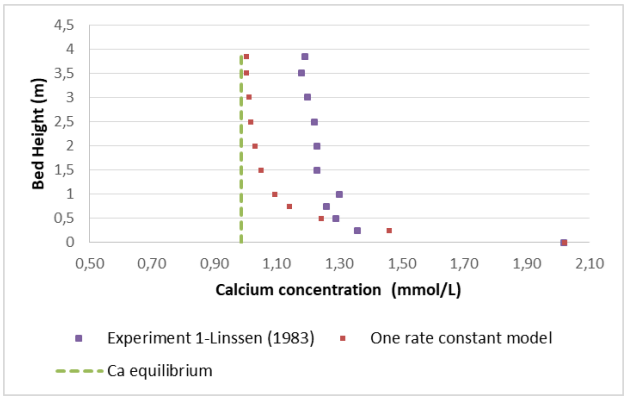

(b)

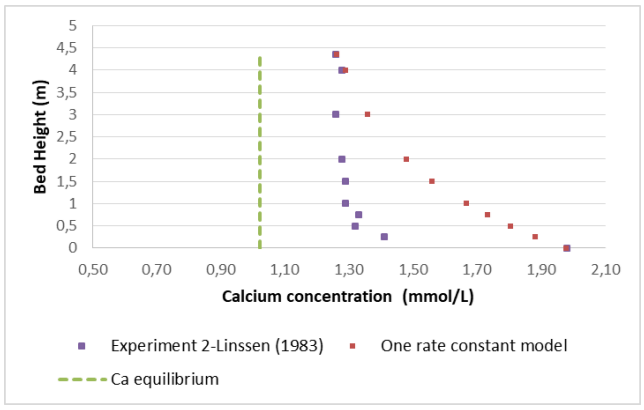

(c)

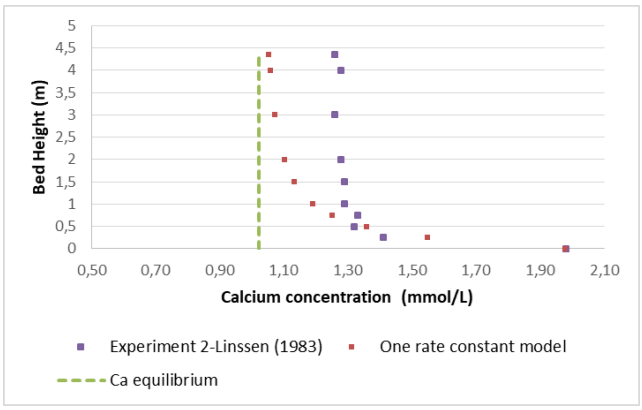

(d)

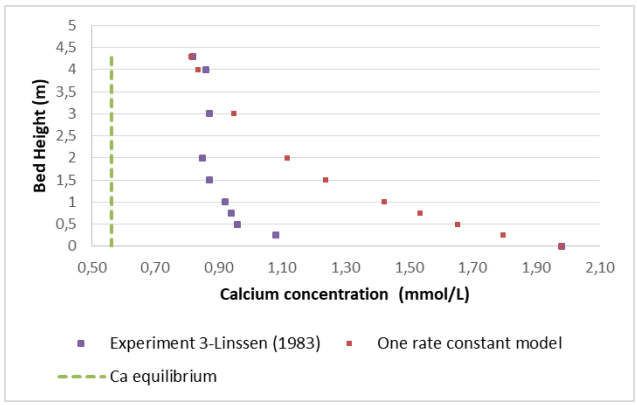

(e)

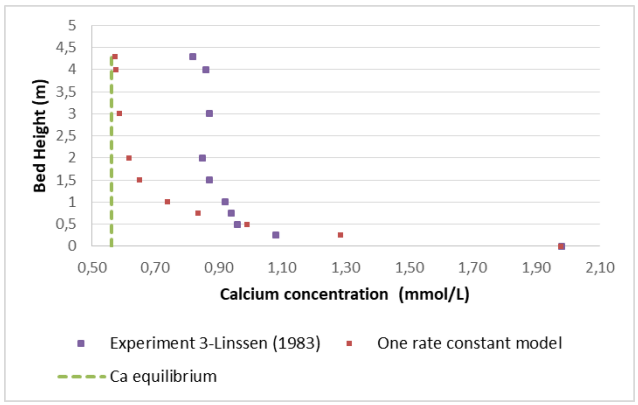

(f)

Figure 30 Measured and modeled calcium concentration profile over the height of the reactor from the Experiments of Linssen (1983) research using the one-rate-constant model

It can be seen from Figure 30 above that it is not possible to accurately predict the calcium profile in a pellet softening reactor using the one-rate-constant model. It is only the bottom part of the reactor or the effluent can be approximated with the one-rate-constant model. Therefore, the two-rate-constants model gives an improved description of the calcium carbonate crystallization inside a pellet softening fluidized bed reactor.

5.6. Recalibration

Nevertheless, if a lower value of k_L is assumed, the two-rate- constants model approximates very well the measured calcium and pH profile as it can be seen in Figure 31.

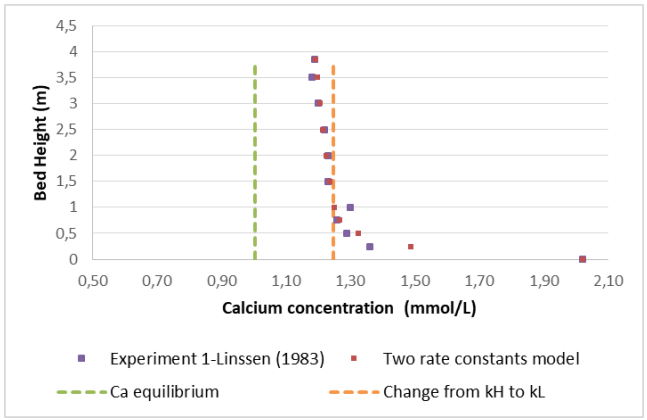

(a)

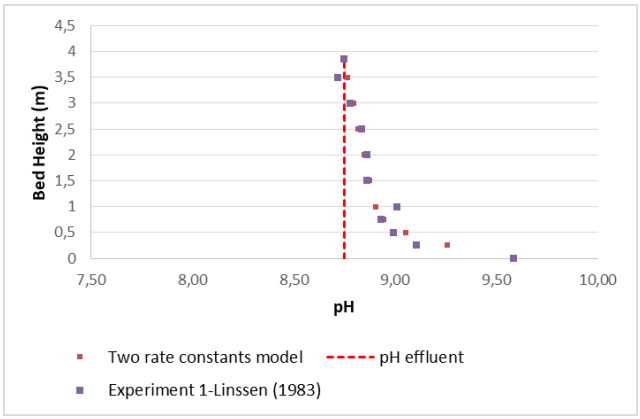

(b)

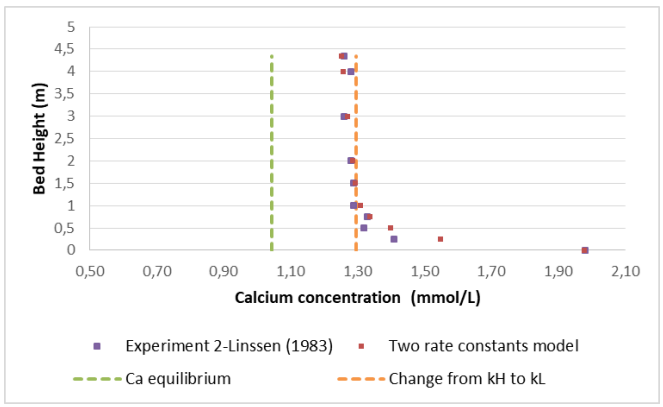

(c)

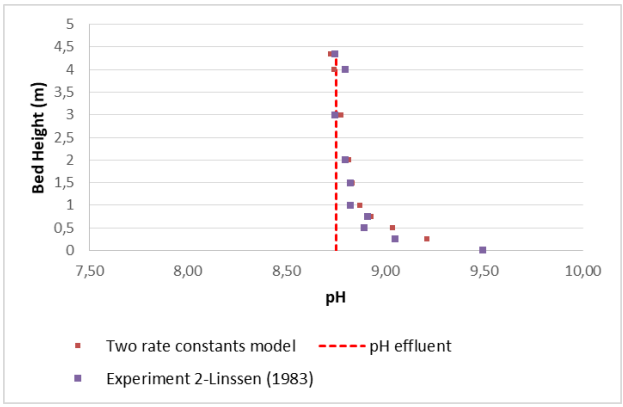

(d)

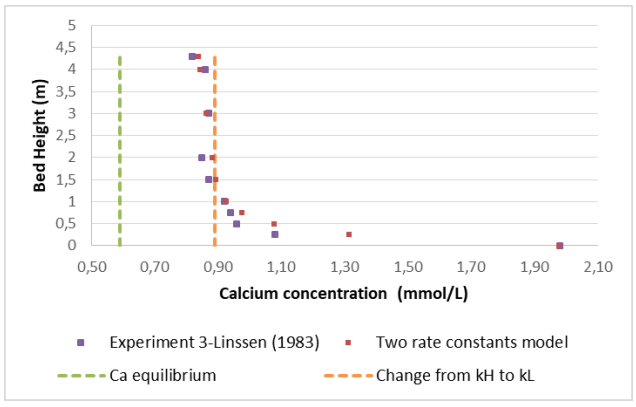

(e)

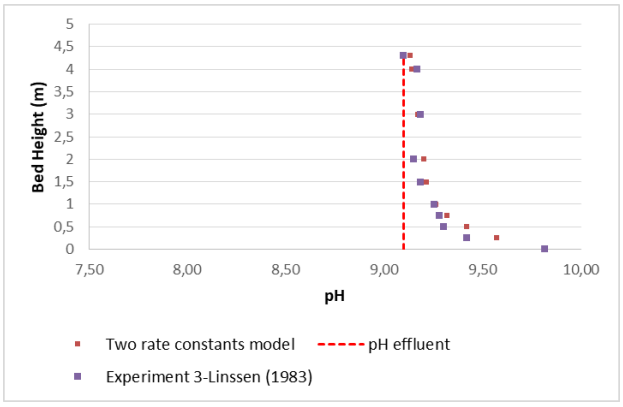

(f)

Figure 31: Measured and modeled pH and calcium reduction using the two-rate-constants model (a) and (b) for Experiment 1 from Linssen (1983), (c) and (d) for Experiment 2 from Linssen (1983) (e) and (f) for Experiment 3 from Linssen (1983)

In Table 9 the input values of the two-rate-constants model for each experiment are shown. Also, the dose of NaOH that was determined based on the effluent pH is shown instead of the NaOH that is given in Linssen (1983) research. It must be noted that for the modeling of the Linssen (1983) experiments a

higher saturation ratio of change than in the PFR Fluidized bed experiments is used. The saturation ratio of change in this case is within the range found in the STR batch experiments.

Table 9 Input values for the parameters of the two-rate-constants model based on the Linssen (1983) Experiments

Two-rate-constants model parameters values-Experiments from Linssen (1983)			
	Experiment 1	**Experiment 2**	**Experiment 3**
Seeding material	sand particles d=0.37-0.79	sand particles d=0.43-0.68	sand particles d=0.43-0.68
Temperature (˚C)	9.8	9.8	10.8
Velocity (m/h)	70	100	100
NaOH dose (mmol/L)	1.027	0.925	1.45
High rate constant (k1T) (mmol/L/s * m)	0.1224	0.1224	0.1224
Low rate constant (k2T) (mmol/L/s * m)	0.004	0.004	0.004
Intercept A_H (-)	13	13	17
Saturation Ratio of change (SRCH) (-)	13.4	13.4	17.4

By comparing the model input values it seems that the high and low rate constant values are identical in all three experiments. The main difference is that in a higher dose the change from a high to a low rate constant takes place to a slightly higher saturation ratio.

5.7. An improved model of calcium carbonate crystallization rate

Based on the experimental results and the validation and recalibration of the model using the Linssen (1983) an improved model for calcium carbonate crystallization kinetics was derived. The equation of the model is:

$$-\frac{dCa}{dt} = k_i * K_{sp} * S(SR - A_i) \quad (39)$$

- the high rate constant is k_H =0.1224 (mol/ L *s^{-1}*m^3/m^2) for calcite SR>13.5
- the low rate constant k_L = 0.004 (mol/ L *s^{-1}*m^3/m^2) for calcite SR<13.5
- the intercept of the high rate constant line is A_H = 13
- the intercept of the low constant line is A_L =1

The saturation ratio of change is the intersection of the two lines. Using this equation several scenarios were studied (see Appendix C.4). However, further investigation of scenarios is necessary to determine the optimal operation of a pellet softening fluidized bed reactor.

6

Discussion

In this section, the experimental results as well the results of the modeling of calcium carbonate crystallization are discussed and explained.

6.1. Discussion about the comparison of the models' predictions with the experimental results

Firstly, the results from the comparison of the prediction models used in this research are described and analyzed. The reason that the two-rate-constants model predicts better the calcium carbonate crystallization is discussed.

The rate of crystallization in both types of experiments was plotted against saturation ratio to determine if the experimental data plot in a straight line as Wiechers predicted or a bending in the line is observed as suggested by Dreybrodt et al. (1997). In Figure 32 the rate of calcium carbonate crystallization rate in Experiment 2 and the plot of the experimental data of Wiechers is shown.

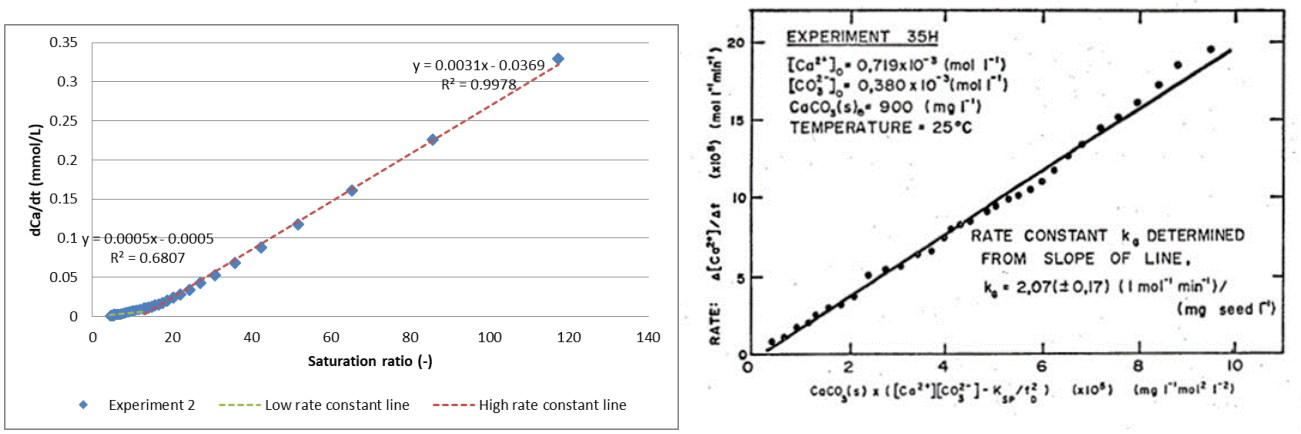

Figure 32 Comparison between the plot of the rate of crystallization against the saturation ratio of Experiment 2 and the experimental data of Wiechers

It can be seen from the graph of Figure 32 that in contrast with the experimental results of Wiechers the data of Experiment 2, do not plot in a straight line. When the saturation ratio decreases a bending of the curve is observed. Therefore, the data can better be plotted as two lines or a "hockey stick" shaped curve. This curved plot of the data is observed in all STR batch experiments.

An explanation for the bending of the curve can be found in literature. A reduction of the crystallization rate is possibly caused by the presence of inhibitors. At the beginning of the experiment that supersaturation is high, crystallization is not sensitive to the effect of inhibitors. As a result, a linear relationship can be used to describe the rate of crystallization similar to the one suggested by other researchers that used artificial hard water with no inhibitors. On the other hand, at low supersaturation surface nucleation becomes the predominant mechanism of crystallization [Dove and Hocella (1993)] that a bending of the curve is observed. Dreybordt et al. (1997) suggest that at low supersaturation

inhibitors on the water or in the surface of the seeding material block surface nucleation and cause a decrease in the growth rate. This observation is in accordance with the mechanism of inhibition proposed by Inskeep and Bloom (1986), Lebron and Suarez (1996) and Reddy (2012) about the inhibition of organic carbon. According to these researchers, organic carbon creates a coating on the surface of the seeding material that is inhibiting the crystallization of calcium carbonate.

Based on Table 1 the organic carbon in the natural influent water is the inhibitor that most likely is affecting calcium carbonate crystallization. Also, the inhibiting effect of dissolved organic carbon is enhanced by the presence of magnesium ions in the water (§2.3.5). The presence of a high concentration of organic carbon in Weesperkarspel natural water is possibly affecting the rate of crystallization due to the binding of the carboxylate groups at the surface of the seeding material. When the supersaturation decreases and surface nucleation is the main mechanism of crystallization, the calcium and carbonate ions are hindered from reaching the surface of the seeding material by the coating of organic carbon and a significant reduction of the rate of crystallization is observed.

In order to investigate further which model describes more accurately the calcium carbonate crystallization kinetics, the experimental results were compared with the predictions of three models. The following models have been examined: the Wiechers model [equation (18)], the one-rate-constant model [equation (29)] and the two-rate-constants model [equation (32)]. The linear models found in literature are mostly empirical and have been derived using experimental measurements.

In Figure 33 the measured pH of the STR batch Experiment 2 and PFR fluidized bed is compared with the predictions of the three models.

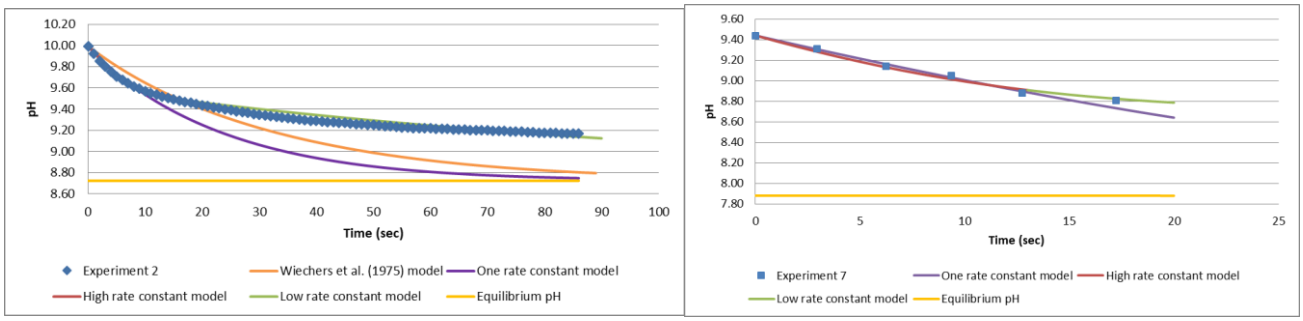

Figure 33 Experiment 2: Measured pH and modeled pH reduction using three models

Based on the results of the STR batch experiments, the one-rate-constant and the Wiechers model can describe accurately enough the beginning of the experiment but do not predict the measured values when the supersaturation of the solution is decreased. These findings agree with the observations from the graph of the rate of crystallization against supersaturation. At the beginning of the experiment, that supersaturation is high the linear models, that have been derived using artificial hard water without inhibitors, predict accurately enough the rate of crystallization. After a few seconds, however, that supersaturation has decreased the predictions of the linear models of Wiechers and one-rate constant model fail to predict the measured pH and calcium reduction. This period of the experiment corresponds to the bending of the curve in the graph of the rate of crystallization against supersaturation that is caused by the inhibiting effect of various compounds. It is important to note, the rate of crystallization at high supersaturation, during the experiments that calcite powder was used as seeding material, is approximately the same as measured in Wiechers research and therefore predicted by Wiechers model. These findings show that Wiechers equation predicts accurately enough the rate of crystallization when inhibition is not important and confirm the assumption that, the inhibitors have no effect at the rate of crystallization at high supersaturation.

It can be concluded then, that the rate of calcium carbonate crystallization, when natural water is used cannot be described with only one-rate-constant. Alternatively, a nonlinear model can be used to predict the calcium carbonate crystallization rate as proposed by Dreybrodt et al. (1997). In this research, the two-rate-constants model is used to describe the non-linear relation between the rate of crystallization

and supersaturation. Based on the results, the two-rate-constants model predicts much more accurately the rate of calcium carbonate crystallization as it can be seen from Figure 33.

The results of the PFR fluidized bed experiments were compared with the one- rate-constant and two-rate-constants models as well. However, in this case, no significant difference in the prediction of calcium carbonate crystallization is observed. This is due to the fact that the saturation ratio in the top of the fluidized bed remains above the SR=13-15. Therefore, the column is not high enough to observe the change from the high to the low rate constant line. Nevertheless, if the one-rate-constant model is used to describe the rate of calcium carbonate crystallization the predicted pH on the top of the reactor deviates slightly from the predicted value. Therefore, it is possible that in the PFR fluidized bed experiments a decrease of the rate constant values is observed as well.

Overall, the two-rate-constants model is an improved model predicts much better the experimental results of the PFR fluidized bed experiments as well as the STR fluidized bed experiments than the linear models found in literature.

For the validation of the two-rate-constants model the measurements of the calcium concentration over the height of a pellet softening fluidized bed reactor from Linssen (1983) were used (see Table 8). According to the results of the model validation (Figure 29), the high rate constant that was determined from the PFR fluidized bed experiments is describing sufficiently well the rate of crystallization in the bottom of the reactor. However, the low rate constant derived from the PFR fluidized bed experiments is largely overestimating the rate of crystallization on the upper part of the reactor. The reason for this deviation is that the column that was used for the PFR fluidized bed experiments was not high enough to determine accurately the low rate constant (§5.6). The low rate constant should be approximately 10 times lower than the value that was determined from the PFR fluidized bed reactor experiments.

As a result, the model was recalibrated using the experiments of Linssen. After, it is recalibrated the two-rate-constants model seems to predict very well the measured calcium concentration over the height of the reactor. The one-rate-constant model, on the other hand, cannot predict accurately the rate of crystallization even if several rate constant values are tested

6.2. Average relative error

To quantify the differences in the predictions between the models the average relative error (ARE) of the three models was calculated using equation (40):

$$ARE = \frac{1}{n}\sum_{i=1}^{n}\left(\frac{\left|y_{calc,i} - y_{exp,i}\right|}{y_{exp,i}}\right) \qquad (40)$$

Where $y_{calc,i}$ is the calculated values, $y_{exp,i}$ are the measured values during the experiment and is the number of measurements. According to the results, a two-rate-constants model [equation (32)] fits the experimental measurements much more accurately than Wiechers or one-rate-constant model. The ARE of the two-rate-constants model is only 3- 5% while the ARE of the Wiechers model is ranging between 19-63%. The ARE if the one-rate-constant model is used is also ranging between 17-32 %. Therefore, the two-rate-constants model improves significantly the prediction of the rate of calcium carbonate crystallization during the STR batch experiments.

Table 10 Average Relative error of STR batch experiments

Average Relative Error			
Experiment No.	**Wiechers**	**one-rate-constant model**	**two-rate-constants model**
1	19.54%	17.17%	3.71%
2	24.99%	32.14%	5.65%
3	55.39%	42.77%	2.14%
4	58.32%	37.60%	3.94%
5	63.07%	27.95%	3.74%

The average relative error was also calculated for the PFR fluidized bed experiments and the experiments of Linssen (1983) that were used for the validation of the model.

Table 11 Average Relative Error of PFR fluidized bed and full-scale reactor experiments

Average Relative Error		
PFR Fluidized Bed Experiments		
Experiment No.	**one-rate-constant model**	**two-rate-constants model**
6	0.68%	0.90%
7	1.42%	1.45%
8	4.43%	0.48%
9	3.22%	3.04%
Linssen (1989) Experiments		
Linssen Exp1	15.94%	1.83%
Linssen Exp2	16.80%	1.97%
Linssen Exp3	35.63%	4.45%

It can be seen from Table 11 that the ARE of the one-rate-constant and two-rate constants model in the PFR fluidized bed experiments is approximately the same. The reason for this result is that the column in the PFR fluidized bed experiments was not high enough to observe the sharp reduction of the rate at low supersaturation. It must be noted though that the ARE of the last measurement in each experiment is significantly decreased when the two-rate constants model is used instead of the one-rate-constant model. In particular, when the one-rate-constant model is used the relative error of the last measured points is approximately 4-10 % while when the two-rate-constants model is used the relative error decreases to approximately 1-4%.

The two-rate-constants is predicting significantly better the calcium reduction during the Linssen experiments compared to the one-rate-constant model. The ARE of the two-rate-constants model is ranging between 1and 4% while the ARE of the one-rate-constant model is ranging between 16 and 30%. Therefore, the calcium reduction in a full-scale fluidized bed reactor can be predicted much more accurately using the two-rate-constants model compared to the linear models found in literature.

6.3. Effect of hydraulic and flow conditions on calcium carbonate crystallization

By comparing the rate of calcium carbonate crystallization during the PFR fluidized bed and the STR batch experiments the effect of the hydraulic and flow conditions on calcium reduction in a pellet softening fluidized bed reactor can be determined. In Figure 34 the graph of the rate of calcium reduction against the saturation ratio of the STR batch Experiment 2 and the PFR fluidized bed Experiment 8 is presented. The rate of calcium reduction has been divided with the specific surface area of the seeding material in each experiment in order to avoid variation due to a different surface area for crystallization.

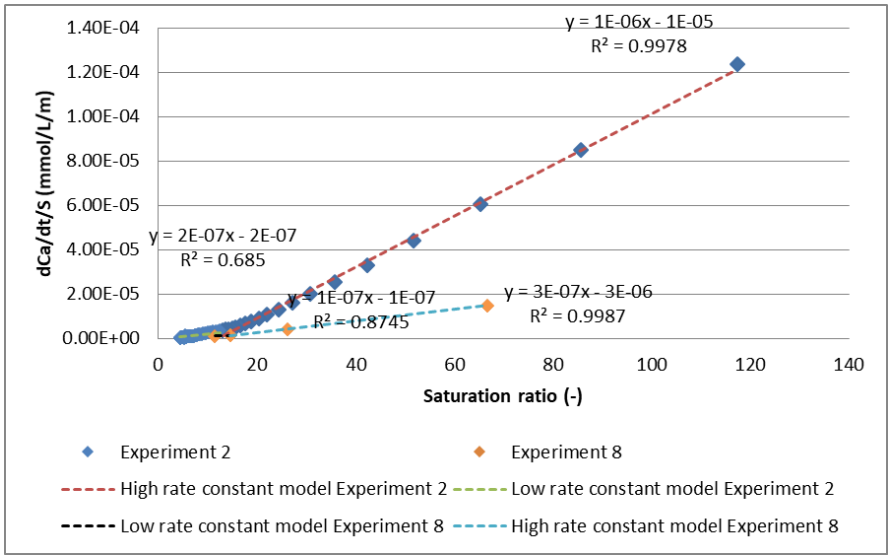

Figure 34 Crystallization rate against calcite saturation ratio

According to Figure 34, the rate of crystallization in the PFR fluidized bed experiment is lower than in the STR batch experiments. In particular, the high rate constant in Experiment 2 is approximately three times higher than in Experiment 8. The low rate constant is also 2 times higher in Experiment 2 compared to Experiment 8. Based on these results, it can be concluded that the hydraulic and flow conditions inside the reactor play an important role in the calcium carbonate crystallization kinetics. Therefore, the rate of transfer of the calcium and carbonate ions in the surface of crystallization seem to influence significantly the hardness reduction process.

An ideal plug flow reactor is considered to behave as a series of batch reactors. Therefore, if the PFR fluidized bed reactor that was used in this research was separated into layers, the rate of calcium carbonate crystallization in each layer should be the same as the one measured during the STR batch reactor experiments. Nevertheless, based on the PFR fluidized bed experiments the rate of crystallization in the column is significantly lower than in the STR batch experiments. The reason for this deviation could be that the flow conditions inside the PFR fluidized bed reactor are not ideal. Especially in the area around the water inlet, radial flow of water and pellets was observed. As a result, the rate of crystallization decreases due to limitations on the rate of mass transfer of the reactants to the crystallization surface.

A full-scale pellet softening fluidized bed reactor is not an ideal plug flow reactor as well. In the bottom of a full-scale pellet softening fluidized bed reactor where the caustic soda is dosed, intensive mixing takes place and radial flow of chemicals is observed. Therefore, there is a mixing zone in the bottom of the reactor that is acting more as a continuously stirred batch reactor (CSTR) rather than a PFR. Therefore, since the flow conditions inside a full-scale reactor are not ideal, a reduction of the calcium carbonate rate is expected as it was observed in the PFR fluidized bed experiments. Overall, it is considered that the flow conditions inside a full-scale pellet softening reactor approximate more the flow conditions inside the column of the PFR fluidized bed experiments rather than flow conditions inside a batch reactor. As a result, it is not possible to use the experimental results of batch experiments to determine the rate of crystallization in a full-scale fluidized bed reactor. Therefore, the assumption of Van Schagen that the calcium carbonate crystallization model needs to be modified to take into account the hydraulic and flow

conditions inside the reactor is verified. Nevertheless, it is not possible to accurately predict using a linear equation even if a different rate constant to take into account the different hydraulic and flow conditions is used. Further study is necessary to accurately determine the effect of hydraulic and flow conditions on calcium carbonate crystallization.

6.4. Effect of temperature on calcium carbonate crystallization

The effect of temperature on the crystallization of calcium carbonate was investigated. STR batch experiments were conducted using the same concentration of seeding material at three different temperatures. In STR batch Experiments 3, 4 and 5, not washed crushed calcite was used as a seeding material and the temperature was adjusted at 5, 10 and 20 ˚C respectively. Although, the same concentration and type of seeding material was used in all three experiments it was not possible to accurately determine the specific surface due to the presence of powder attached to the crushed calcite particles. Therefore, the difference in calcium carbonate crystallization rate between the three experiments can be attributed to the different SSA of the seeding material that was used rather than the changes in temperature. As a result, it was not possible to accurately detect the influence of temperature on calcium carbonate crystallization rate. However, in Experiments 3, 4 and 5 a difference in the shape of the curve during the change from a high to a low rate constant in the rate v_s saturation ratio graph was observed.

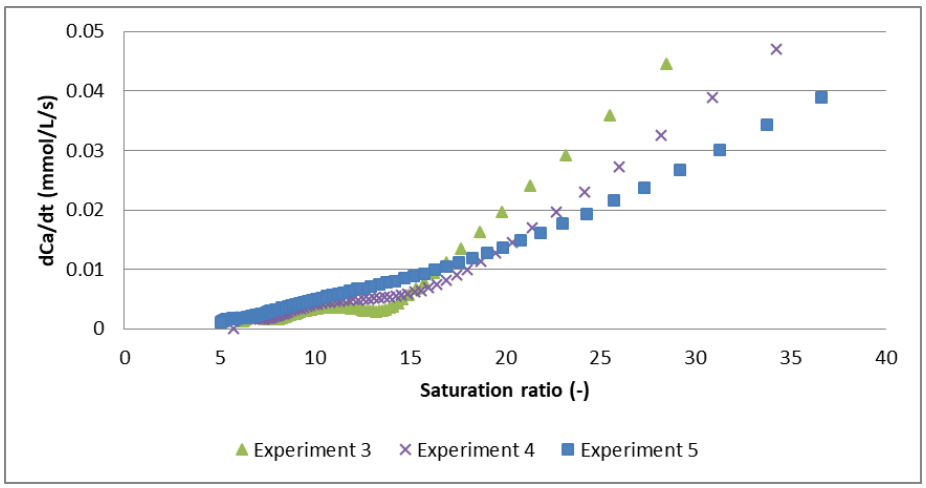

Figure 35 Crystallization rate against calcite saturation ratio in Experiments 3, 4 and 5

As it can be seen from Figure 35 during Experiment 3 that the temperature of the water was low (approximately 5˚C), the slope of the line of the rate of calcium reduction against the saturation ratio changes abruptly from a high to a much lower value, while in Experiment 5, that the temperature of the water was much higher, a smooth transition is observed. Therefore, although the effect of temperature cannot be accurately quantitatively determined using the experimental results, it is observed that the higher the temperature the smoother the transition from a high rate constant to a low rate constant line.

6.5. Effect of using a different type of seeding material on calcium carbonate crystallization

Moreover, two different types of seeding material were used during the PFR fluidized bed experiment. In Experiments 6 and 7 calcite pellets were used as seeding material while in Experiment 8 and 9 the column was filled with crushed calcite. In Figure 36 the calcium carbonate crystallization rate during the PFR Fluidized Bed experiments is plotted against the saturation ratio. The rate has been divided with the specific surface area in order to eliminate the differences due to different crystallization surface between the experiments.

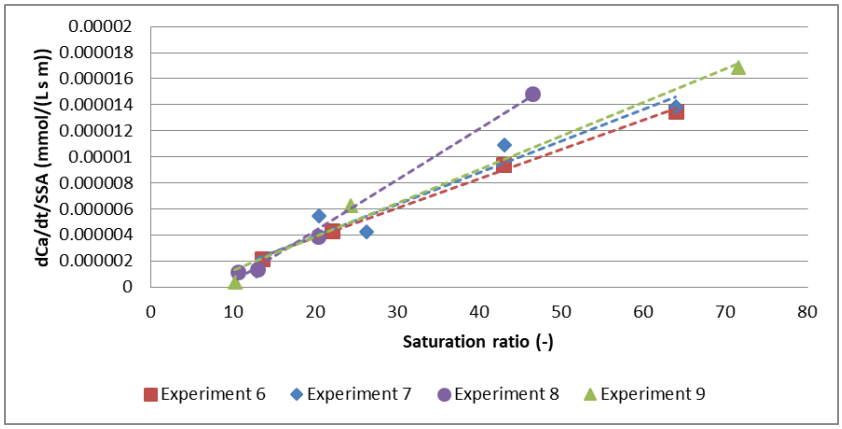

Figure 36 Calcium carbonate crystallization rate against calcite saturation ratio of all PFR fluidized bed experiments

Based on Figure 36 there seems to be no significant difference on the rate of crystallization of calcium carbonate due to the use of a different type of seeding material.

6.6. Remarks on the design of a pellet softening fluidized bed reactor

The results of this research can be used to improve the design and operation of a full-scale pellet softening fluidized bed reactor. Several operational scenarios can be tested in order to determine the optimal operational state for the pellet softening process. In Appendix C.4 the effect of reducing the diameter of the seeding material as well as the up-flow velocity was investigated. Nevertheless, no significant improvement of the calcium removal was observed.

Based on the results of this research, the following remarks should be considered while designing a pellet softening fluidized bed reactor:

- Firstly, the quality of the influent hard water needs to be determined. It is possible that the presence of inhibitors in the hard water causes a reduction of the rate of calcium carbonate crystallization at low supersaturation. In particular, the concentration of natural organic carbon seems to have a significant effect on the rate of calcium carbonate at a low saturation ratio. Removing the dissolved organic carbon using Ion Exchange (IEX) technology could result in an increased calcium carbonate crystallization rate in the top of the reactor. According to Hsu and Singer (2009) (§2.3.6), the calcium removal can increase approximately 20% if the concentration of natural organic matter in the water decreases from 8.3 to 1.5 mg/L.

- In case that a high concentration of inhibitors is present in the water, the two-rate-constants model should be used instead of the one-rate-constant model for the prediction of the calcium carbonate crystallization rate inside a pellet softening fluidized bed reactor. However, several model parameters need to be determined. To be able to use the two-rate-constants model, it is necessary to determine three parameters: the high rate constant, the low rate constant and the intercept of the high rate constant line. The high rate constant is not sensitive to water quality changes and a value of approximately 0.1224 can be used. The low rate constant on the other hand seems to be affected by the concentration of inhibitors in the water and needs to be determined experimentally based on the water quality of the influent water. STR batch experiments cannot be used to establish the model parameters since in these flow conditions the rate of calcium carbonate crystallization is overestimated. Therefore, PFR fluidized bed experiments are necessary in order to determine the rate of crystallization of calcium carbonate at a low saturation ratio.

- An important finding of this research is that the largest part of the calcium concentration is removed in the bottom of the reactor while in the top the rate of calcium carbonate crystallization is much lower. Van den Hout (2016) argued that building a higher reactor would result in a higher removal of calcium with a lower dose of caustic soda. This is due to the fact that the linear model by Wiechers was used during this research. As a result, the rate of crystallization on the upper part of the reactor was largely overestimated. Nevertheless, according to the two-rate-constants

model, the rate of crystallization in the top of the reactor is significantly lower than predicted by Van den Hout. Therefore, building a higher reactor with a higher fluidized bed will not have a significant effect on the calcium removal and consequently will not reduce the caustic soda consumption.

- In this research, it was not possible to accurately determine the effect of temperature on calcium carbonate crystallization kinetics. It seems that there is not an important change in the rate of crystallization when the temperature is ranging between 10- 20 °C. However, the influence of more extreme temperatures on the hydraulic and chemical conditions in a pellet softening fluidized bed needs to be taken into account.

7

Conclusions and Recommendations

7.1. Conclusions

From the experimental and modeling results of this research, an improved understanding of calcium carbonate crystallization kinetics under various hydraulic and chemical conditions was achieved. In particular, the following concluding remarks can be made:

- The linear model proposed by Wiechers et al. (1975), Van Schagen (2008 b,c) cannot predict the calcium carbonate crystallization rate when natural water with inhibiting compounds is used. In the top of the reactor, a deviation of more than 0.5 between the modeled and measured pH is observed. Even if a different rate constant value than the one proposed by Wiechers is used, as Van Schagen et al. (2008) suggested the average related error of the one-rate-constant model is still ranging between 16 and 35 %.
- Alternatively, an improved two-rate-constants model can be used to predict the calcium carbonate crystallization rate. A high rate-constant model is used to predict the crystallization in the bottom of the reactor where the supersaturation is high and a low rate constant is used for the top of the reactor where the saturation ratio has decreased below 13-17. In this case, the model is able to predict more accurately the rate of calcium carbonate crystallization and the average related error decreases to 1-4%.
- The hydraulic and flow conditions inside the reactor affect markedly the crystallization rate of calcium carbonate. The rate of crystallization seems to bε 3 times lower in a PFR fluidized bed compared to STR batch experiments where vigorous stirring is applied. Hence, the diffusion of ions on the surface of the seeding material seems to play an important role in the calcium carbonate crystallization kinetics as Van Schagen suggested. However, even if a lower rate constant is used in order to take into account the different flow conditions the rate of crystallization at low supersaturation is still overestimated.
- The results of this research are not accurate enough to determine the effect of temperature on calcium carbonate kinetics. Nevertheless, a difference in the shape of the pH reduction curve is observed. When the temperature is high, a smooth transition from the high rate constant to the low rate constant line can be seen while at a low temperature the change is much more abrupt.
- The type of seeding material that is used seems to have little influence on the calcium carbonate crystallization kinetics. Using seeding material with a different diameter or a rougher surface does not have an impact on calcium carbonate crystallization kinetics.

Overall, with the two-rate-constants model developed in this research the prediction of the pH and calcium concentration profile inside a pellet softening fluidized bed reactor is significantly improved. The models that have been used so far for the prediction of calcium carbonate crystallization inside a pellet softening fluidized bed reactor assume a linear relationship between the rate of crystallization and supersaturation. However, the linear models overestimate the rate of crystallization on the upper region of the reactor that supersaturation is low. Using the two-rate-constants model a more accurate

representation of the hardness reduction over the height of the reactor is obtained. Therefore, it can be used to test several operational scenarios in order to optimize the pellet softening process and improve the design of a fluidized bed reactor. Furthermore, from this research, the importance of water quality on calcium carbonate crystallization kinetics is underlined. That inhibiting compounds present in the influent water can have an important impact on calcium carbonate crystallization kinetics and should be further studied. These findings can be used to improve the operation of a pellet softening fluidized bed reactor by defining and removing the most significant inhibitors.

7.2. Recommendations

Although the two-rate-constants can predict sufficiently well the calcium and pH reduction over the height of the pellet softening fluidized bed reactor, further research is necessary to improve the understanding of calcium carbonate crystallization under various hydraulic and chemical conditions. The determination of the influence of a number of factors such as the concentration and type of inhibitors on calcium carbonate crystallization kinetics is necessary in order to be able to accurately predict and optimize the hardness reduction process.

Further research regarding the influence of inhibitors such as dissolved organic carbon in the rate of calcium carbonate crystallization is required. Especially, the influence of the saturation ratio and the temperature of the solution on the inhibiting effect of organic carbon should be investigated. In order to improve the pellet softening process, the concentration of inhibitors in the water from the influent stream of WPK water treatment plant should be reduced. In this case, it is possible that a high rate constant is used to describe the rate of crystallization in the whole reactor. The rate of crystallization at a supersaturation lower than 13-17 would be, therefore, significantly higher. Dissolved organic carbon can be removed from the water before the softening process using ion exchange (IEX) technology [Grefte et al. (2011)]. The calcium reduction rate in a fluidized bed reactor using water with a lower content in organic carbon, should be measured and compared with the results of this research, to determine the inhibiting effect on calcium carbonate kinetics.

The possibility that a new equilibrium is established when inhibitors are present in the solution should also be checked. In this research, the duration of the experiments was only a few minutes. The crystallization of calcium carbonate should be measured for a longer period of time in order to clarify if a new equilibrium is established. In case that a new equilibrium is reached, the supersaturation of calcium carbonate which is the driving force for the crystallization is lower than measured in this research.

Furthermore, the PFR fluidized bed experiments need to be repeated in a higher column in order to be able to determine the low rate constant more accurately. Also, a higher number of measurements on the top of the reactor is necessary in order to accurately detect the saturation ratio that the change from a high rate constant to a low rate constant takes place.

In a pellet softening reactor the mixing of the caustic soda takes place in the bottom of the reactor. In the mixing zone of the reactor, the hydraulic conditions deviate from a plug flow reactor due to turbulence. In this research, the mixing of caustic soda took place in a static mixer before the reactor. Mixing at the bottom of the PFR fluidized bed reactor instead of prior to the column would give a more accurate representation of the hydraulic conditions inside a pellet softening reactor.

It is also important to define the effect of temperature on the calcium carbonate kinetics. Determining the rate of calcium carbonate crystallization for a larger range of temperatures is necessary.

Bibliography

Links

USGS (2017), https://wwwbrr.cr.usgs.gov/projects/GWC_coupled/phreeqc/, retrieved on December 2017

Mineral data publishing, (2001-2005) http://rruff.info/doclib/hom/calcite.pdf, Retrieved on May 2018

Reference

Aldaco, R., Garea, A., & Irabien, A., (2007). Calcium fluoride recovery from fluoride wastewater in a fluidized bed reactor. *Water Research*, *41*(4), 810-818.

Astilleros, J. M., Fernández-Díaz, L.& Putnis, A., (2010). The role of magnesium in the growth of calcite: An AFM study. *Chemical Geology*, *271*(1), 52-58.

Brečević, L. & Kralj, D., (2007). On calcium carbonates: From fundamental research to application, *Croatica Chemica Acta*, 80 (3-4), pp. 467-484.

Crittenden, J. C.; Trussell, R. R., Hand, D.W., Howe, K. J., & Tchobanoglous, G., (2017). MWH's Water Treatment - Principles and Design (3rd Edition), John Wiley & Sons

Davis, K. J., Dove, P. M., & De Yoreo, J. J., (2000). The role of Mg2+ as an impurity in calcite growth. *Science*, *290*(5494), 1134-113

Dhanaraj, G., Byrappa, K., Prasad, V., & Dudley, M. (Eds.), (2010). *Springer handbook of crystal growth*. Springer Science & Business Media.

Dijk, van, J. C., (1993). Softening: Water treatment without waste material: the Dutch experiences with pellet reactors. In *Softening: Water treatment without waste material: the Dutch experiences with pellet reactors*. Delft University of Technology: Faculty of Civil Engineering.

Dijk, van, J.C. & Wilms, D.A., (1991). Water treatment without waste material-fundamentals and state of the art of pellet softening", Journal Water Supply, Research and Technology: AQUA, 40(5), pp. 263-280

Dirken, P., Baars, E.T., Graveland, A.J. & Woensdregt, C.F., (1990). "On the crystallization of calcite {CaCO3} during the softening process of drinking water in a pellet reactor with fluidized beds of quartz, garnet and calcite seeds", 11th Symposium on industrial crystallization

Faure, G., (1998). *Principles and applications of geochemistry: a comprehensive textbook for geology students*. Prentice Hall.

Flaathen, T. K., Oelkers, E. H., Gislason, S.R. & Aagaard, P. (2011). The effect of dissolved sulfate on calcite precipitation kinetics and consequences for subsurface CO2 storage, *Energy Procedia*, *4*, 5037-5043.

Gebauer, D. & Cölfen, H. (2011). Prenucleation clusters and non-classical nucleation. *Nano Today*, *6*(6), 564-584.

Gebauer, D., Völkel, A. & Cölfen, H. (2008). Stable prenucleation calcium carbonate clusters. *Science*, *322*(5909), 1819-1822.

Gefte, A. (2013), Removal of Natural Organic Matter Fractions by Anion Exchange: Impact on drinking water treatment processes and biological stability.

Graveland, A.J., Dijk, van, J.C., Moel, de, P.J. & Oomen, J.H.C.M. (1983), Developments in water softening by means of pellet reactors, Journal AWWA, 75(12), pp. 619-625

Grefte, A., Dignum, M., Baghoth, S. A., Cornelissen, E. R., & Rietveld, L. C. (2011). Improving the biological stability of drinking water by ion exchange. *Water Science and Technology: Water Supply*, *11*(1), 107-112.

Hamer, F. W. (2016). Calcium carbonate precipitation during subsurface injection of RO-brine: The effect on the hydraulic conductivity, Graduation thesis, Delft University of Technology

Helm van, der, A. W. C., Kramer, O. J. I., Hooft J. F. M., & De Moel P. J. (2015), Plant wide chemical water stability modeling with PHREEQC for drinking water treatment, In *IWC 2nd International Water Conference: New Developments in IT & Water, Rotterdam, The Netherlands, 8-10 February 2015; Authors version*. IWC.

Herzog, R. E., Shi, Q., Patil, J. N., & Katz, J. L. (1989), Magnetic water treatment: the effect of iron on calcium carbonate nucleation and growth. *Langmuir*, *5*(3), 861-867.

Hout, van den, L. (2016), Modellering van de hardheidsreductie, Optimalisatie van het hardheidsreductieproces door het ontwikkelen van een laagjesmodel waarbij de koppeling is gemaakt tussen de waterchemie en hydraulica, Graduation thesis, Hogeschool Utrecht, Institute for Life Science and Chemistry

Hsu, S., & Singer, P. C. (2009). Application of anion exchange to control NOM interference on lime softening. *American Water Works Association. Journal*, *101*(6), 85.

Hu, R. Z., Huang, T. L., Wen, G., & Yang, S. Y. (2017), Modeling particle growth of calcium carbonate in a pilot-scale pellet fluidized bed reactor, *Water Science and Technology: Water Supply*, *17*(3), 643-651.

Inskeep, W. P., Bloom, P. R. (1986), Kinetics of calcite precipitation in the presence of water-soluble organic ligands, *Soil Science Society of America Journal*, *50*(5), 1167-1172.

Jones, A. G. (2002), *Crystallization process systems*. Butterworth-Heinemann, Vol 5, p 137-142.

Kashchiev, D. (2008), Towards a better description of the nucleation rate of crystals and crystalline monolayers, *The Journal of Chemical Physics*, 129, 164701

Kramer, O.J.I., Jobse, M.A., Baars, E.T., Helm, A.W.C., van der, Colin, M.G., Kors, L.J., & Vugt W.H., van (2015), Model-based prediction of fluid bed state in full-scale drinking water pellet softening reactors, IWA congress, "New Developments in IT & Water Conference", Conference paper, pp. 1-26

Lebron I. and Suarez I.L. (1996), Calcite nucleation and precipitation kinetics as affected by dissolved organic matter at 25˚C and pH > 7.5, *Geochimica et Cosmochimica Acta*, p2765-2776

Lewis, A., Seckler, M., Kramer, H., & Van Rosmalen, G. (2015), *Industrial crystallization: fundamentals and applications*, Cambridge University Press

Lin, Y. P., & Singer, P. C. (2005), Inhibition of calcite crystal growth by polyphosphates, *Water Research*, *39*(19), 4835-4843.

Lindsay, W. L. (1979), *Chemical equilibria in soils*. John Wiley and Sons Ltd.

Linssen P.H.J.M. (1983), *Thermodynamische en reaktiekinetische apecten van de hardhead reduktie in de drinkwaterbereiding,* Gemeentewaterleidingen Amsterdam.

Liu Z., Dreybrodt W. (1997), Dissolution kinetics of calcium carbonate minerals in H20-CO2 solutions in turbulent flow: The role of the diffusion boundary layer and the slow reaction $H_2O + CO_2 \leftrightarrow H^+ + HCO_3^-$, *Geochimica et Cosmochimica Acta*, Vol. 61, No. 14, pp. 2879-2889,

Mazzotti, M., (2015). Introduction to Chemical Engineering: Chemical Reaction Engineering, Swiss Separation Processes Laboratory (SPL), ETH Federal Institute of Technology Zurich

Moel, de, P. J., Verberk, J. Q., & Dijk, van, J. C. (2007), *Drinking water: principles and practices*. World Scientific Publ.

Nancollas G. H., Reddy M. M., (1974 b), The kinetics of crystallization of scale forming minerals, *Society of Petroleum Engineers Journal,* 14, p 117-126.

Nancollas G.H., Reddy M.M., (1971), The Crystallization of Calcium Carbonate: II Calcite Growth Mechanism, *Journal of Colloid and Interface Science*, Vol. 37, No. 4, p 824-828

Nielsen, L. C., De Yoreo, J. J., & DePaolo, D. J. (2013), General model for calcite growth kinetics in the presence of impurity ions. *Geochimica et Cosmochimica Acta*, *115*, 100-114.

Ostwald, W. (1897). Studien über die Bildung und Umwandlung fester Körper. *Zeitschrift für physikalische Chemie*, *22*(1), 289-330.

Parsiegla, K. I., & Katz, J. L. (1999), Calcite growth inhibition by copper (II): I. Effect of supersaturation. *Journal of crystal growth*, *200*(1), 213-226.

Plummer, L. N., & Busenberg, E. (1982), The solubilities of calcite, aragonite and vaterite in CO2-H2O solutions between 0 and 90 C, and an evaluation of the aqueous model for the system CaCO3-CO2-H2O. *Geochimica et cosmochimica acta*, *46*(6), 1011-1040.

Reddy M.M., Plummer L.N. and Busenberg E., (1981), Crystal growth of calcite from calcium bicarbonate solutions at constant P_{CO2} and 25°C: a test of a calcite dissolution model, *Geochimica et Cosmochimica Acta,* Vol 45, p 1281-1289

Reddy, M. M. (2012), Calcite growth-rate inhibition by fulvic acid and magnesium ion—Possible influence on biogenic calcite formation. *Journal of Crystal Growth*, 352(1), 151-154.

Reddy, M. M., & Nancollas, G. H. (1976), The crystallization of calcium carbonate: IV. The effect of magnesium, strontium and sulfate ions, *Journal of Crystal Growth*, *35*(1), 33-38.

Rietveld L.(2015), *Softening*, Drinking water treatment, Delft University of Technology

Schagen van K. M., Rietveld, L. C., & Babusška, R. (2008), Dynamic modeling for optimization of pellet softening, *Journal of Water Supply: Research and Technology-AQUA*, *57*(1), 45-56.

Schagen van, K.M. (2009), Model-Based Control of Drinking-Water Treatment Plants, ISBN: 978-90-8957-008-6, Ph.D. thesis

Schagen, van, K.M., Rietveld, L.C. Babuška, R. & Baars, E.T. (2008), Control of the fluidized bed in the pellet softening process, *Chemical Engineering Science*, 63, pp. 1390-1400

Schetters, M. J. A. (2013), Grinded Dutch calcite as seeding material in the pellet softening process", TU Delft

Schetters, M.J.A., Hoek, van der, J.P., Kramer, O.J.I., Kors, L.J., Palmen, L.J., Hofs, B. & Koppers, H. (2015), Circular economy in drinking water treatment: reuse of grinded pellets as seeding material in the pellet softening process, *Water Science and Technology*, 71(4), pp. 479-486

Sheikholeslami, R., & Ong, H. W. K. (2003), Kinetics and thermodynamics of calcium carbonate and calcium sulfate at salinities up to 1.5 M. *Desalination*, *157*(1-3), 217-234.

Tai C. Y. (1999), Crystal growth kinetics of two-step growth process in liquid fluidized-bed crystallizers, Journal *of Crystal Growth*, 206 pp 109-118

Tai C.Y., Chien W-C., Chen C.-Y. (1999), Crystal Growth Kinetics of Calcite in a Dense Fluidized-Bed Crystallizer**,** *AIChE Journal*, Vol. 45, No. 8, p1605-1614

Tai C.Y., Hsiao-Ping Hsu, (2001), Crystal growth kinetics of calcite and its comparison with readily soluble salts*, Powder Technology*, 121, 60–67

Takasaki, S., Parsiegla, K. I., & Katz, J. L. (1994), Calcite growth and the inhibiting effect of iron (III). *Journal of Crystal Growth*, *143*(3-4), 261-268.

W. Ostwald , (1902),Lehrbuch für allgemeine Chemie, Vol II, Engelman, Leipzig,

Waternet. (2010). Het draait om water. Watercyclusplan 2010-2015. Amsterdam.

Weischers H.N.S., Sturrock P., Marais G.v.R. (1975), Calcium carbonate crystallization kinetics, *Water Research* Vol. 9. pp 835 to 845, Pergamon Press, Printed in Great Britain

Yoreo, de, J. J., & Vekilov, P. G. (2003), Principles of crystal nucleation and growth, *Reviews in mineralogy and geochemistry*, 54(1), 57-93.

Zhang, Y., & Dawe, R. A. (2000), Influence of Mg 2+ on the kinetics of calcite precipitation and calcite crystal morphology, *Chemical Geology*, *163*(1), 129-

APPENDIX A – STR Batch Reactor Experiments

A.1 Water quality of influent of Weesperkarspel treatment plant

In Table A. 1 and Table A. 2 the water quality of the influent of WPK water treatment plant the dates that the water was abstracted to be used for the STR batch experiments is shown.

Table A. 1 Water of the influent stream of WPK water treatment plant on 12/07/2017

Module **Calcite kinetics (PWP and Wiechers model)**
Dissolution and precipitation of Calcite

Sample description	WPK TimeVal			12-07-2017 13:20	Test data	*Assumption: mg/L =mg/kgs =mg/kgw*	
Basic data							
	Temperature	t	°C		19,9		
	Oxygen	O2	mg/L		8,7	0,27	mmol/kgw
	pH	pH	-		7,57		
	Total organic carbon	TOC	mg/L C		6,6	0,55	mmol/kgw
	Silicate	Si	mg/L Si		5	0,17	mmol/kgw
	Conductivity (measured, at 20 °C)	EC	µS/cm		472	47,2	mS/m
Cations	Calcium	Ca	mg/L		70,6	1,76	mmol/kgw
	Magnesium	Mg	mg/L		6,68	0,27	mmol/kgw
	Sodium	Na	mg/L		24,1	1,05	mmol/kgw
	Potassium	K	mg/L		2,5	0,06	mmol/kgw
	Ammonium (inert)	NH4	mg/L N		0,01	0,000	mmol/kgw
Anions	Alkalinty (as HCO3)	HCO3	mg/L		203	3,33	mmol/kgw
	Chloride	Cl	mg/L		55	1,57	mmol/kgw
	Nitrate	NO3	mg/L N		0,9	0,02	mmol/kgw
	Sulfate	SO4	mg/L		6,5	0,07	mmol/kgw
	Bromide	Br	mg/L		0,09	0,00	mmol/kgw
	Nitrite (inert)	NO2	mg/L N		0,0	0,00	mmol/kgw

Table A. 2 Water quality of the influent stream of WPK water treatment plant on 04/07/2017

AQUATIC CHEMISTRY for Engineers

Module **Calcite kinetics (PWP and Wiechers model)**
Dissolution and precipitation of Calcite

Sample description	WPK TimeVal			04-07-2017 10:20	Test data	*Assumption: mg/L =mg/kgs =mg/kgw*	
Basic data							
	Temperature	t	°C		19,7		
	Oxygen	O2	mg/L		8,7	0,27	mmol/kgw
	pH	pH	-		7,72		
	Total organic carbon	TOC	mg/L C		6,6	0,55	mmol/kgw
	Silicate	Si	mg/L Si		5	0,17	mmol/kgw
	Conductivity (measured, at 25 °C)	EC	µS/cm		462	46,2	mS/m
Cations	Calcium	Ca	mg/L		68,4	1,71	mmol/kgw
	Magnesium	Mg	mg/L		6,68	0,27	mmol/kgw
	Sodium	Na	mg/L		24,1	1,05	mmol/kgw
	Potassium	K	mg/L		2,5	0,06	mmol/kgw
	Ammonium (inert)	NH4	mg/L N		0,01	0,000	mmol/kgw
Anions	Alkalinty (as HCO3)	HCO3	mg/L		199	3,26	mmol/kgw
	Chloride	Cl	mg/L		55	1,57	mmol/kgw
	Nitrate	NO3	mg/L N		0,9	0,02	mmol/kgw
	Sulfate	SO4	mg/L		6,5	0,07	mmol/kgw
	Bromide	Br	mg/L		0,09	0,00	mmol/kgw
	Nitrite (inert)	NO2	mg/L N		0,0	0,00	mmol/kgw

A.2 STR batch experimental results

A.2.1 Experiment 1-results

A.2.1.1 Species distribution analysis

In the following figures the calcium species distribution in the solution is shown. The total calcium concentration is also plotted against time and the equilibrium concentration is shown.

In Figure A. 2 the saturation ratio and the saturation index of calcite during the experiment is presented while in Figure A. 3 the concentration of calcium that is removed from the solution and the calcium carbonate crystallization potential (CCCP) are shown. Also, the calcium reduction rate is plotted against time. It is obvious that the rate of crystallization significantly decreases and almost reaches zero after a certain period of time.

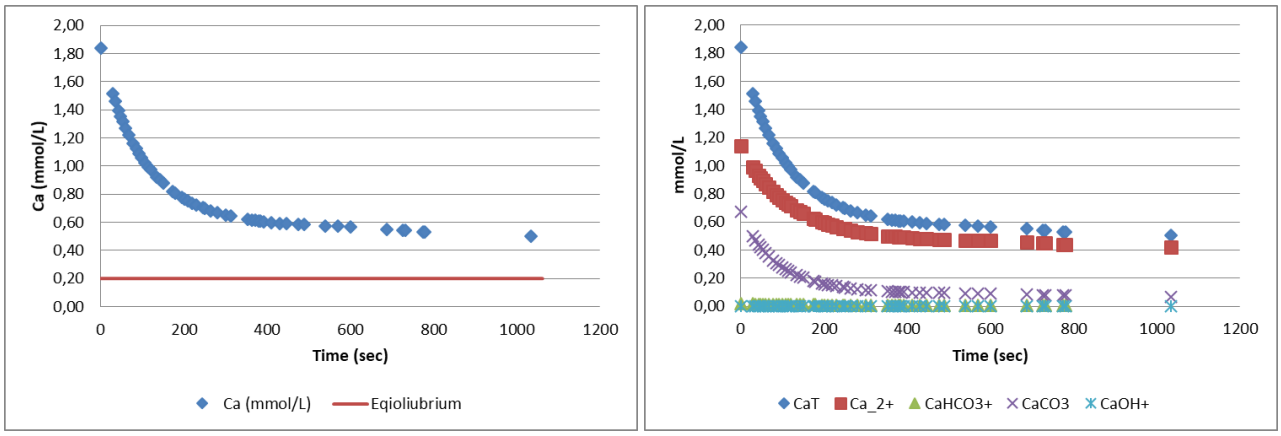

Figure A. 1 Experiment 1: Total calcium concentration and species distribution

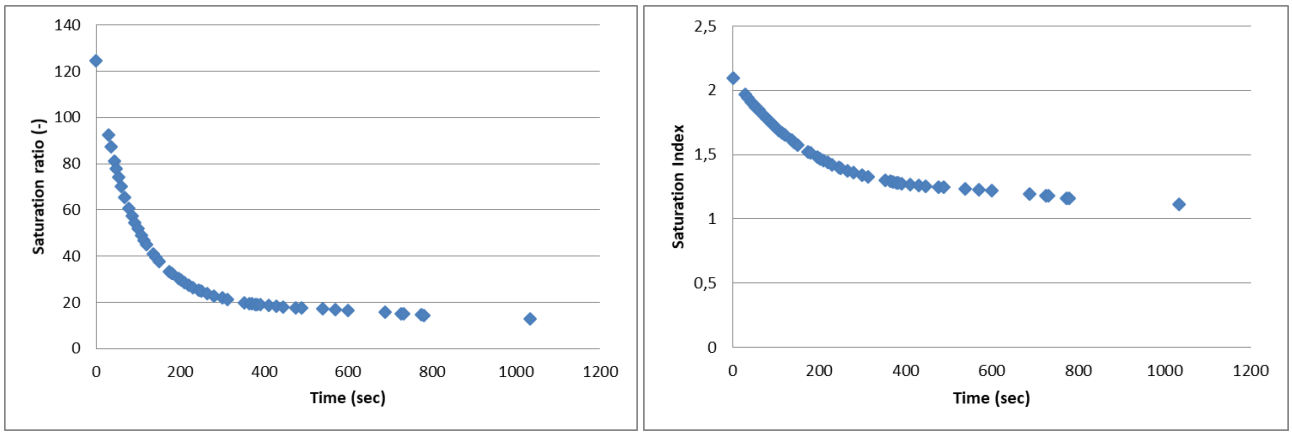

Figure A. 2 Experiment 1: Saturation ratio and saturation index

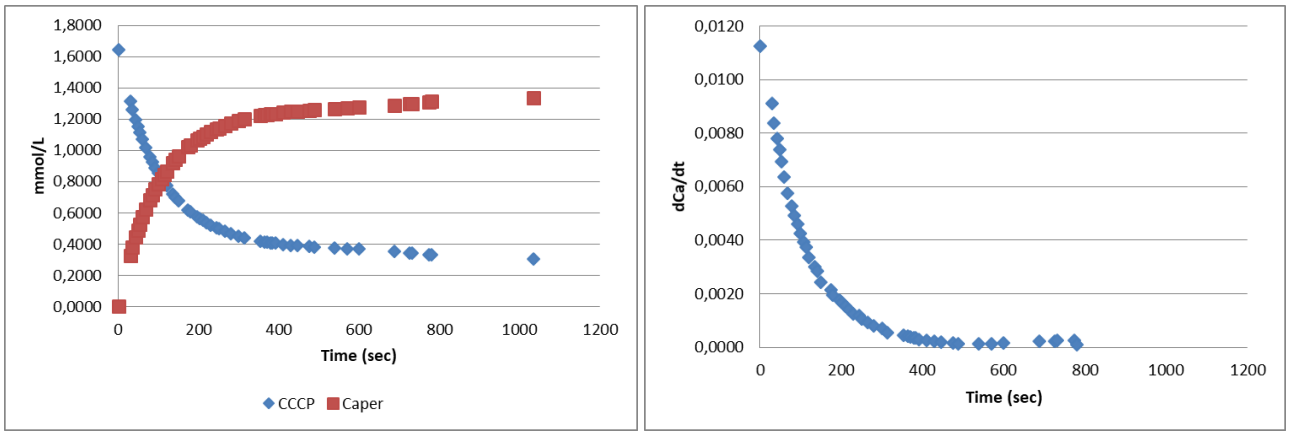

Figure A. 3 Experiment 1: Concentration of removed calcium and CCCP-Rate of calcium carbonate crystallization

A.2.2 Experiment 2-results

A.2.2.1 Particle size distribution analysis

A particles size distribution analysis took place in the TU Delft laboratory in order to define the specific surface area of the calcite powder that was used as seeding material in Experiment 1.

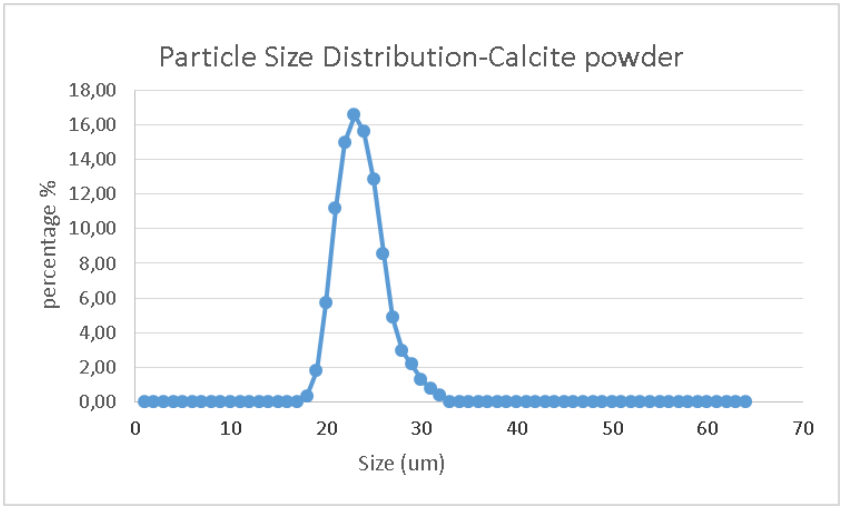

Figure A. 4 Particle size distribution of Merck calcite powder

Based on the results of the analysis the d50 of the powder is approximately 24um. The specific surface area is ranging between 2000-6000 m^2/m^3. In the following table the calculated specific surface area of the seeding material that was used in Experiment 2 based on the particle size distribution analysis is shown.

Table A. 3 Experiment 2: Particle size distribution analysis of calcite powder

size	%Volume	Volume of particles	Surface (m-1)
74.00	0.33%	2.12E-13	2.96E+00
62.23	1.82%	1.26E-13	1.94E+01
52.33	5.69%	7.50E-14	7.22E+01
44.00	11.19%	4.46E-14	1.69E+02
37.00	14.99%	2.65E-14	2.69E+02
31.11	16.56%	1.58E-14	3.54E+02
26.16	15.63%	9.37E-15	3.97E+02
22.00	12.83%	5.58E-15	3.87E+02
18.50	8.56%	3.32E-15	3.07E+02
15.56	4.86%	1.97E-15	2.07E+02
13.08	2.93%	1.17E-15	1.49E+02
11.00	2.17%	6.97E-16	1.31E+02
9.25	1.30%	4.14E-16	9.33E+01
7.78	0.74%	2.47E-16	6.32E+01
6.54	0.40%	1.46E-16	4.06E+01
	sum Surface area (m-1)		2662.14

A.2.2.2 Species distribution analysis

In the following figures the calcium species distribution in the solution is shown. The total calcium concentration is also plotted against time and the equilibrium concentration is shown.

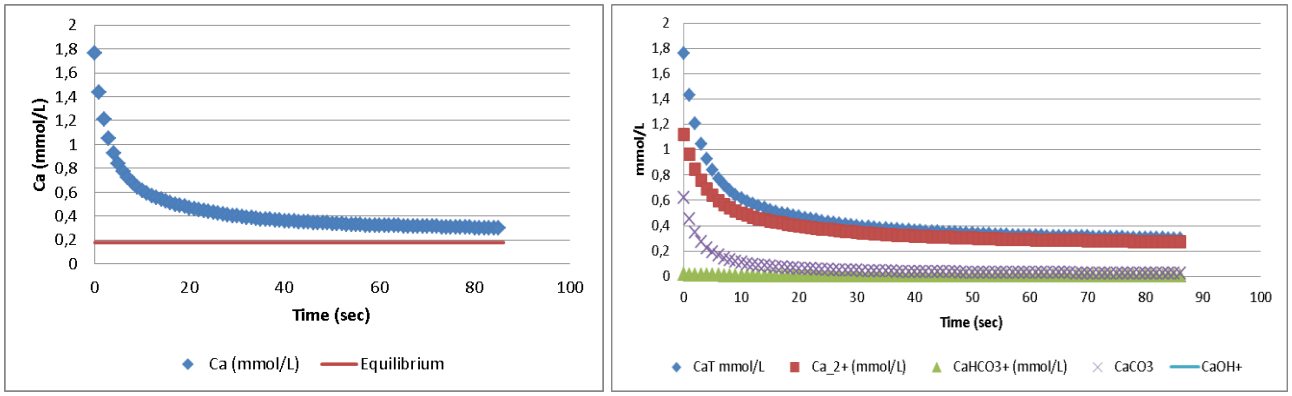

Figure A. 5 Experiment 2: Total calcium concentration and species distribution

In Figure A. 6 the saturation ratio and the saturation index during the experiment is presented. It can be clearly seen that in the beginning of the experiment a saturation ratio of 120 and a Saturation index of approximately 2 is reached.

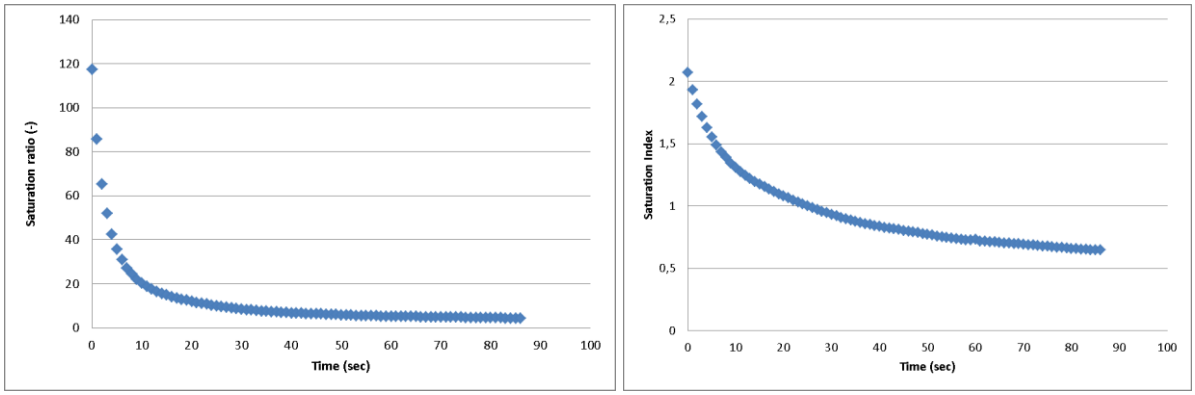

Figure A. 6 Experiment 2: Saturation ratio and saturation Index

In Figure A. 7 the concentration of calcium that is removed from the solution and the calcium carbonate crystallization potential (CCCP). Also the calcium reduction rate is plotted against time. It is obvious that the rate of crystallization significantly decreases and almost reaches zero after a certain period of time.

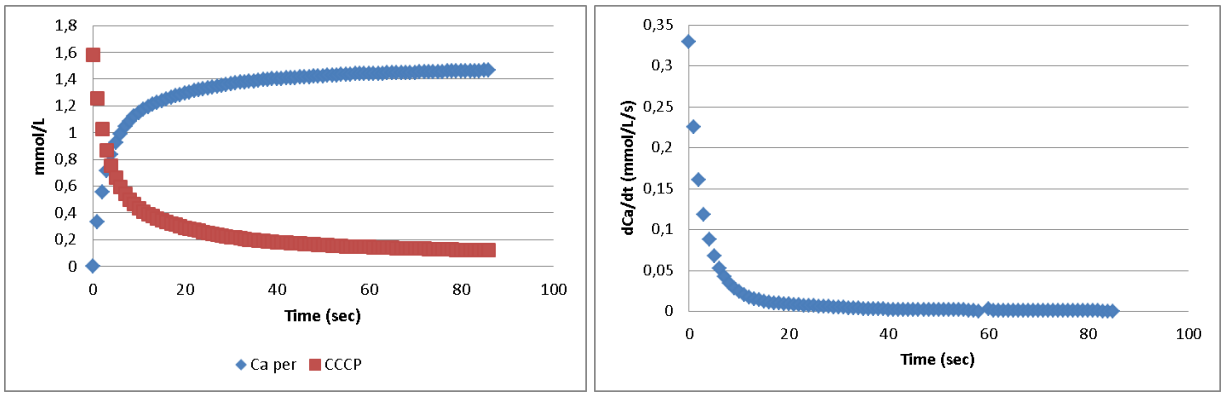

Figure A. 7 Experiment 2: Concentration of removed calcium and CCCP-Rate of calcium carbonate crystallization

A.2.3 Experiment 3-results

A.2.3.1 Species distribution analysis

In the following figures the calcium species distribution in the solution is shown. The total calcium concentration is also plotted against time and the equilibrium concentration is shown

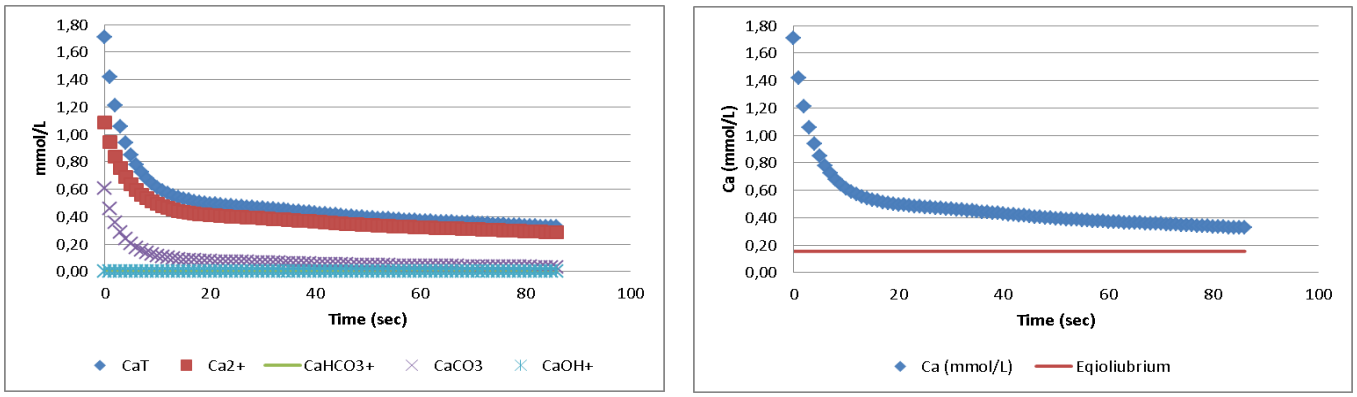

Figure A. 8 Experiment 3: Total calcium concentration and species distribution

In Figure A. 9 the saturation ratio and the saturation index during the experiment is presented. It can be clearly seen that in this experiment the initial saturation ratio is slightly lower. In the beginning of the experiment, a saturation ratio of 117 and a Saturation index of approximately 2 is reached.

In Figure A. 10 the amount of calcium that is removed from the solution and the calcium carbonate crystallization potential is shown. Also the calcium reduction rate is plotted against time. It is obvious that the rate of crystallization significantly decreases and almost reaches zero after a certain period of time.

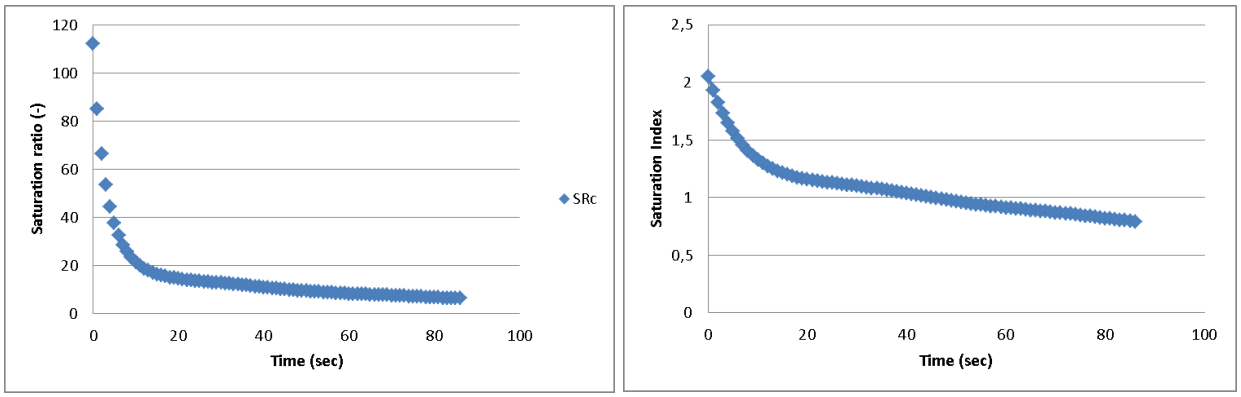

Figure A. 9 Experiment 3: Saturation ratio and saturation index

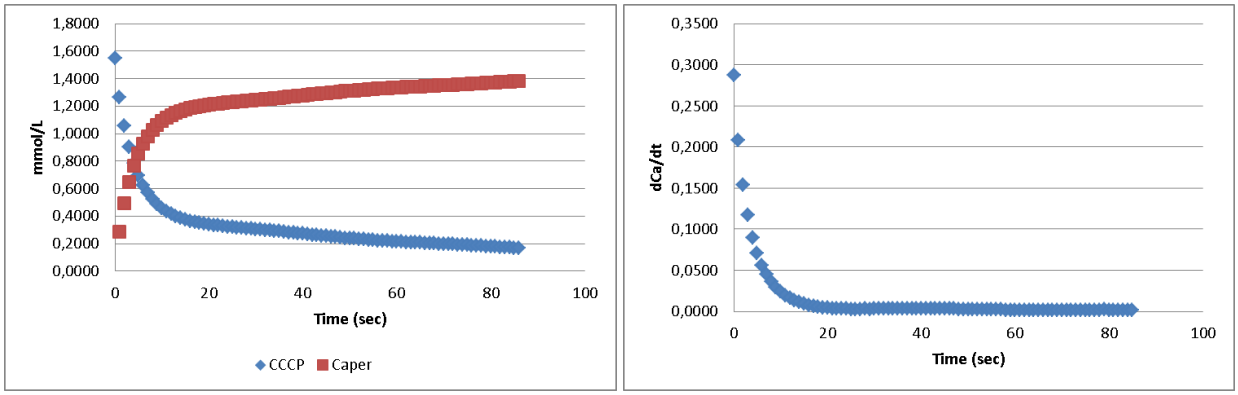

Figure A. 10 Experiment 3: Concentration of removed calcium and CCCP-Rate of calcium carbonate crystallization

A.2.4 Experiment 4-Results

A.2.4.1 Species distribution analysis

In the following figures the calcium species distribution in the solution is shown. The total calcium concentration is also plotted against time and the equilibrium concentration is shown.

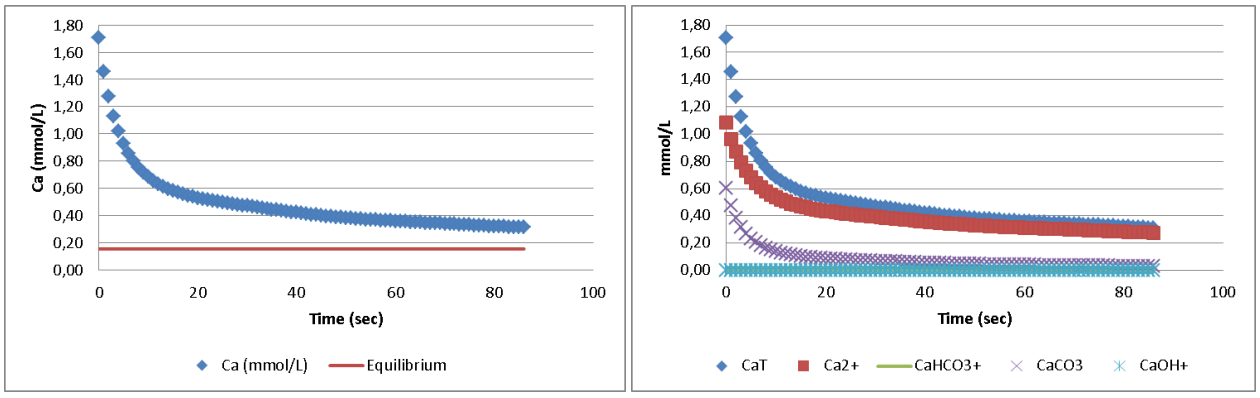

Figure A. 11 Experiment 4: Total calcium concentration and species distribution

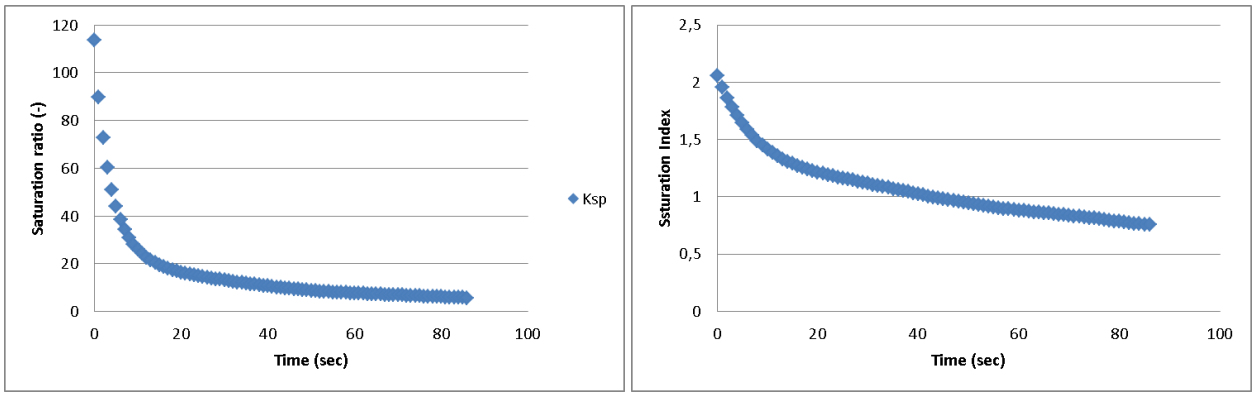

Figure A. 12 Experiment 4: Saturation ratio and saturation index

In Figure A. 11 the calcite saturation index and saturation ratio during Experiment 4 is shown and in Figure A. 12 the amount of calcium that is removed from the solution and the calcium carbonate crystallization potential (CCCP) is shown. Also the calcium reduction rate is plotted against time.

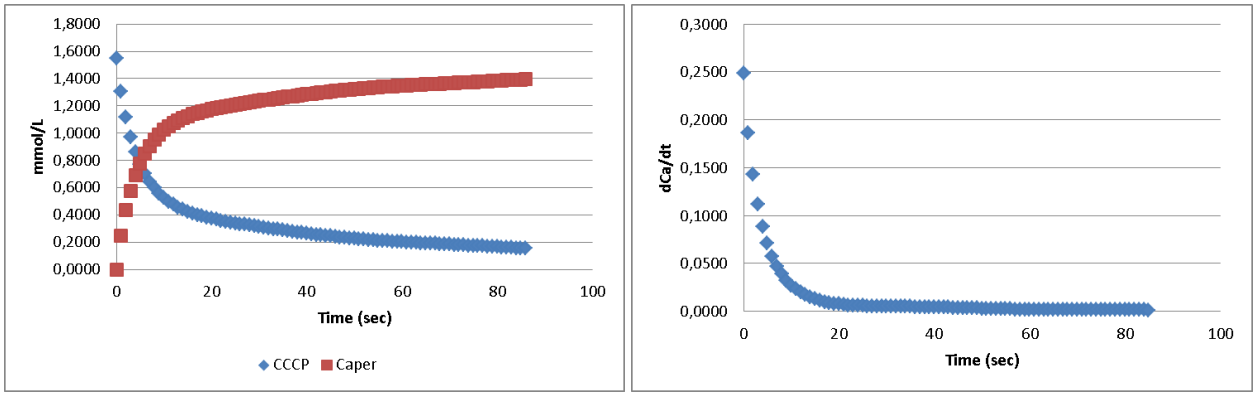

Figure A. 13 Experiment 4: Concentration of removed calcium and CCCP-Rate of calcium carbonate crystallization

A.2.5 Experiment 5-results

A.2.5.1 Species distribution analysis

In the following figures the calcium species distribution in the solution is shown. The total calcium concentration is also plotted against time and the equilibrium concentration is shown.

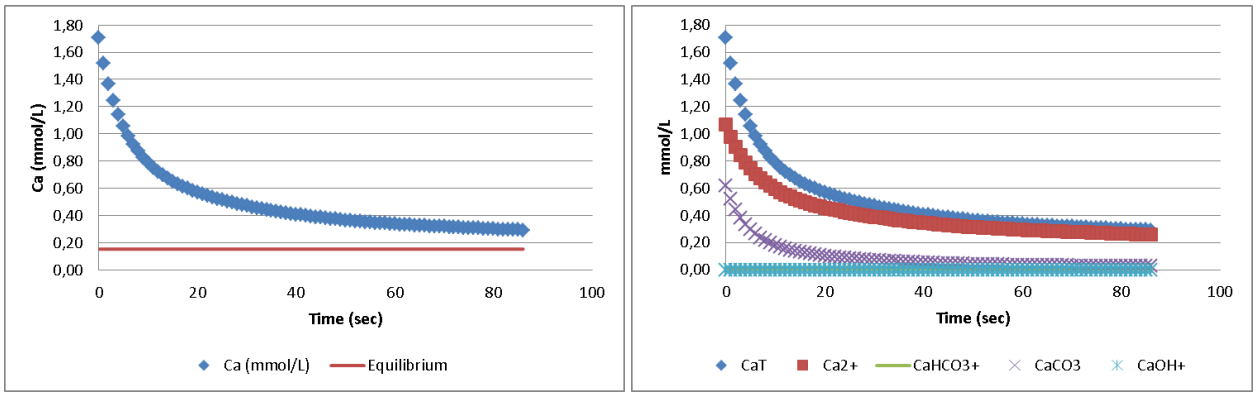

Figure A. 14 Experiment 5: Total calcium concentration and species distribution

In the following figure the saturation ratio and the saturation index during the experiment is presented.

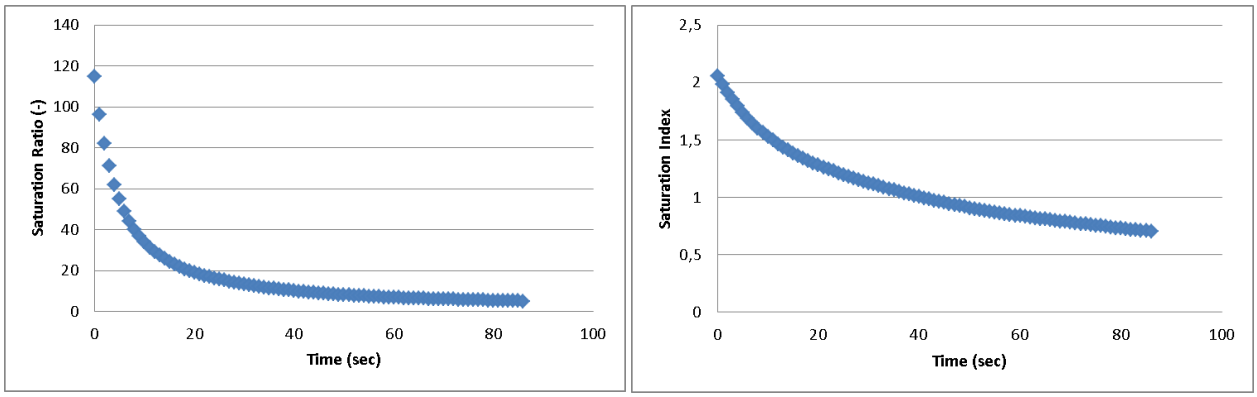

Figure A. 15 Experiment 5: Saturation ratio and saturation index

In Figure A. 16 the amount of calcium that is removed from the solution and the calcium carbonate crystallization potential (CCCP) is shown.

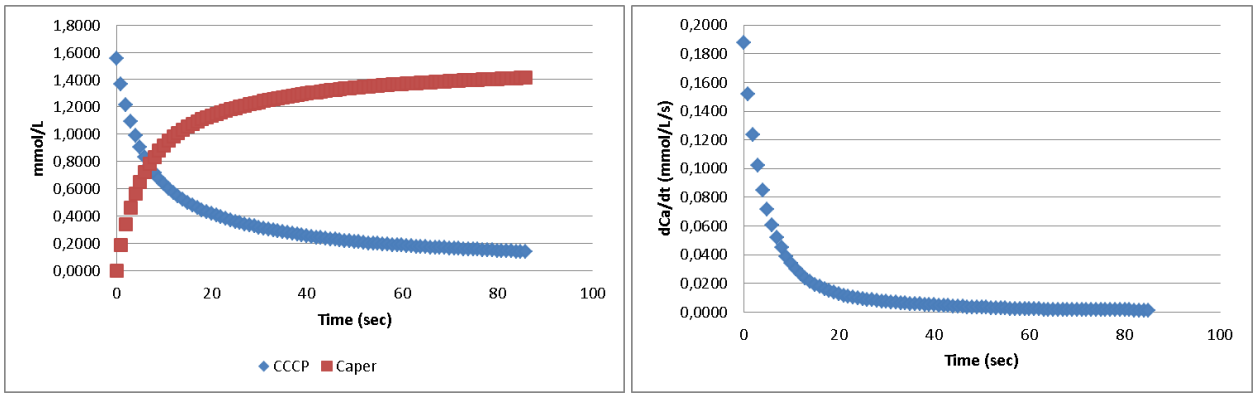

Figure A. 16 Experiment 5: Concentration of removed calcium and CCCP-Rate of calcium carbonate crystallization

A.2.6 SSA calculations for the STR batch experiments

Experiment 1

Table A. 4 Experiment 1: Particle size distribution analysis of calcite powder

size	%Volume	Volume of particles	Surface (m^{-1})
74.00	0.33%	2.12E-13	9.87E-02
62.23	1.82%	1.26E-13	6.48E-01
52.33	5.69%	7.50E-14	2.41E+00
44.00	11.19%	4.46E-14	5.63E+00
37.00	14.99%	2.65E-14	8.97E+00
31.11	16.56%	1.58E-14	1.18E+01
26.16	15.63%	9.37E-15	1.32E+01
22.00	12.83%	5.58E-15	1.29E+01
18.50	8.56%	3.32E-15	1.02E+01
15.56	4.86%	1.97E-15	6.92E+00
13.08	2.93%	1.17E-15	4.96E+00
11.00	2.17%	6.97E-16	4.37E+00
9.25	1.30%	4.14E-16	3.11E+00
7.78	0.74%	2.47E-16	2.11E+00
6.54	0.40%	1.46E-16	1.35E+00
	sum Surface area (m-1)		88.74

Experiment 2

Table A. 5 Experiment 2: Particle size distribution analysis of calcite powder

size	%Volume	Volume of particles	Surface (m-1)
74.00	0.33%	2.12E-13	2.96E+00
62.23	1.82%	1.26E-13	1.94E+01
52.33	5.69%	7.50E-14	7.22E+01
44.00	11.19%	4.46E-14	1.69E+02
37.00	14.99%	2.65E-14	2.69E+02
31.11	16.56%	1.58E-14	3.54E+02
26.16	15.63%	9.37E-15	3.97E+02
22.00	12.83%	5.58E-15	3.87E+02
18.50	8.56%	3.32E-15	3.07E+02
15.56	4.86%	1.97E-15	2.07E+02
13.08	2.93%	1.17E-15	1.49E+02
11.00	2.17%	6.97E-16	1.31E+02
9.25	1.30%	4.14E-16	9.33E+01
7.78	0.74%	2.47E-16	6.32E+01
6.54	0.40%	1.46E-16	4.06E+01
	sum Surface area (m-1)		2662.14

Experiments 3, 4 and 5

In Experiments 3, 4and 5 the same concentration and specific surface area of seeding material was used. The SSA was calculated based on the methodology in §3.2. The results are shown in Table A. 6.

Table A. 6 Experiments 3, 4, 5: Calculation of SSA

d(m)=	5.50E-04
Volume of pellet (m^3)	8.71E-11
Mass of pellet (g)	2.36E-04
density (kg /m^3)	2.71E+03
Surface of single pellet (m^2)	9.50E-07
Volume of reactor (m^3)	5.14E-04
Specific Surface Area (m^2/m^3)	3.00E+02
Surface of pellets (m^2)	1.50E-01
Number of pellets	1.58E+05
Volume of pellets (m^3)	1.38E-05
Volume of solution (m^3)	5.00E-04
Volume of pellets (ml)	13.75
Gross Volume of pellets (ml)	22.92
Mass of pellets (g)	37.26

APPENDIX B – PFR Fluidized Bed Reactor Experiments

This appendix deals with the presentation of the water quality of the influent water for the PFR fluidized bed experiments.

B.1 Water quality of influent of Weesperkarspel treatment plant

In Table B. 1 the water quality of the influent of WPK water treatment plant the dates that the water was abstracted to be used for the Fluidized Bed Reactor experiments is shown.

Table B. 1 Water of the influent stream of WPK water treatment plant on 15/08/2017

AQUATIC CHEMISTRY for Engineers

Module **Calcite kinetics (PWP and Wiechers model)**
Dissolution and precipitation of Calcite

Sample description	WPK TimeVal		##########	Test data	*Assumption: mg/L =mg/kgs =mg/kgw*	
Basic data	Temperature	t	°C	19,4		
	Oxygen	O2	mg/L	8,2	0,26	mmol/kgw
	pH	pH	-	7,78		
	Total organic carbon	TOC	mg/L C	6,7	0,56	mmol/kgw
	Silicate	Si	mg/L Si	4	0,16	mmol/kgw
	Conductivity (measured, at 25 °C)	EC	µS/cm	465	46,5	mS/m
Cations	Calcium	Ca	mg/L	64,3	1,60	mmol/kgw
	Magnesium	Mg	mg/L	6,97	0,29	mmol/kgw
	Sodium	Na	mg/L	24,7	1,08	mmol/kgw
	Potassium	K	mg/L	2,7	0,07	mmol/kgw
	Ammonium (inert)	NH4	mg/L N	0,00	0,000	mmol/kgw
Anions	Alkalinty (as HCO3)	HCO3	mg/L	198	3,25	mmol/kgw
	Chloride	Cl	mg/L	60	1,69	mmol/kgw
	Nitrate	NO3	mg/L N	0,8	0,01	mmol/kgw
	Sulfate	SO4	mg/L	6,8	0,07	mmol/kgw
	Bromide	Br	mg/L	0,09	0,00	mmol/kgw
	Nitrite (inert)	NO2	mg/L N	0,0	0,00	mmol/kgw

B.2 SSA calculations for the PFR fluidized bed experiments

Experiments 6

Table B. 2 Calculations of inlet nozzle volume and the

Inlet Nozzle Volume								
Hexagon				Cylinder				Total Volume
2*apothek e	side (m)	Area (m2)	Volume (m3)	D (m)	H(m)	Area (m2)	Volume (m3)	Nozzle (m3)
16.76	9.68E-03	2.43E-04	1.51E-06	5.02E-02	3.50E-02	1.98E-03	6.92E-05	7.08E-05

Layer No	Fixed Bed Height (cm)	Fluidized Bed Height (cm)	Layer weight (g)	Sum Weight (g)	Nett Pellet Volume (m3)	Layer Volume (m3)	porosity	SSA (m2/m3 water)	Con (g/L)
-	0	0	0	0	0	0	-	0	
0	0	0	0	0	0	0	-	0	
1	10	14.50	1000.72	1000.72	3.71E-04	7.25E-04	0.49	5921	1380
2	15	35.60	1500.32	2501.04	9.26E-04	1.88E-03	0.51	5481	1328
3	15	56.90	1500.48	4001.52	1.48E-03	3.05E-03	0.51	5344	1311
4	15	78.00	1453.96	5455.48	2.02E-03	4.21E-03	0.52	5224	1296

Experiment 7

Inlet Nozzle Volume								
Hexagon				Cylinder				Total Volume
2*apotheke	side (m)	Area (m2)	Volume (m3)	D (m)	H(m)	Area (m2)	Volume (m3)	Nozzle (m3)
16.76	9.68E-03	2.43E-04	1.51E-06	5.02E-02	3.50E-02	1.98E-03	6.92E-05	7.08E-05

Layer number	Fixed Bed Height (cm)	Fluidized Bed Height (cm)	Layer weight (g)	Sum Weight (g)	Nett Pellet Volume (m3)	Layer Volume (m3)	porosity	SSA (m2/m3 water)	Conc (g/L)
-	0	0	0	0	0	0	-	0	
0	0	0	0	0	0	0	-	0	
1	10	14.2	1000.42	1000.42	3.71E-04	7.09E-04	48%	6205	1412
2	20	28	1000.14	2000.56	7.41E-04	1.47E-03	49%	5786	1365
3	30	41.8	1000.22	3000.78	1.11E-03	2.22E-03	50%	5659	1350
4	40	55.9	1000.08	4000.86	1.48E-03	3.00E-03	51%	5536	1335
5	55	76.3	1500.18	5501.04	2.04E-03	4.12E-03	51%	5547	1336

Experiment 8

Inlet nozzle Volume								
Hexagon				Cylinder				Total Volume
2*apotheke	side (m)	Area (m2)	Volume (m3)	D (m)	H(m)	Area (m2)	Volume (m3)	Nozzle (m3)
16.76	9.68E-03	2.43E-04	1.51E-06	5.02E-02	3.50E-02	1.98E-03	6.92E-05	7.07E-05

Layer number	Fixed Bed Height (cm)	Fluidized Bed Height (cm)	Layer weight (g)	Sum Weight (g)	Nett Pellet Volume (m3)	Layer Volume (m3)	porosity	SSA (m2/m3 water)	Conc (g/L)
-	0	0	0	0	0	0	-	0	
0	0	0	0	0	0	0	-	0	
1	10	21	1000.06	1000.06	3.70E-04	1.08E-03	66%	5681	925
2	20	43.5	1000.52	2000.58	7.41E-04	2.32E-03	68%	5131	864
3	30	66.5	1000.24	3000.82	1.11E-03	3.58E-03	69%	4914	839
4	35	79	500.46	3501.28	1.30E-03	4.26E-03	70%	4767	821

Experiment 9

Inlet Nozzle Volume								
Hexagon				Cylinder				Total Volume
2*apotheke	side (m)	Area (m2)	Volume (m3)	D (m)	H(m)	Area (m2)	Volume (m3)	Nozzle (m3)
16.76	9.68E-03	2.43E-04	1.51E-06	5.02E-02	3.50E-02	1.98E-03	6.92E-05	7.08E-05

Layer number	Fixed Bed Height (cm)	Fluidized Bed Height (cm)	Layer weight (g)	Sum Weight (g)	Nett Pellet Volume (m3)	Layer Volume (m3)	porosity	SSA (m2/m3 water)	Conc (g/L)
-	0	0	0	0	0	0	-	0	
0	0	0	0	0	0	0	-	0	
1	10	20	1000.82	1000.82	3.71E-04	1.03E-03	64%	6163	975
2	15	41	1000.84	2001.66	7.41E-04	2.18E-03	66%	5625	919
3	15	65	1000.38	3002.04	1.11E-03	3.50E-03	68%	5087	859

Appendix C-Experiments of Linssen (1983)

In this paragraph the experimental results of the research of Linssen (1983) that was used for the validation of the model is shown.

C.1 Experimental results from Linssen (1983): Experiment 1

Table C. 1 Experiment 1 from Linssen (1983): Experimental conditions

	Experiment 1
Date	21/03/1983
Water flow [m^3/h]	420
Temperature [℃]	9.3
NaOH dose (mmol/L)	1.04
Fluidized Bed Height [m]	3.85
Ca influent [mmol/L]	2.02
Ctotal influent [mmol/L]	3.6
CO_2 influent [mmol/L]	0.3
Type of seeding material	sand
Diameter of seeding material at the top [mm]	0.37
Diameter of seeding material at the top [mm]	0.79
pH effluent	8.75

Table C. 2 Experiment 1 from Linssen (1983): Measurement of Ca. Ct. porosity pellet diameter and specific surface area over the head of the reactor

Experiment 1						
Height [m]	**Ca [mmol/L]**	**Ct [mmol/L]**	**SSA [m^2/m^3]**	**e [mm]**	**d [mm]**	**Contact Time [sec]**
In	2.02	3.60	2430	0.68	0.79	0
0.25	1.36	3.19	2430	0.68	0.79	7.7
0.5	1.29	3.13	2340	0.7	0.77	15.9
0.75	1.26	3.16	2530	0.73	0.64	24.9
1	1.3	3.16	2620	0.76	0.55	34.6
1.5	1.23	3.05	2690	0.78	0.49	53.2
2	1.23	3.05	2550	0.8	0.47	72.8
2.5	1.22	3.00	2570	0.82	0.42	93.3
3	1.2	3.02	2570	0.82	0.42	112.0
3.5	1.18	3.01	2270	0.86	0.37	137.0
3.85	1.19	3.01	2270	0.86	0.37	150.7

C.2 Experimental results from Linssen (1983): Experiment 2

Table C. 3 Experiment 2 from Linssen (1983): Experimental conditions

Experiment 2	
Date	04/05/1983
Water flow [m^3/h]	535
Temperature [℃]	10.8
NaOH dose (mmol/L)	1.02
Fluidized Bed Height [m]	4.35
Ca influent [mmol/L]	1.98
Ct influent [mmol/L]	3.63
CO_2 influent [mmol/L]	0.3
Type of seeding material	sand
Diameter of seeding material at the top [mm]	0.43
Diameter of seeding material at the bottom [mm]	0.68
pH effluent	8.75

Table C. 4 Experiment 2 from Linssen (1983): Measurement of Ca. Ct. porosity. pellet diameter and specific surface area over the head of the reactor

Experiment 2						
Height [m]	**Ca [mmol/L]**	**Ct [mmol/L]**	**SSA [m^2/m^3]**	**e (porosity) [mm]**	**d (diameter) [mm]**	**Contact Time [sec]**
in	1.98	3.63	-	-	-	0.0
0.25	1.41	3.11	2640	0.68	0.68	7.7
0.5	1.32	3.04	2340	0.7	0.68	15.9
0.75	1.33	3.05	2310	0.73	0.67	24.9
1	1.29	3.02	2280	0.76	0.59	34.6
1.5	1.29	2.98	2430	0.78	0.45	53.2
2	1.28	3.00	2250	0.8	0.46	72.8
3	1.26	2.97	2420	0.82	0.46	112.0
4	1.28	2.98	2150	0.82	0.43	149.3
4.35	1.26	2.98	2150	0.86	0.43	170.2

C.3 Experimental results from Linssen (1983): Experiment 3

Table C. 5 Experiment 3 from Linssen (1983): Experimental conditions

Experiment 3	
Date	04/05/1983
Water flow [m^3/h]	535
Temperature [℃]	10.8
NaOH dose (mmol/L)	1.38
Fluidized Bed Height [m]	4.3
Ca initial [mmol/L]	1.98
Ct initial [mmol/L]	3.6
CO_2 influent [mmol/L]	0.3
Type of seeding material	sand
Diameter of seeding material at the top [mm]	0.43
Diameter of seeding material at the bottom [mm]	0.68
pH effluent	8.75

Table C. 6 Experiment 3 from Linssen (1983): Measurement of Ca. Ct. porosity pellet diameter and specific surface area over the head of the reactor

Experiment 3						
Height [m]	**Ca [mmol/L]**	**Ct [mmol/L]**	**SSA [m^2/m^3]**	**e [mm]**	**d [mm]**	**Contact Time [sec]**
in	1.98	-	-	-	-	0.0
0.25	1.08	2.98	2640	0.7	0.68	6.3
0.5	0.96	2.77	2340	0.73	0.68	13.0
0.75	0.94	2.75	2310	0.74	0.67	19.8
1	0.92	2.67	2280	0.78	0.59	27.9
1.5	0.87	2.64	2430	0.82	0.45	43.9
2	0.85	2.60	2250	0.83	0.46	59.3
3	0.87	2.59	2420	0.81	0.46	86.8
4	0.86	2.57	2150	0.85	0.46	121.5
4.3	0.82	2.51	2150	0.85	0.43	130.6

C.4 Scenario study

In order to optimize the operation of a pellet softening reactor and in particular to minimize the use of chemicals, several operational scenarios for a pellet softening fluidized bed reactor were tested. The Layers-model [Hout (2016). Kramer et al. (2015)] was used to determine the hydraulic conditions inside a pellet softening reactor while the two-rate-constants model was used to model the calcium carbonate seeded crystallization kinetics.

According to the two-rate-constants model that was developed in this research the largest reduction of calcium takes place at the bottom of the reactor. The rate of crystallization in the top of the reactor is much lower. In order to increase the rate of crystallization at the top of the reactor. an increase in the specific surface area of the seeding material is necessary. If the velocity of the water inside the reactor is decreased then a higher crystallization surface area is available. The effect of using seeding material with a uniform diameter over the height of the reactor on the rate of calcium reduction at the top of the reactor was also investigated. In this case. a high specific surface area is offered in the top as well as in the bottom of the reactor.

In order to investigate the effect of having a low velocity of water. in a pellet softening reactor in combination with seeding material with a uniform or a non-uniform diameter over the height of the reactor two scenarios are tested. In Table C. 7 the operational scenarios for the pellet softening fluidized bed reactor are shown.

Table C. 7 Operational scenarios for the pellet softening fluidized bed reactor

	Scenario 1	Scenario 2
Velocity (m/h)	80	60
Effluent TH (mmol/L)	1.4	1.4
By pass (%)	0	0
NaOH dose (mmol/L) uniform calcite pellet diameter d=1.1-1mm	1.067	1.042
NaOH dose (mmol/L) uniform calcite pellet diameter d=0.6-0.7mm	1.059	1.027
NaOH dose (mmol/L) non-uniform calcite pellet diameter	1.047	1.015

In Figure C. *1 Calcium reduction over the height of the pellet softening fluidized bed reactor according to scenario 1*

and **Σφάλμα! Το αρχείο προέλευσης της αναφοράς δεν βρέθηκε.** the calcium reduction over the height of the reactor according to scenario 1 and scenario 2 are shown.

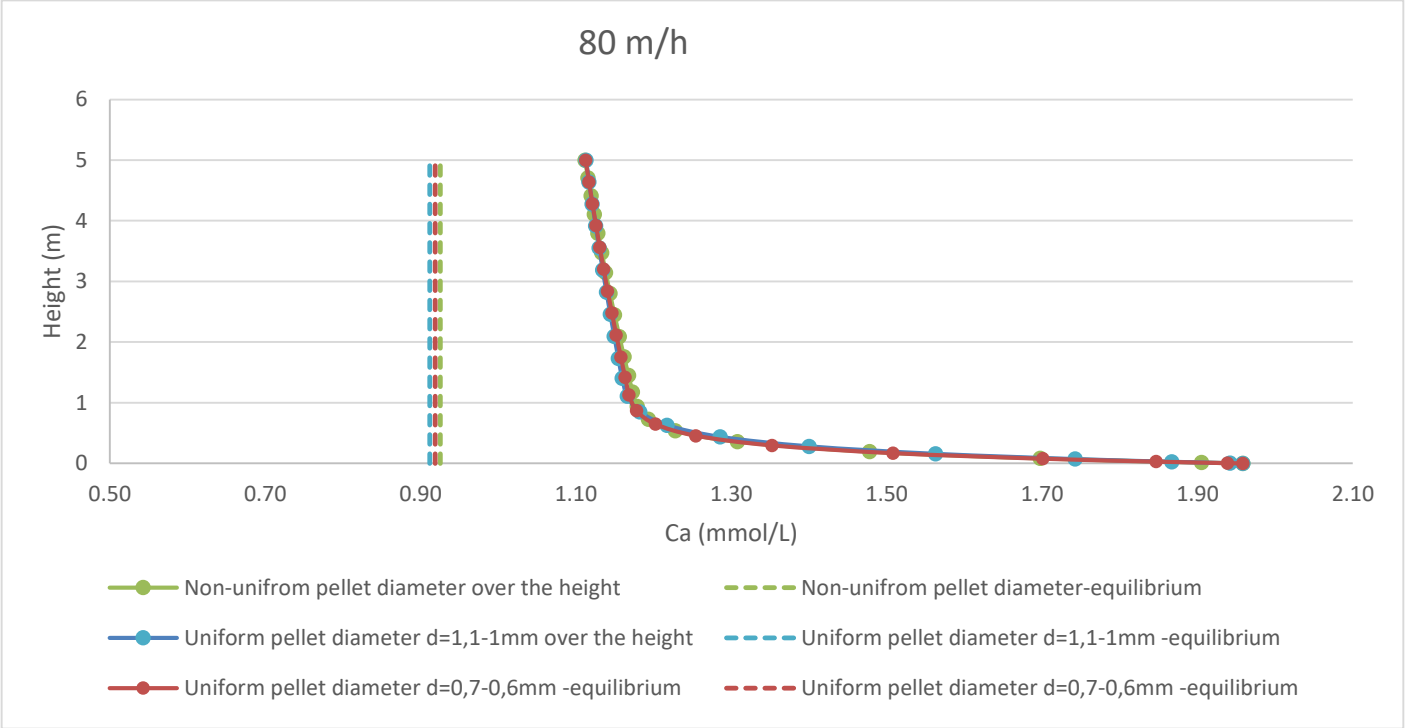

Figure C. 1 Calcium reduction over the height of the pellet softening fluidized bed reactor according to scenario 1

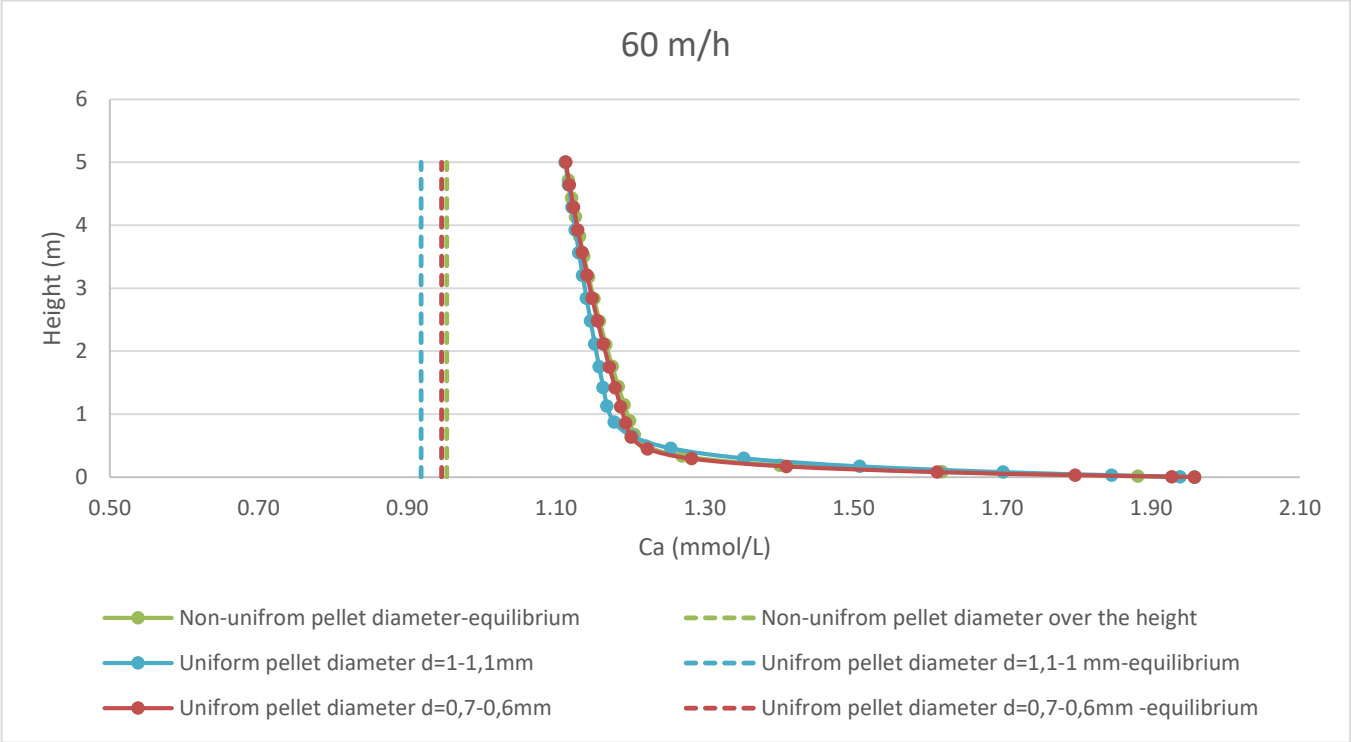

Figure C. 2 Calcium reduction over the height of the pellet softening fluidized bed reactor according to scenario 2

Based on Table C. 7and Figure C. 1 when the velocity is 80 m/h. there is a very small difference in the calcium reduction profile over the height of the reactor if a uniform diameter seeding material is used or not. Also a slightly higher dose should be added to the solution to reach a total hardness (TH) of 14 mmol/L in the top of the reactor, compared to using a non-uniform seeding material. In this case the use of a uniform diameter seeding material is not improving the operation of the pellet softening fluidized bed reactor.

On the other hand, if the velocity of the water inside the reactor is reduced to 60 m/h the difference between a uniform and a non-uniform diameter inside the pellet softening fluidized bed reactor is slightly

higher. However, a reactor filled with uniform diameter seeding material with a diameter d >0.6mm is still not performing better than a reactor with a non-uniform diameter seeding material.

Overall, it can be concluded that the operation of a pellet softening reactor can be improved and the dosing of caustic soda reduced only if the velocity of the water inside the reactor is lower than 60 m/h and the diameter of the seeding material is smaller than 0.6mm.